

For Reference

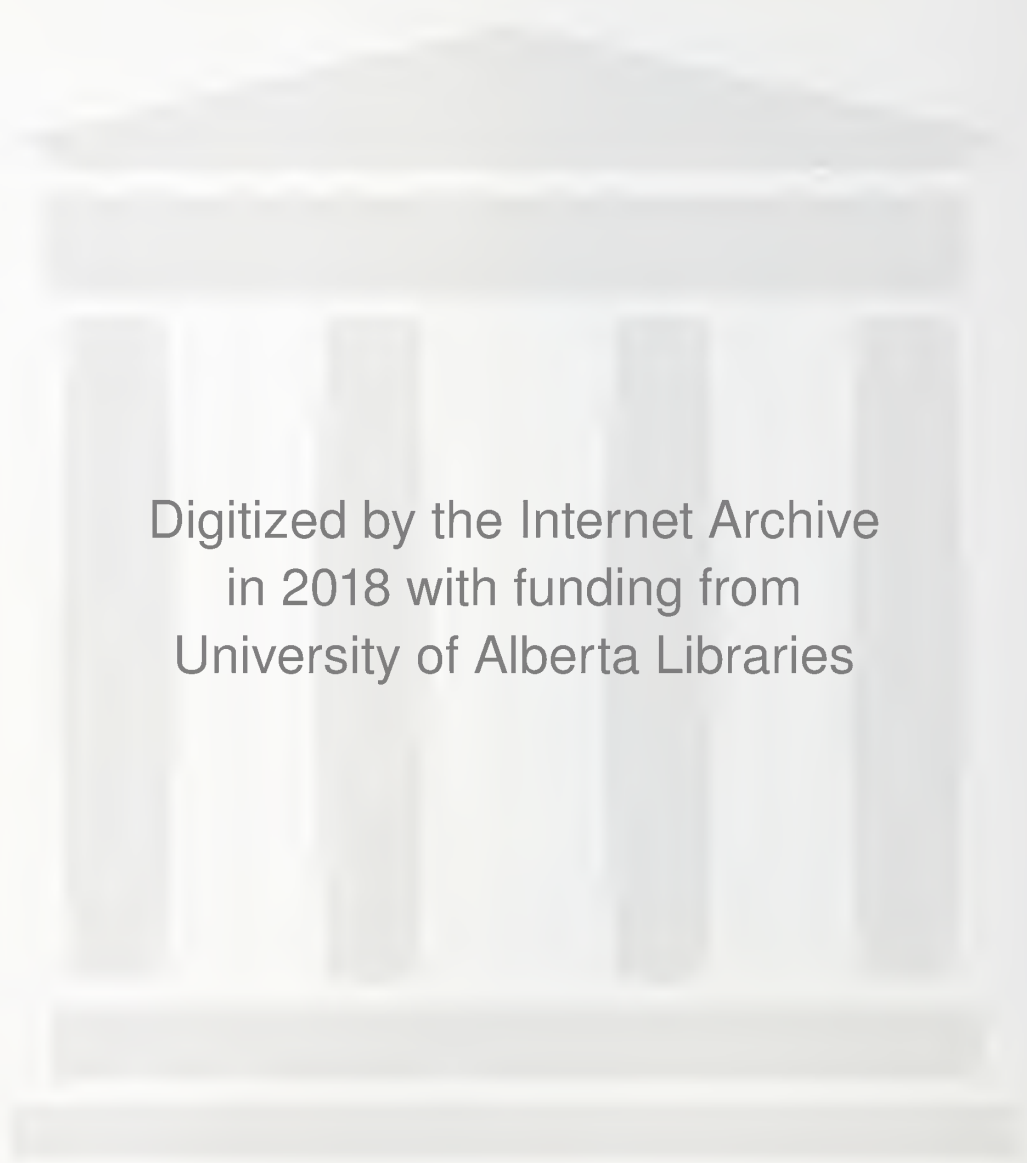
NOT TO BE TAKEN FROM THIS ROOM

FURTHER STUDIES IN PRESTRESSED
CONCRETE

FEDUNEC & LAVIOLETTE

Ex LIBRIS
UNIVERSITATIS
ALBERTAENSIS





Digitized by the Internet Archive
in 2018 with funding from
University of Alberta Libraries

<https://archive.org/details/FedunecLaviolette1954>

54.
7.
THE UNIVERSITY OF ALBERTA

FURTHER STUDIES IN PRESTRESSED CONCRETE

A DISSERTATION

SUBMITTED TO THE SCHOOL OF GRADUATE STUDIES
IN PARTIAL FULFILMENT OF THE REQUIREMENTS FOR THE DEGREES
OF MASTER OF SCIENCE

FACULTY OF ENGINEERING
DEPARTMENT OF CIVIL ENGINEERING

by

W.S. Fedunec

T.W. Laviolette

Under the Direction of Dr. R.N. McManus

EDMONTON, ALBERTA,

April 3, 1954

ABSTRACT

Experimental studies were made of the flexural behavior of six unbonded prestressed concrete beams employing the patented Lee-McCall system. The six rectangular beams which were designed and tested were divided into two groups; one having percentages of steel of 0.0073, the other have percentages of steel of 0.012. Two of the beams were constructed with vertical joints in the concrete at midspan.

Deflections, steel strains, and the deformations in the central portion of the beam span were observed.

In the load-deflection curves, there was no marked deviation from the straight line up to loads which were 90% of the cracking load. The cracking loads predicted by the usual (elastic) design relationship were found to be 6% to 15% on the safe side. There was an indication that during bending plane sections rotated about an axis which was lower than the centre of gravity axis, but the axis of rotation was noted to rise as the loads were increased.

At failure, the ratio of the moment arm to the effective depth (commonly called j) was determined to be 0.91 to 0.93.

An average value of 0.0039 inches/inch was obtained for the ultimate compressive strain of concrete.

ACKNOWLEDGEMENTS

The authors wish to express their appreciation to:

Dr. R.M. McManus for his guidance during the experimental program and his constructive criticisms during the writing of the manuscript.

Mr. Edwin Foo and Mr. R. Yacyshyn for their generous assistance with the experimental work.

TABLE OF CONTENTS

PAGE

I Introduction

A Brief History of Prestressed Concrete.....	1
The Lee-McCall System.....	2
Earlier Work.....	4

II Scope of the Studies 6

III Design Theory 7

IV Design of the Beams

Notation Used.....	10
Notation Used for the Test Beams.....	11
Selection of the Size and Shape of Beams.....	11
Location of the Steel.....	12
Estimation of Cracking Loads.....	16

V Experimental Procedures

Materials Used.....	20
Instrumentation Used.....	20
Construction of the Beams.....	20
Post-Tensioning of the Beam.....	22
Testing Procedures.....	22

VI Presentation of Results..... 23

VII Discussion of Results

Load-Deflection Characteristics.....	27
The Axis About Which Sections Rotated.....	27
Concrete Strains.....	28
The Cracking Loads.....	29
Steel Stresses.....	29
Ultimate Loads.....	31
Physical Characteristics of the Failures.....	33

TABLE OF CONTENTS (Continued)

PAGE

VIII <u>Conclusions</u>	94
<u>Bibliography</u>	95
<u>Appendix A</u> - Static Tests Performed on Lee-McCall Bars and Bar-Nut Assemblies.....	96
<u>Appendix B</u> - Extensometers.....	101

LIST OF PLATES

<u>PLATE</u>	<u>NAME</u>	<u>PAGE</u>
1	figure a - Enlarged Detail of Lee-McCall Thread ..	5
	figure b - Details of a Lee-McCall Jack.....	5
2	Detail of Beam U.....	11
	Detail of Beam O.....	11
3	Details of Beam U-S.....	12
	Details of Beam O-S.....	12
4	figure c - Detail of Gauge Point.....	25
	figure d - Testing Apparatus.....	25
5	Beam U-1, Deflection of North Third Point.....	30
6	Beam U-1, Deflection of Centre Point.....	31
7	Beam U-1, Deflection South Third Point.....	32
8	Beam U-2, Deflection of North Third Point.....	33
9	Beam U-2, Deflection of Centre Point.....	34
10	Beam U-2, Deflection of South Third Point.....	35
11	Beam O-1, Deflection of North Third Point.....	36
12	Beam O-1, Deflection of Centre Point.....	37
13	Beam O-1, Deflection of South Third Point.....	38
14	Beam O-2, Deflection of North Third Point.....	39
15	Beam O-2, Deflection of Centre Point.....	40
16	Beam O-2, Deflection of South Third Point.....	41
17	Beam U-S1, Deflection of North Third Point.....	42
18	Beam U-S1, Deflection of Centre Point.....	43
19	Beam U-S1, Deflection of South Third Point.....	44
20	Beam O-S1, Deflection of North Third Point.....	45
21	Beam O-S1, Deflection of Centre Point.....	46
22	Beam O-S1, Deflection of South Third Point.....	47

LIST OF PLATES, Continued

<u>PLATE</u>	<u>NAME</u>	<u>PAGE</u>
23	Beam U-1, Extension of Top Extensometers.....	47
24	Beam U-1, Shortening of Bottom Extensometer.....	48
25	Beam U-2, Extension of Top Extensometer.....	50
26	Beam U-2, Shortening of Bottom Extensometer.....	51
27	Beam O-1, Extension of Top Extensometer.....	52
28	Beam O-1, Shortening of Bottom Extensometer.....	53
29	Beam O-2, Extension of Top Extensometer.....	54
30	Beam O-2, Shortening of Bottom Extensometer.....	55
31	Beam U-31, Extension of Top Extensometer.....	56
32	Beam U-31, Shortening of Bottom Extensometer.....	57
33	Beam O-31, Extension of Top Extensometer.....	58
34	Beam O-31, Shortening of Bottom Extensometer.....	59
35	Beam U-1, Position of Axis of Rotation.....	60
36	Beam U-2, Position of Axis of Rotation.....	61
37	Beam O-1, Position of Axis of Rotation.....	62
38	Beam O-2, Position of Axis of Rotation.....	63
39	Beam U-31, Position of Axis of Rotation.....	64
40	Beam U-32, Position of Axis of Rotation.....	65
41	Beam U-1, Strain in Top Concrete Fibre.....	66
42	Beam U-2, Strain in Top Concrete Fibre.....	67
43	Beam O-1, Strain in Top Concrete Fibre.....	68
44	Beam O-2, Strain in Top Concrete Fibre.....	69
45	Beam U-31, Strain in Top Concrete Fibre.....	70
46	Beam O-31, Strain in Top Concrete Fibre.....	71
47	Beam U-2, Steel Strains.....	72
48	Beam U-1, Steel Strains.....	73
49	Beam O-2, Steel Strains.....	74
50	Beam U-31, Steel Strains.....	75

LIST OF PLATES, Continued

<u>PLATE</u>	<u>NAME</u>	<u>PAGE</u>
51	Beam O-S1, Steel Strains.....,	76
52	Beam U-2, Steel Stresses.....	77
53	Beam O-1, Steel Stresses.....	78
54	Beam O-2, Steel Stresses.....	79
55	Beam U-S1, Steel Stresses.....	80
56	Beam O-S1, Steel Stresses.....	81
57	Maximum, Observed Steel Stresses.....	82
58	Stress Strain Curve for Macalloy Steel.....	91
59	Stress Strain Curve for Macalloy Steel.....	92
60	Extensometer, Assembly and Details.....	104
62	Details of End Anchorage Plates.....	105

LIST OF FIGURES

<u>FIGURE</u>	<u>NAME</u>	<u>PAGE</u>
3	Side View of Forms.....	26
4	End View of Forms.....	26
5	Stages in the Preparations of Bars.....	27
6	Typical Post-tensioning Procedure.....	27
7	Physical Characteristics of the Failures.....	34
8	Failure Zone in Beam U-1.....	35
9	Closeup of the Failure in Beam U-1.....	35
10	Beam O-1 under a load of 31.5 kips.....	36
11	Horizontal Cracks in Beam U-S1.....	36
12	Typical Fractures in Macalloy Bars.....	100

I INTRODUCTION

In this investigation several prestressed concrete beams were designed and tested. The beams were post-tensioned with unbonded, Lee-McCall bars.

A Brief History of Prestressed Concrete

The idea of prestressed concrete, first conceived in 1886 (by P.H. Jackson of San Francisco), is as old as the idea of reinforced concrete; but the early attempts to apply prestressing were not successful because mild steels and low strength concretes were used. A French engineer, E. Freyssinet, was the first to fully realize the cause of the early failures. In 1929, he showed that high strength materials, worked at correspondingly high stresses, were essential if sufficient precompression was to be retained after creep and shrinkage losses had occurred.

By 1940, large scale practical application of prestressing had taken place in Europe. Three systems were evolved: Hoyer's system of "long line" pre-tensioning, Freyssinet's system for post-tensioning, and Magnel's system for post-tensioning. All of these systems used relatively small wires, and hence a considerable amount of skilled labour. But European engineers were able to offset the additional labour with the saving in materials.

On this continent, a machine was developed in 1943 for performing circular prestressing. Linear prestressing was not employed till 1950 because it was generally believed that the techniques evolved in Europe were too labour-consuming to be competitive. However, both the Magnel and Freyssinet

systems have now been used successfully in North America. Another system was developed here: the Roebling system. It employs factory-tailored, prestretched, strand reinforcement which is supplied in exact lengths and with special end fittings. Presently, several larger structures are making use of the Lee-McCall system which was developed and widely used in England. This system, with its bar type tensioning units and its threaded anchorages, was utilized in the construction of 2,200.-50 foot long, precast girders for the recently completed Tampa Bay Bridge in Florida.

The majority of prestressed concrete structures have been of the bonded variety, i.e. the steel is bonded to the concrete. Unbonded prestressed concrete members, those in which the steel is entirely separated from the concrete except at the end anchorages, are known to have lower strengths and less favorable failure characteristics than corresponding bonded members. Yet they have been used, apparently advantageously, in many instances. The first prestressed bridge in America, one of three short spans built in Tennessee in 1950, used unbonded Roebling cables. Unbonded cables were also employed in a bridge at Danvers, Massachusetts. Many so-called trussed girder type of bridges which have been constructed in Europe have unbonded tensioning units.

The Lee-McCall System

Because the Lee-McCall System has been used in the beams studied here, it will be discussed much more fully than other systems which may be as important or more so.

The Lee-McCall system has two distinguishing features; the relatively large-sized tensioning units, and the "high efficiency" nut-and-thread anchorages. It was developed - in the late forties - as a result of the collaboration of D.H. Lee, an English engineer, and McCall's Macalloy Ltd., Sheffield.

The tensioning units vary in size from $\frac{1}{2}$ in. to $1\frac{1}{8}$ in. in diameter. These bars are of silicon/manganese alloy steel, and they are cold-worked over their full length. The cold-working, "McCall's Process", assures an ultimate strength of 145 k.s.i. and a 0.2% proof stress of 130 k.s.i.. During the cold-working process the bars are subjected to stresses which are well above the working stress.

The anchorage device consists essentially of a partially tapered, fine thread and a comparatively long nut. On the bar, the thread is of a normal (National Fine Series) type except that the last few threads are gradually increased in diameter to full bar diameter at the root. In the nut, there is also some normal type of thread, but the rest is correspondingly tapered. The threads in the tapered portion are not engaged under working loads (figure a, plate 1). They engage successively only when the stress on the last adjacent root is relatively high, and the load on the bar is approaching the ultimate.

This "high efficiency" nut will develop very nearly the full strength of the bar. However, the nut has to be seated in its proper spot on the bar if full advantage is to be taken of its "high efficiency".

The two important advantages of the Lee-McCall system are:

1. A single bar replaces many wires - with a resulting

labour saving.

2. The thread-and-nut anchorage virtually eliminates slippage.

The disadvantage that arises is that bar lengths and extensions must be accurately computed because the nut has to be in its proper spot if the desired high efficiency is to be obtained. Small adjustments are possible by shimming; split washers facilitate rapid shimming.

Tensioning is accomplished by means of a hydraulic jack that is specially adapted to screw onto a 4 in. long extension which is provided on the tensioning unit. It is not unusual to tension either from one end or from both ends. The jacks are often equipped with a scale and vernier for measuring bar extension, so that a much better indication of initial steel stress can be obtained than with a fluid pressure gage.

Earlier Work

A thesis entitled "An Investigation in Prestressed Concrete" was presented in 1951 by H.L. Reid, M.Sc. Two beams were designed and tested in that work. Six similar beams, with varying amounts of prestress, have been tested since then. All of these beams were prestressed with pre-tensioned and bonded wires.

The studies reported here have been conducted on beams of the same proportions, but unbonded, post-tensioned bars have been used.

FIGURE a

ENLARGED DETAIL OF LEE-McCALL THREAD AND H.E. NUT

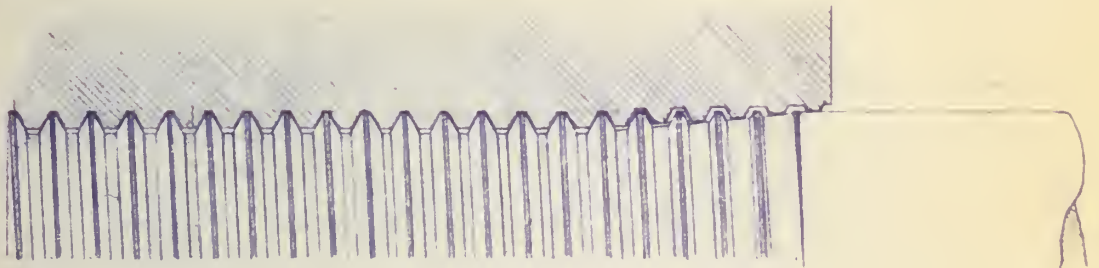
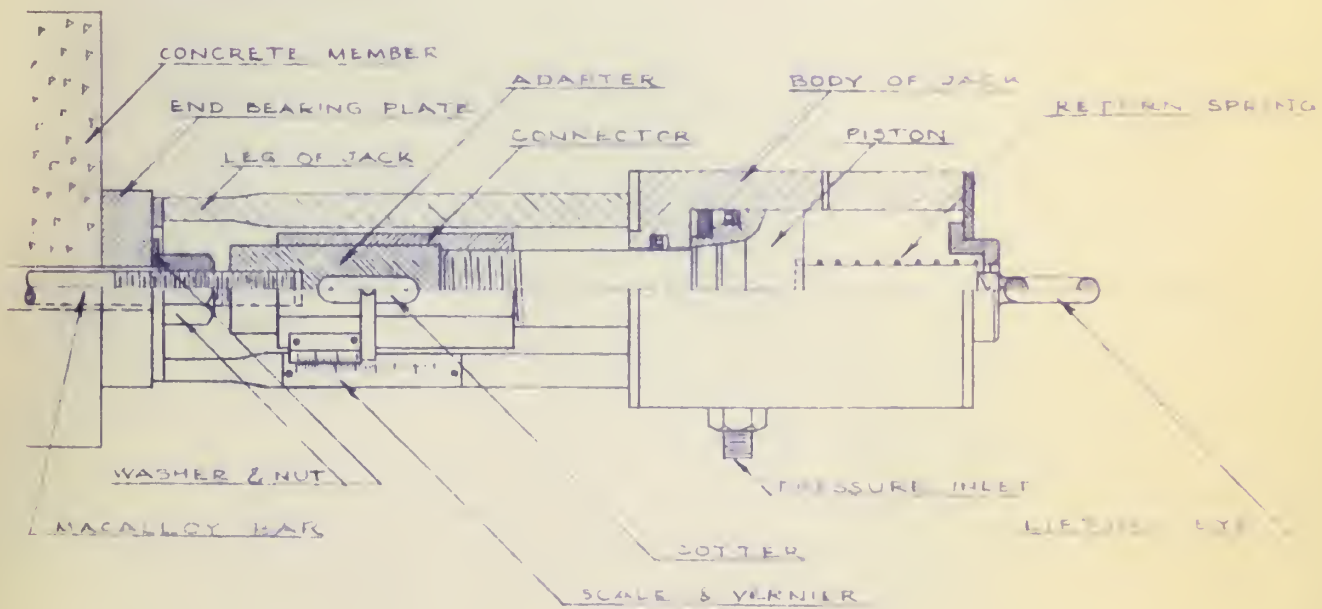


FIGURE b

DETAILS OF A LEE McCALL JACK



II SCOPE OF THE STUDIES

The primary aim of these studies was to obtain experimental data on the flexural behavior of prestressed concrete beams which utilize post-tensioned, unbonded reinforcement.

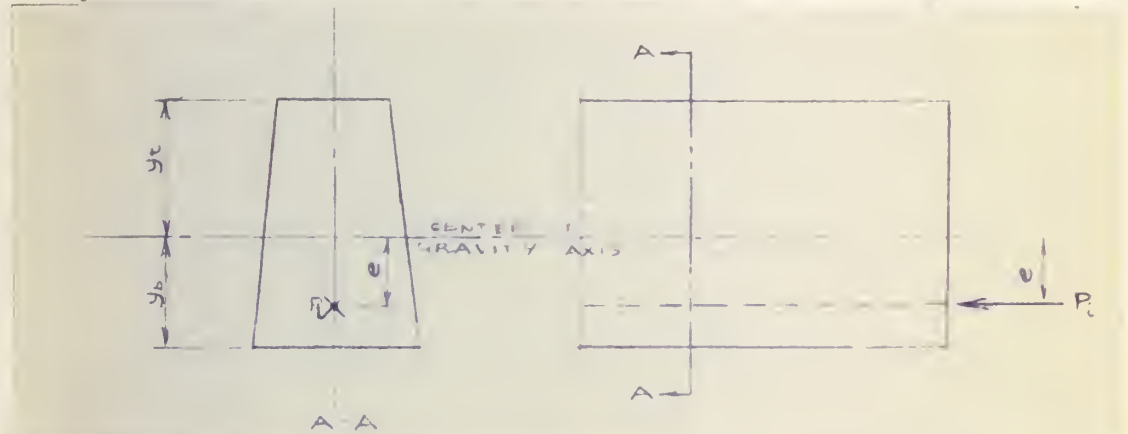
Six rectangular beams were designed, three with a percentage of steel of 0.0073, and three with a percentage of steel of 0.012. One beam from each group of three was constructed with a vertical joint in the concrete at midspan. The beams were post-tensioned with the patented Lee-McCall units.

The load-deflection characteristics, the steel strains, the cracking and failure loads, the axes about which sections rotated, the compressive strains in the concrete, and failure characteristics were observed when the beams were tested. Each beam was subjected to two cycles of loading.

III DESIGN THEORY

A prestressed concrete beam in its working range has no (or very small) tensile stresses. Thus the elastic theory for homogeneous sections will indicate flexural stresses with a reasonable degree of accuracy. The elastic design relationship that is commonly used is a form of the well known formula, $f = \frac{P}{A} \pm \frac{Pey}{I}$, for eccentrically loaded, homogeneous and elastic columns.

Consider a prismatic beam which has a section that is symmetrical about a vertical axis (in the figure below).



If the section, of net area A and of moment of inertia about the centre of gravity axis I_{cg} , is precompressed (as shown above) with a force of P_i , then the tensile stresses at the top and bottom fibres will be:

$$1. \text{ ----- } c_t = -\frac{P}{A} + \frac{P_i e y_t}{I}$$

$$\text{and } 2. \text{ ----- } -c_b = -\frac{P}{A} - \frac{P_i e y_b}{I}, \text{ respectively.}$$

Consider that the section is also subjected to a bending moment, M , which causes compressive stresses in the top fibre. Then the tensile stress at the top fibres will be:

$$3. \text{ ----- } c_t = -\frac{P_i}{A} + \frac{P_i e y_t}{I} - \frac{M y_t}{I}$$

If r is the radius of gyration of the section, then

$$4. \text{ ----- } c_t = \frac{P_i}{A} \left(\frac{ey_t}{r^2} - 1 \right) - \frac{My_t}{I}$$

The compressive stress in the bottom fibres will be:

$$5. \text{ ----- } c_b = \frac{P_i}{A} \left(\frac{ey_b}{r^2} + 1 \right) - \frac{My_b}{I}$$

Formulae 4 and 5 can be used to compute the flexural stresses in a prestressed concrete beam provided the beam has not cracked and the maximum compressive stresses fall on a reasonably elastic portion of the stress-strain curve.

During post-tensioning the effective area and the effective moment of inertia will be those for the concrete section alone. If then a bond is established between the steel and concrete by grouting, then I and A under loads applied after grouting are generally assumed to be those for the so-called transformed section which considers the effects of both the steel and the concrete. However, if a beam is left unbonded, it will act as a statically indeterminate (tied) structure when external loads are applied. It has been found from tests that the change in steel stress under working loads is small. Thus it is a common practice in computing working stresses in an unbonded beam to neglect the effect of the steel; the I and A which are effective during post-tensioning are used.

Shearing stresses for a prestressed concrete beam which has not cracked can be computed with the elastic relationship for homogeneous sections, viz. $v = \frac{VQ}{Ib}$, where v is the shearing stress at a fibre of distance y from

the centre of gravity axis, V is the shearing force at the section, I is the moment of inertia of the section about the centre of gravity axis, b is the width of the section at the fibre considered, and Q is the statical moment about the centre of gravity axis of that area either above or below the fibre considered.

IV DESIGN OF THE BEAM

1. Notation Used

- A, the cross-sectional area of the beam.
- A_s , the cross-sectional area of the steel.
- b, the width of the beam.
- c_b , the compressive stress in the extreme bottom fibre.
- c_t , the tensile stress in the extreme top fibre.
- c_{db} , the bottom fibre stress due to M_d .
- c_{dt} , the top fibre stress due to M_d .
- d, the effective depth - top fibre to the steel.
- e, the eccentricity of the prestressing force about the centre of gravity axis.
- f'_c the standard concrete cylinder strength.
- $f''_c = 0.85f'_c$.
- I_{cg} , moment of inertia about the centre of gravity axis.
- M_d , the bending moment due to w_d .
- M_{cr} , the bending moment that will cause cracking.
- n, the ratio $\frac{E_s}{E_c}$.
- P_i , the initial prestressing force.
- P_{cr} , the total load that will cause cracking (third point loading).
- r, radius of gyration of the beam section.
- w_d , the uniformly distributed dead load per unit length.
- \bar{y} , the distance to the centre of gravity axis from the mid-height axis.
- y_b , the distance to the extreme bottom fibre from the centre of gravity axis.
- y_t , the distance to the extreme top fibre from the centre of gravity axis.

2. Notation Used for the Test Beams

The code used to refer to the beams is as follows:

Beam U-1 is a beam with two bars and one of a single monolithic pour.

Beam U-2 is a beam with two bars and one of a single monolithic pour.

Beam O-1 is a beam with three bars and one of a single monolithic pour.

Beam O-2 is a beam with three bars and one of a single monolithic pour.

Beam U-S1 is a beam with two bars and one having a joint in the concrete at midspan.

Beam O-S1 is a beam with three bars and one having a joint in the concrete at midspan.

Details of the beams of types U and O are given in plate 2; of types U-S and O-S in plate 3.

3. Selection of the size and shape of beams

Prestressed concrete beams previously built and tested at the University have been of 10' - 0" span and 6" x 12" rectangular cross-section. In order to get a comparison with those beams, which utilized pretensioned wires, it was decided to retain the same size and shape of beam. It was found that this size of beam would give the desired percentages of steel when either two or three $\frac{1}{2}$ " ϕ Macalloy bars were used.

It should be noted that the design procedure here, where the size of section is selected first and the strength

is then computed, is the reverse of what it would be in a practical design problem, where the section is selected to meet a required strength.

4. Location of the Steel

It should be realized that the locations of the steel as shown in Plates 2 and 3 are not the only ones that would have been satisfactory. In choosing the locations which were used the following courses were adopted.

1. At midspan, the eccentricity of the steel was made as large as feasible in order to obtain the highest possible cracking load (and ultimate load). The tensile stress in the top fibre under the initial prestressing force was the governing factor.

2. Over the middle third, the eccentricity was maintained constant because the bending moment was to be constant in this region (1/3 point loading).

3. Over the supports, the centre of gravity of the steel was located within the kern of the section to avoid tensile stresses in the top fibres.

4. At the ends, the steel was located near mid-height to avoid anchoring the high prestressing forces near the bottom edge.

More practical factors were also considered. A minimum spacing of $3\frac{1}{2}$ in. was maintained between bars at the ends so that the standard jacking equipment could be used. To simplify construction the position of the bottom bars of Beam O was made the same as that of the bars in Beam U.

A trial and error process was employed -- a location was chosen for the steel; the stresses were then checked with formulas 4 and 5. The following computations, carried out for the section at midspan, illustrate how the stresses were checked.

Beam U (the beam with 2 bars, shown in plate 2)

Considering the midspan section, and assuming the cross-section area of a $\frac{1}{2}$ " ϕ bar wrapped with mastic and paper as 0.5 sq. ins., we have:

The net area of concrete, $A = 6(12) - 2(0.5) = 71$ sq. ins.

The position of the centre of gravity of the concrete alone,

$$\bar{y} = \frac{2(0.50) \times 3.5}{72 - 2(0.50)} = \frac{3.5}{71} = 0.049 \text{ in. above mid-height.}$$

The moment of inertia of the concrete section about its centre of gravity axis,

$$\begin{aligned} I_{cg} &= \frac{6 \times 12 \times 12 \times 12}{12} - 1 \times 3.5^2 - 71 \times 0.05^2 \\ &= 864 - 12.25 - 0.17 = 852 \text{ in}^4. \end{aligned}$$

and $r^2 = \frac{852}{71} = 12.0 \text{ in}^2$, where r is the corresponding radius of gyration.

Due to dead load, which is effective during post-tensioning, we have:

$$w_d = 75 \text{ lbs./ft.}$$

$$M_d = \frac{1}{8} \times 75 \times 100 \times 12 = 11,200 \text{ in. lbs.}$$

$$c_{dt} = c_{db} = \frac{11,200 \times 6}{852} = 80 \text{ p.s.i.}$$

If the steel rods are tensioned to 100 k.s.i. (the value recommended with the Lee-McCall system) the initial force in one rod will be:

$$P_i = \frac{\pi}{4} \left(\frac{1}{2}\right)^2 \times 100,000 = 19,600 \text{ lbs.}$$

Immediately after tensioning the concrete stresses at the midspan section will be:

$$c_t = \frac{P_i}{A} \left(\frac{ey_t}{r^2} - 1 \right) - c_{dt}$$

$$= \frac{2 \times 19,600}{71} \left(\frac{3.55 \times 5.95}{12} - 1 \right) - 80 = 340 \text{ p.s.i.}$$

(tension).

$$\text{and } c_b = \frac{P_i}{A} \left(\frac{ey_b}{r^2} + 1 \right) - c_{dt}$$

$$= \frac{2 \times 19,600}{71} \left(\frac{3.55 \times 5.95}{12} + 1 \right) - 80 = 1,460 \text{ p.s.i.}$$

(compression).

Since shrinkage cracks in these short beams were highly unlikely, it was thought that the concrete could safely carry 400 to 500 p.s.i. of tension at the topmost fibre. The 1,460 p.s.i. of compression stress is only $\left(\frac{1,460}{5,000} = \right) 0.29f'_c$ and quite permissible.

These stresses will be nearly the same over the middle third of the beam. As the bars are raised towards the ends, c_t will change to a compression stress and c_b will decrease till $c_t = c_b = \frac{39,200}{71} = 550 \text{ p.s.i.}$ when the steel is at mid-height.

Beam O (the beam with 3 bars, shown in plate 2)

Following the same procedure as with Beam U we get:

$$A = 6 \times 12 - 3 \times 0.5 = 70.5 \text{ sq. ins.}$$

$$\bar{y} = \frac{3 \times 0.5 \times 2.83}{70.5} = 0.06 \text{ ins. (above mid-height).}$$

$$I_{cg} = \frac{6 \times 12 \times 12 \times 12}{12} - 1.5 \times 2.83^2 - 70.5 \times 0.06^2$$

$$= 852 \text{ in}^4.$$

$$r^2 = 12.1 \text{ in}^2.$$

Thus, immediately after tensioning

$$\begin{aligned}c_t &= \frac{3 \times 19,600}{70.5} \left(\frac{2.89 \times 6.06}{12.1} - 1 \right) - 80 \\&= 270 \text{ p.s.i. (tension)} \\c_b &= \frac{3 \times 19,600}{70.5} \left(\frac{2.89 \times 6.06}{12.1} + 1 \right) - 80 \\&= 1,970 \text{ p.s.i. (compression).}\end{aligned}$$

These stresses, too, are permissible.

Beam U-S (the beam with 2 bars and a joint in the concrete, shown in plate 3)

Following the same procedure we have:

$$\begin{aligned}A &= 2 \times 12 - 3 \times 0.5 = 70.5 \text{ sq. ins.} \\ \bar{y} &= \frac{2.25^2}{71} = 0.03 \text{ ins.} \\ I_{cg} &= 864 - 2.25^2 - 71 \times 0.03^2 = 859 \text{ in}^4. \\ r^2 &= \frac{859}{71} = 12.1 \text{ in}^2.\end{aligned}$$

Immediately after prestressing:

$$\begin{aligned}c_t &= \frac{2 \times 19,600}{71} \frac{2.28 \times 5.97}{12.1} - 1) - 80 \\&= -10 \text{ p.s.i. (tension)} \\c_b &= \frac{2 \times 19,600}{71} \left(\frac{2.28 \times 6.03}{12.1} + 1 \right) - 80 \\&= 1,100 \text{ p.s.i. (compression).}\end{aligned}$$

Because of the intentional separation at midspan, it was not feasible to permit tension anywhere in this section.

Beam O-S (the beam with 3 bars and a joint in the concrete, shown in plate 3)

Doing similarly for this beam:

$$\begin{aligned}A &= 70.5 \text{ sq. ins.} \\ \bar{y} &= \frac{1.5 \times 2}{70.5} = 0.04 \text{ ins.} \\ I_{cg} &= 864 - 1.5 \times 2^2 - 70.5 \times 0.04^2 = 858 \text{ in}^4.\end{aligned}$$

$$\begin{aligned}
c_t &= \frac{3 \times 19,600}{70.5} \left(\frac{2.04 \times 5.96}{12.2} - 1 \right) - 80 \\
&= -100 \text{ p.s.i. (tension)} \\
&= 100 \text{ p.s.i. (compression)} \\
c_b &= \frac{3 \times 19,600}{70.5} \left(\frac{2.04 \times 6.04}{12.2} + 1 \right) - 80 \\
&= 1,600 \text{ p.s.i. (compression)}.
\end{aligned}$$

Here again there was a separation at midspan and no tension was permissible.

It was decided to bend the bars in parabolic shapes because the relatively large size of the bars made long radius bends necessary and because the parabolic shape is easily calculated.

5. Estimation of Cracking Loads

The cracking loads were estimated to be as follows: 15.5 kips for Beam U, 19 kips for Beam O, 13.2 kips for Beam U-S, and 16.7 kips for Beam O-S. These computations were based on an assumed ultimate tensile strength of 750 p.s.i. ($0.15f_c'$) for the concrete. The section properties computed as in part 3 and formula 5 were used. The computations for Beam U follow:

from part 3:

$$I_{cg} = 852 \text{ in}^4.$$

$$y_b = 6.05 \text{ ins.}$$

For cracking to occur the bottom fibre stress has to change by:
 $750 + 1,450 = 2,200 \text{ p.s.i.}$

No loss of prestressing force has been assumed because it will be smaller (in the short period before the beam is tested) than the accuracy to which the prestressing can be established.

If M_{cr} is the cracking moment,

$$M_{cr} = \frac{2,200 \times 852}{12 \times 6.05} \text{ ft. lbs.}$$

$$= 25.8 \text{ ft. kips.}$$

Since "third point" loading will be used, the cracking load

$$\text{is } P_{cr} = \frac{M_{cr}}{10} \times 3 \times 2 = 15.5 \text{ kips.}$$

6. Shearing stresses

At the ends of prestressed beams, shear is not usually a governing factor because there is seldom enough bending moment to cause cracking - thus the whole section is available to resist shearing forces. Where cracking does occur the shearing stresses are concentrated on a smaller area of section. They could therefore be critical, especially in regions of combined high shearing forces and high bending moments. A region of such combined high forces and high moments does exist with the beams that were tested here, but previous tests have shown that shearing stresses are not critical with beams of this particular size and shape.

The diagonal tension stresses (resulting from the combined direct and shearing stresses) in prestressed concrete beams are very considerably reduced by the initial longitudinal compression.

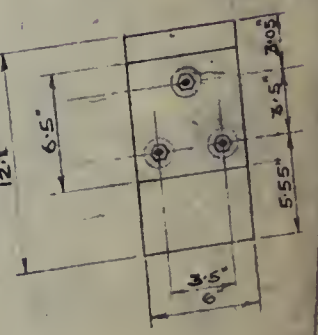
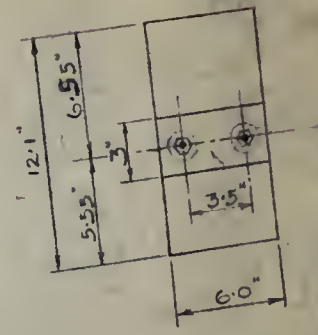
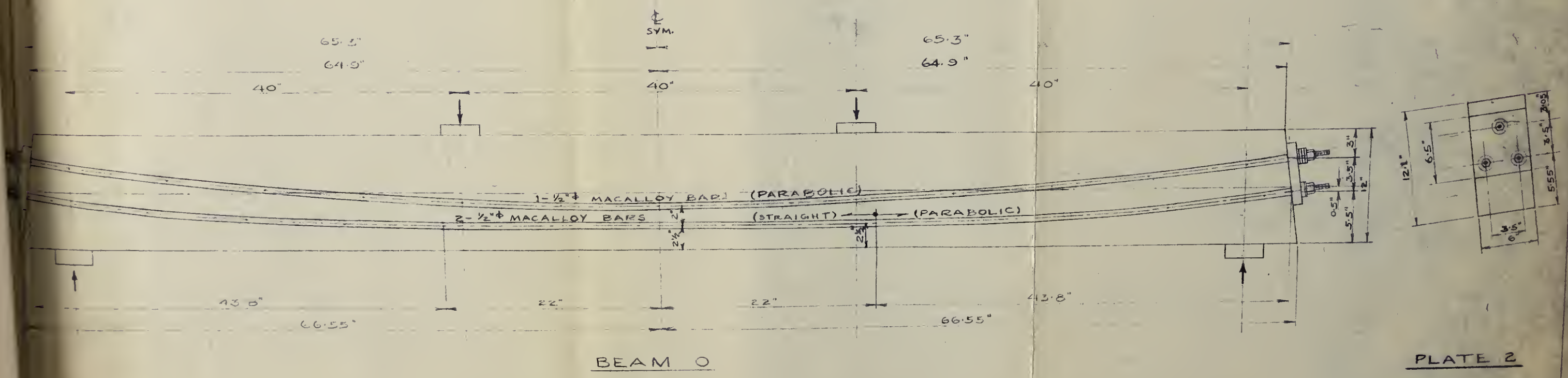
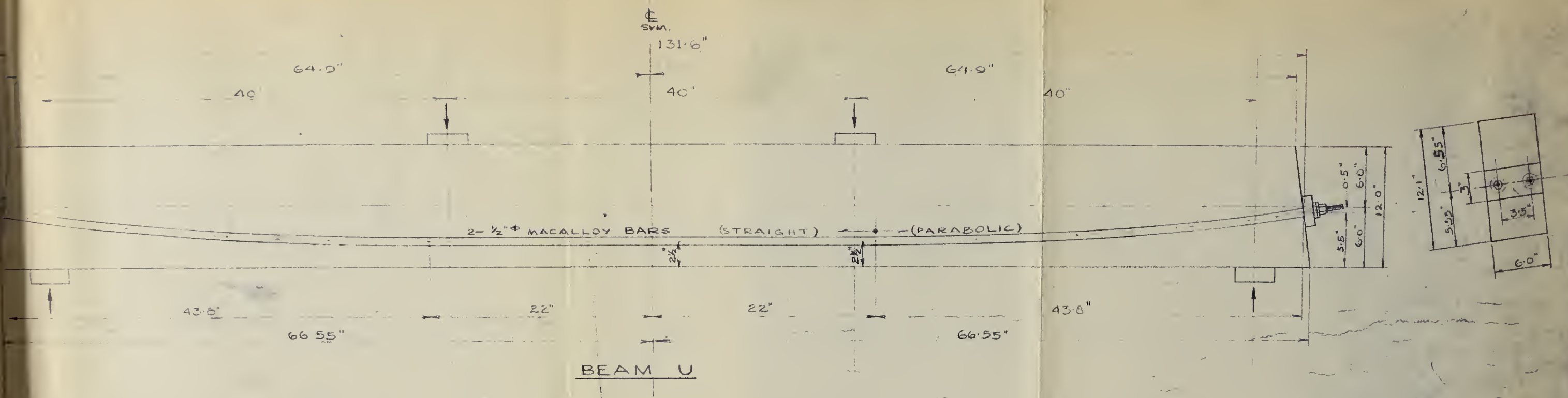


PLATE 2

SCALE: 1/10 SIZE

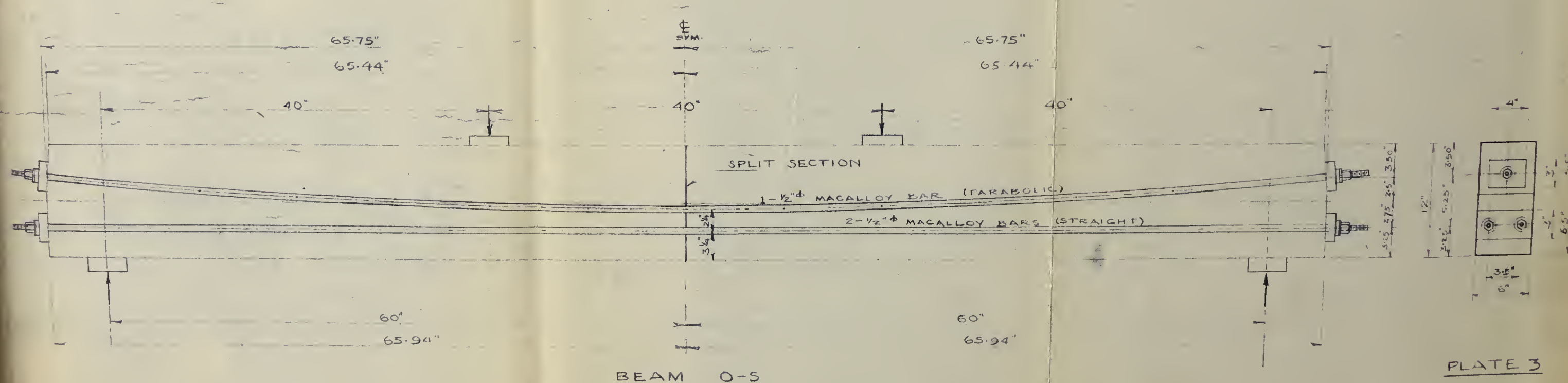
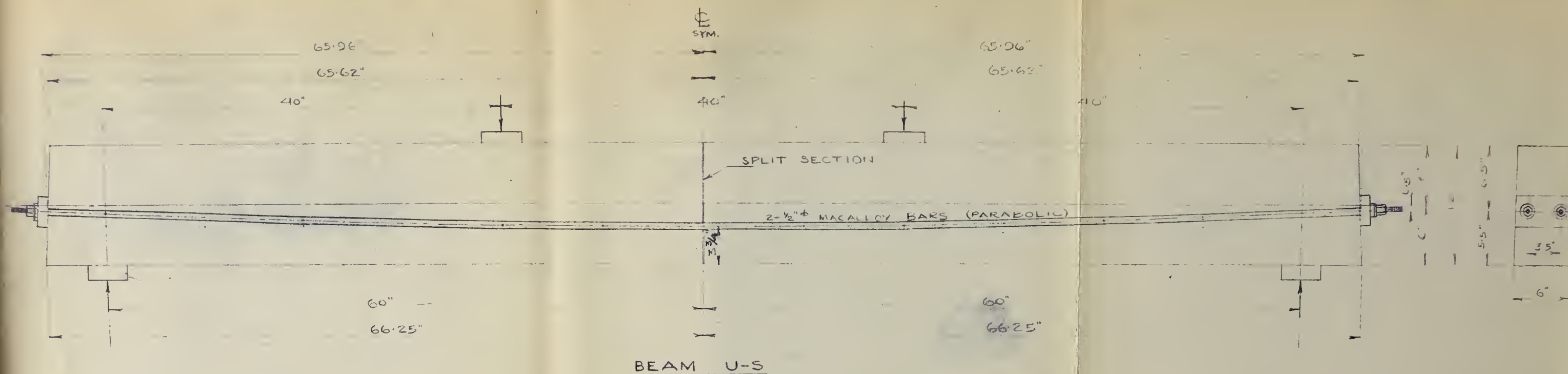


PLATE 3

SCALE: $\frac{1}{10}$ SIZE

V EXPERIMENTAL PROCEDURES

A. Materials Used

Concrete--- The concrete was designed to give a 28 day standard cylinder strength of 5200 p.s.i. and a 3 in. slump. It employed 3/4 in. rounded aggregate, Elk Island Sand, and Portland Cement.

Steel--- Prestressing was accomplished with Lee-McCall tensioning units which had been supplied by the Stressteel Corporation. The bars were $\frac{1}{2}$ in. in diameter and measured 11' - 2" between the inside faces of the nuts.

B. Instrumentation Used

Steel strains were measured, at approximately the midpoint of each bar, with SR-4, Type A-3, Baldwin - Southwark electric gauges. The recording instrument was a Baldwin Type L Strain Indicator.

The deformation of the centre 12 in. of the beam was observed by means of two sliding jigs which were fitted with Ames dials and attached to the beam three inches above its top face and three inches below its bottom face. This apparatus, henceforth referred to as the extensometers, is illustrated in Plate 60, Appendix B. The concrete strains and the axis about which sections rotated were computed from these extensometer readings by assuming Bernoulli's Hypothesis.

C. Construction of the Beams

Preparation of Bars--- As the bars were to be unbonded, they were first coated with a 1/8 inch thick layer

of mastic (Barrett's Plastic-Elastigum) and then wrapped with a heavy building paper.

Preparations for Instrumentation--- Near the centre of each bar a gauge point, consisting of two SR-4, Type A-3 electric strain gauges was established. The gauges, after they had been applied according to Baldwin-Southwark instructions, were waterproofed with three thin layers of Petrolastic Asphalt. Plastic coated wire leads were used. Furthermore, the gauge point was encased in mastic and protected on top by a metal shield (see figure c, plate 4) which also formed a cavity in the concrete so that the gauge point could safely move $1/8$ in. upwards and $5/16$ in. longitudinally when the bar was tensioned.

There were provided 4 - $7/16$ in. diameter by 20 in. long bars to which the extensometers (discussed in Appendix B) could be fastened. Figure 4 illustrates the manner in which these rods were placed.

Forming--- Figures 3 and 4 depict the forming techniques that were employed. Plywood forms were used, and $1/4$ in. diameter form ties held the tensioning rods in their proper locations. The form ties were well greased so that they could be removed when the concrete had set.

The metal division which formed the split section in Beams U-S and O-S was well greased to avoid any bond.

Placing of Concrete--- Each beam was completely poured over a period of one hour. No mechanical vibration was used. One standard cylinder was taken from each of the four batches of concrete required for a single beam.

Curing of Beams--- From the day after they were poured till the day before they were tested, the beams were kept continually wet by means of a weeping hose (made of untreated canvas) that had been placed along the tops of the beams. All bare lead wires had to be carefully waterproofed to avoid damage to the electric gauges.

D. Post-Tensioning of the Beams

The post-tensioning procedure and the standard Stressteel equipment that was used are illustrated in figure 6. Tensioning was carried out from one end only. In beams with three bars the centre bar was tensioned first. In beams with only two bars, the bars were brought to the desired stress in two stages in order to avoid the high tensile stresses which would have resulted in one of the top corners of the beam had the bar on the opposite side been stressed to 100 k.s.i. in one stage.

The thickness of washers that was required with each bar was determined as follows:

1. The bar was pulled to the desired stress.
2. The nut was seated in its proper position -- that is moderately wrench tight.
3. The distance between the nut and the anchor plate was measured.

An appropriate number of split shimming washers was then inserted between the anchor plate and the nut.

E. Testing Procedures

The testing apparatus is illustrated in Plate 4,

figure d. The following testing procedure was used.

1. Each beam was loaded to its cracking load in 1 kip increments.
2. It was then unloaded in two steps.
3. It was allowed to stand without load for 1 hour.
4. It was then loaded to 15 kips, in 3 increments.
5. Finally, it was loaded to failure in 1 kip increments.

Beam U-1 was subjected to 3 such cycles of loading-the 2nd cycle was up to 20 kips.

Before the test and after each increment of load, the following data was observed:

1. The deflection of the mid-point - with an Ames dial.
2. The deflections of the third-points - with Ames dials.
3. The steel strains in all bars - with electric gauges.
4. The extensometer readings - details of the extensometers are given in appendix B.

All readings were taken when the beam had reached a steady-state under the particular load.

In the case of Beam U-1, steel strains could not be obtained because the electric gauges had been short-circuited during pouring, and extensometer readings were obtained only during the 3rd cycle because of mechanical difficulties.

In each beam one SR-4 gauge was singled out and "followed to failure". With Beam U-2 it was also possible

to obtain extensometer readings while the beam was sustaining its ultimate load.

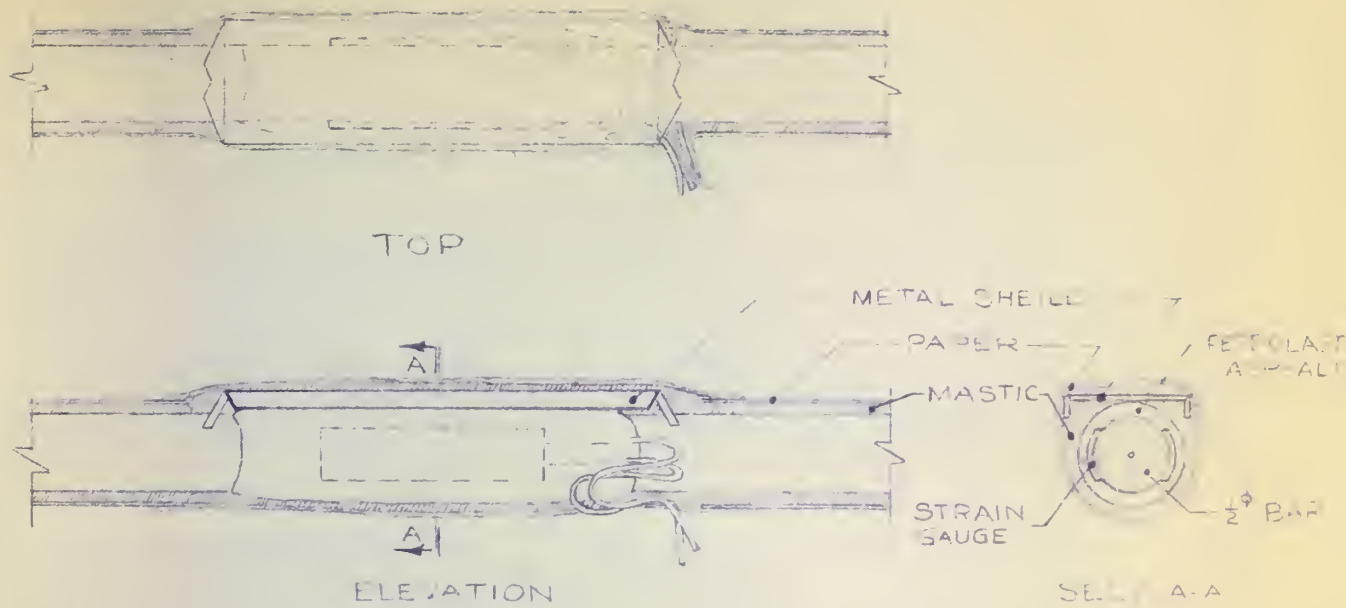


FIG. DETAIL OF GAUGE POINT

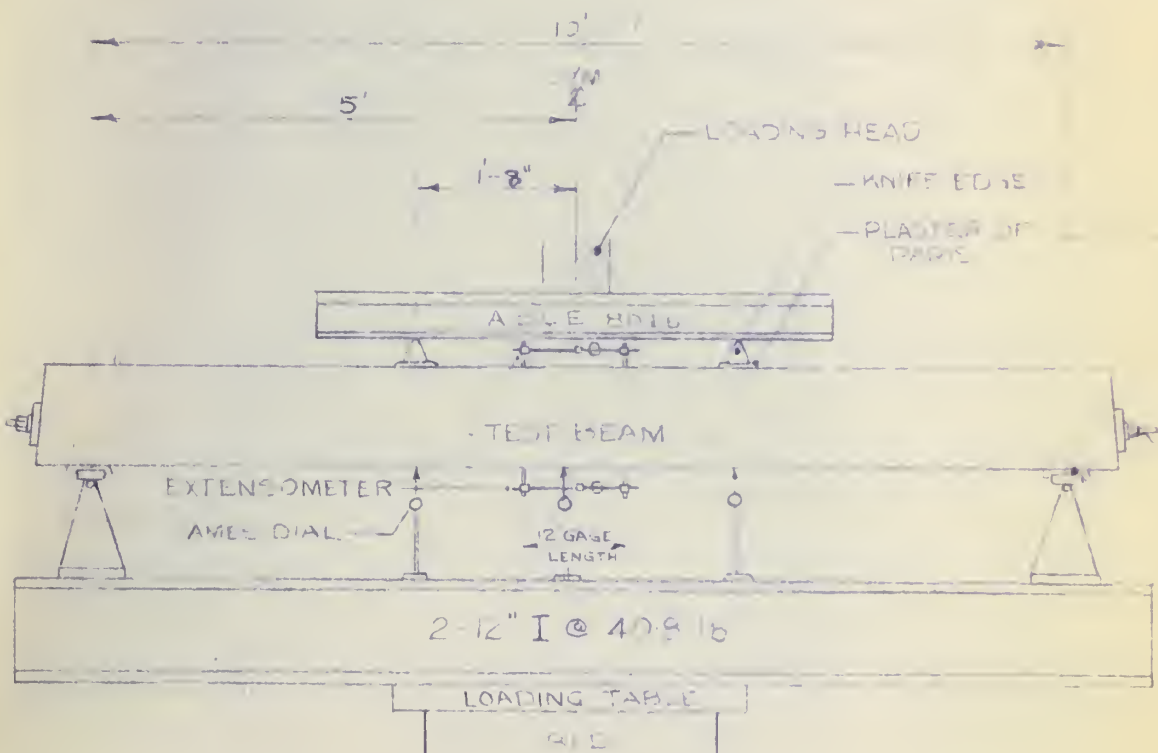


FIG TESTING APPARATUS



Figure 3. (above)

Side view of the forms
- showing how the bars
were held in place.

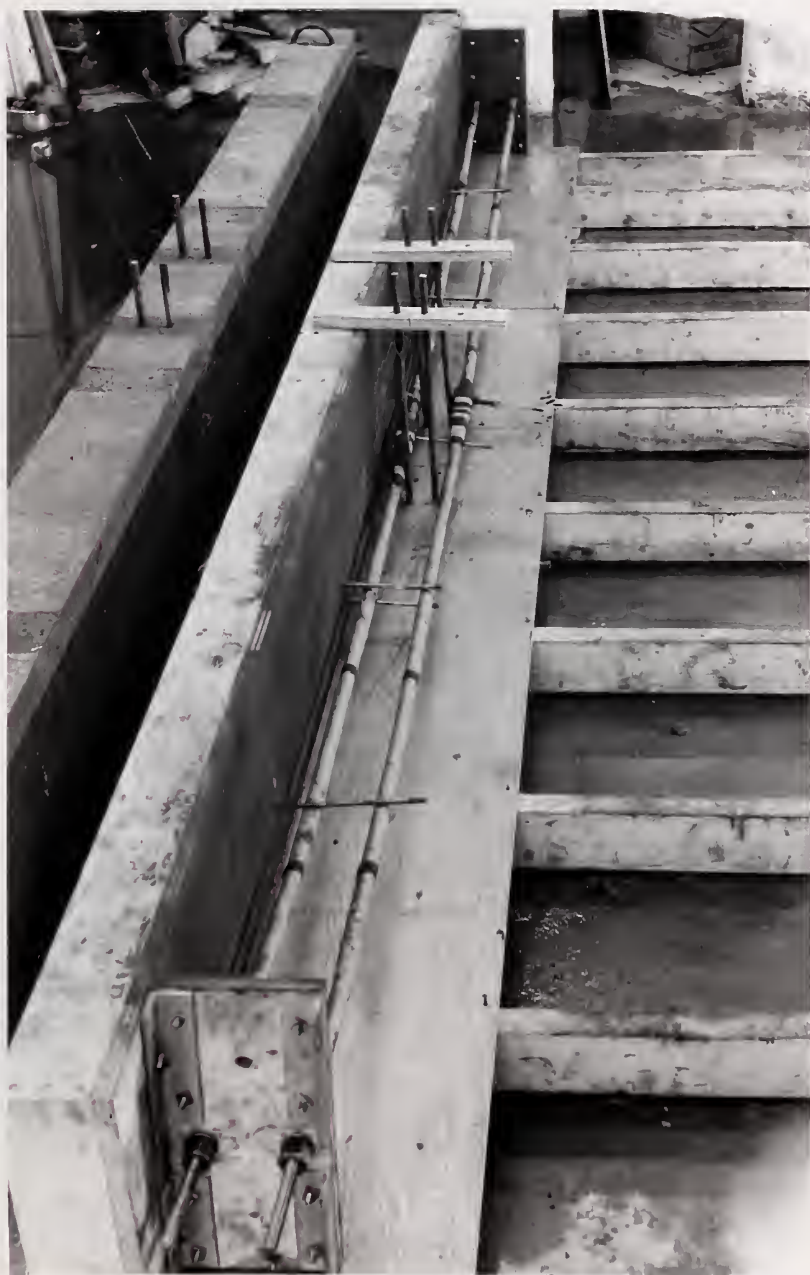


Figure 4. (left)

End view of the forms.



Figure 5. Various stages in preparation of the bars.



Figure 6. Typical post-tensioning procedure.

VI PRESENTATION OF RESULTS

Plates 5 to 22 inclusive, show the Load-Deflection curves for the six beams which were tested. Deflections at midspan and those under both load points have been plotted against the total applied load. It should be noted that the term "cycle" has been used to refer to the loading stage of the loading-unloading cycle. Since the loading stages of the first cycles invariably plotted very close to the loading stages of the second cycles it was decided not to differentiate between points obtained during loading and those obtained during unloading. Further, only the points that fell outside the thickness of the curve are shown.

Plates 23 to 34 inclusive, illustrate graphically the extensometer readings which were observed when the beams were tested. It should be remembered that the extensometers were:

1. located at midspan
2. placed 3 inches above and below the top and bottom faces, respectively, of the beam.
3. measuring strain over a gauge length of twelve inches.

Plates 35 to 40 inclusive depict the mean positions of the axes about which rotation of sections occurred during each 2 kip increment of loading. These positions have been computed from the extensometer readings on the basis that plane sections before bending remain plane after bending*.

* which fact is well substantiated by Hognestad's work, see reference 7.

The computed compressive strains in the top concrete fibre at midspan are shown in Plates 41 to 46 inclusive. These computations too were based on the assumption that plane sections remain plane.

Plates 47 to 51 inclusive, show the Steel Strain vs. Load curves for five of the beams. Such data was not obtained from Beam U-1 because the electric gauges in that beam had been damaged during the pouring process. These curves were converted to Steel Stress-Load curves, Plates 52 to 56 inclusive, by using the stress-strain curve given in Plate 59, Appendix A.

Other data, including concrete strengths, cracking loads, ultimate loads, etc., is presented in Table II.

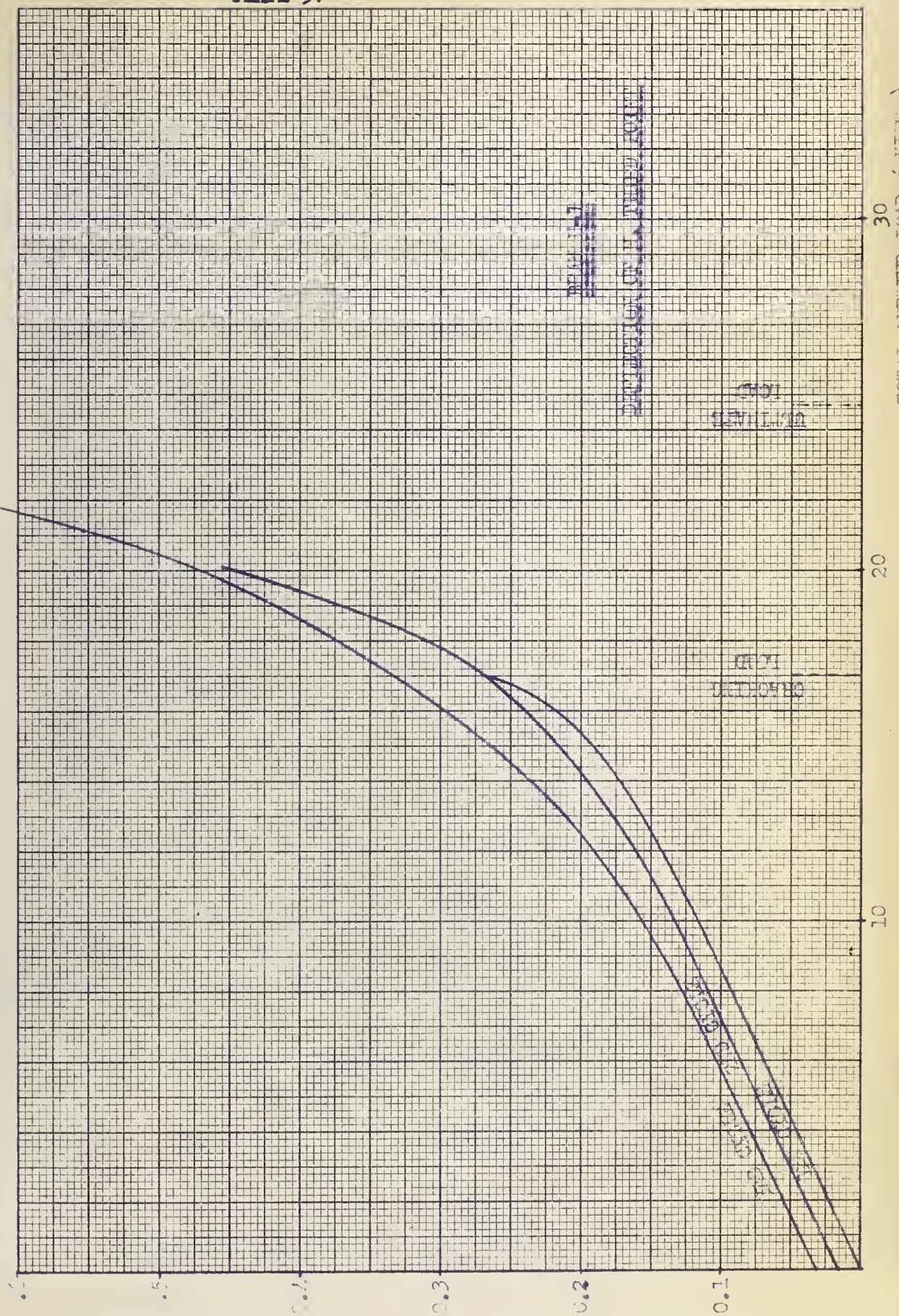


PLATE 6.

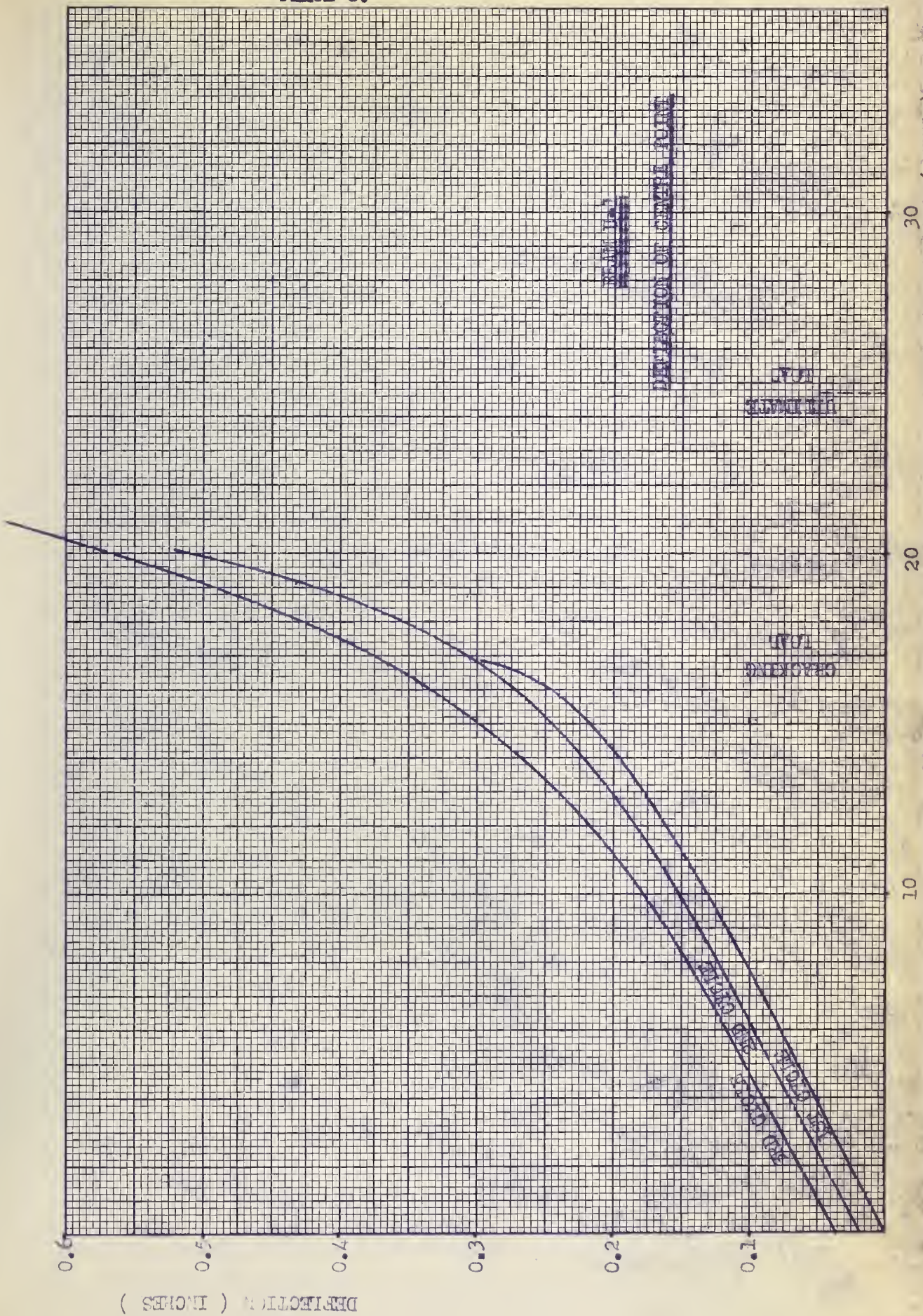


PLATE 7.

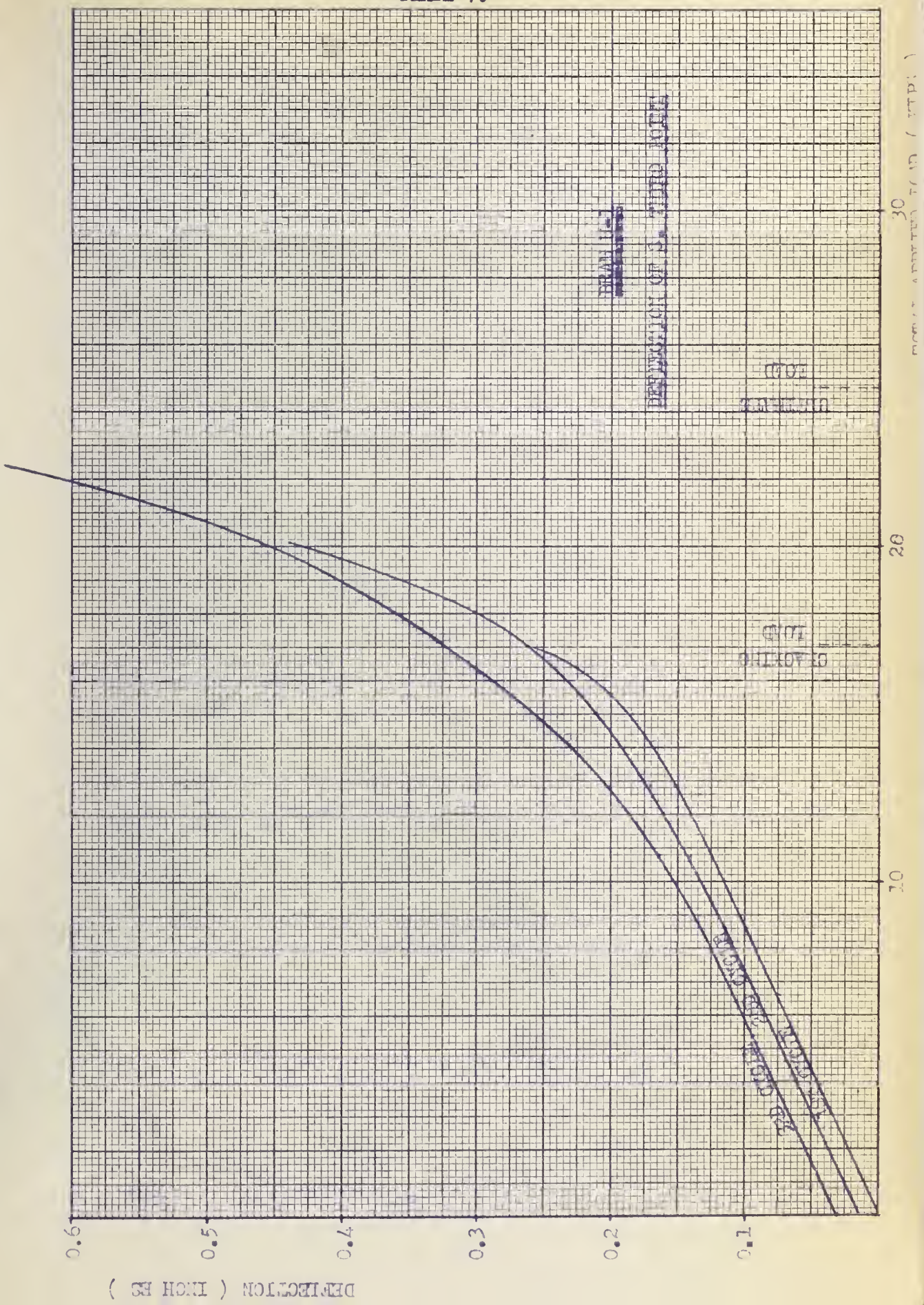


PLATE 8.

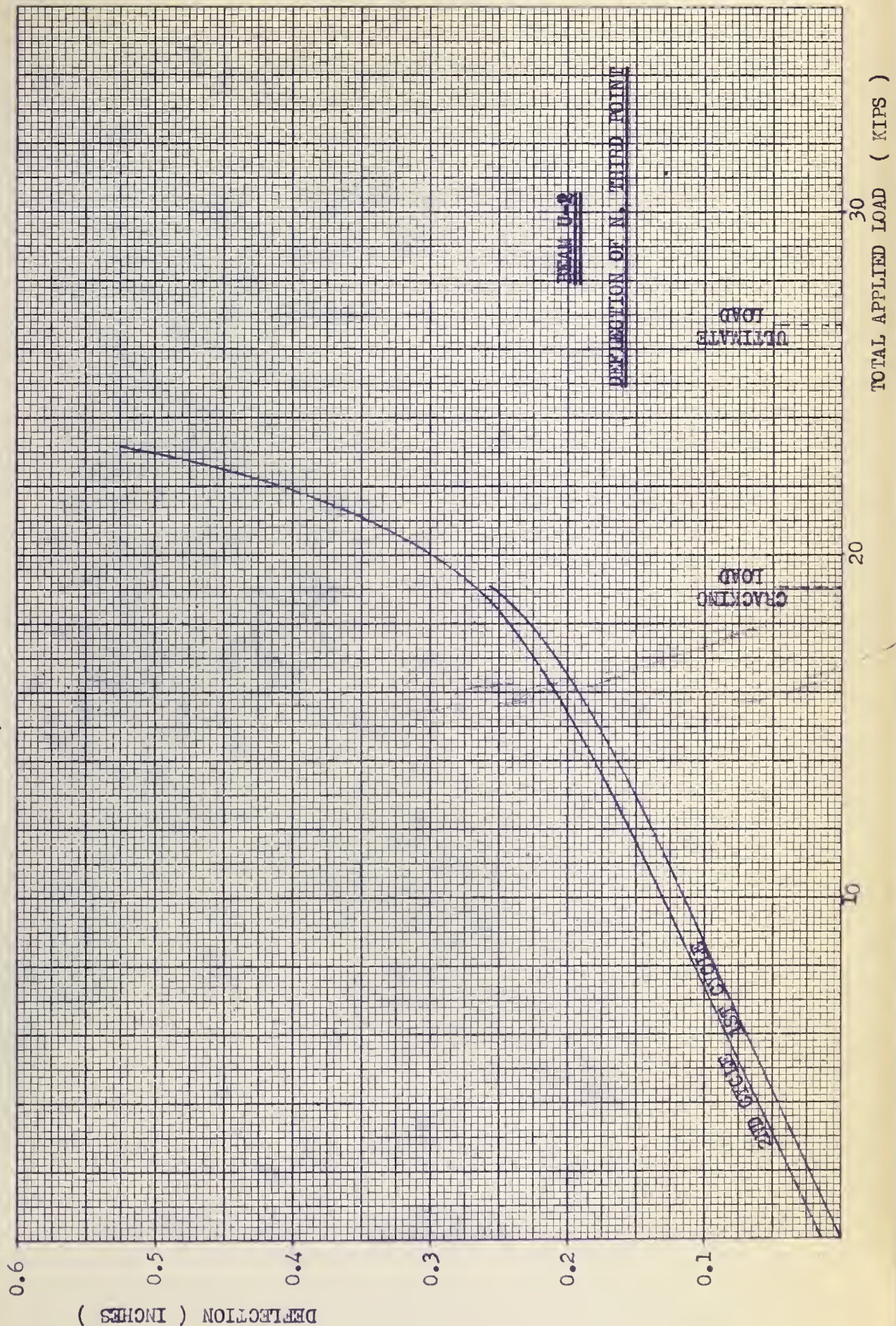
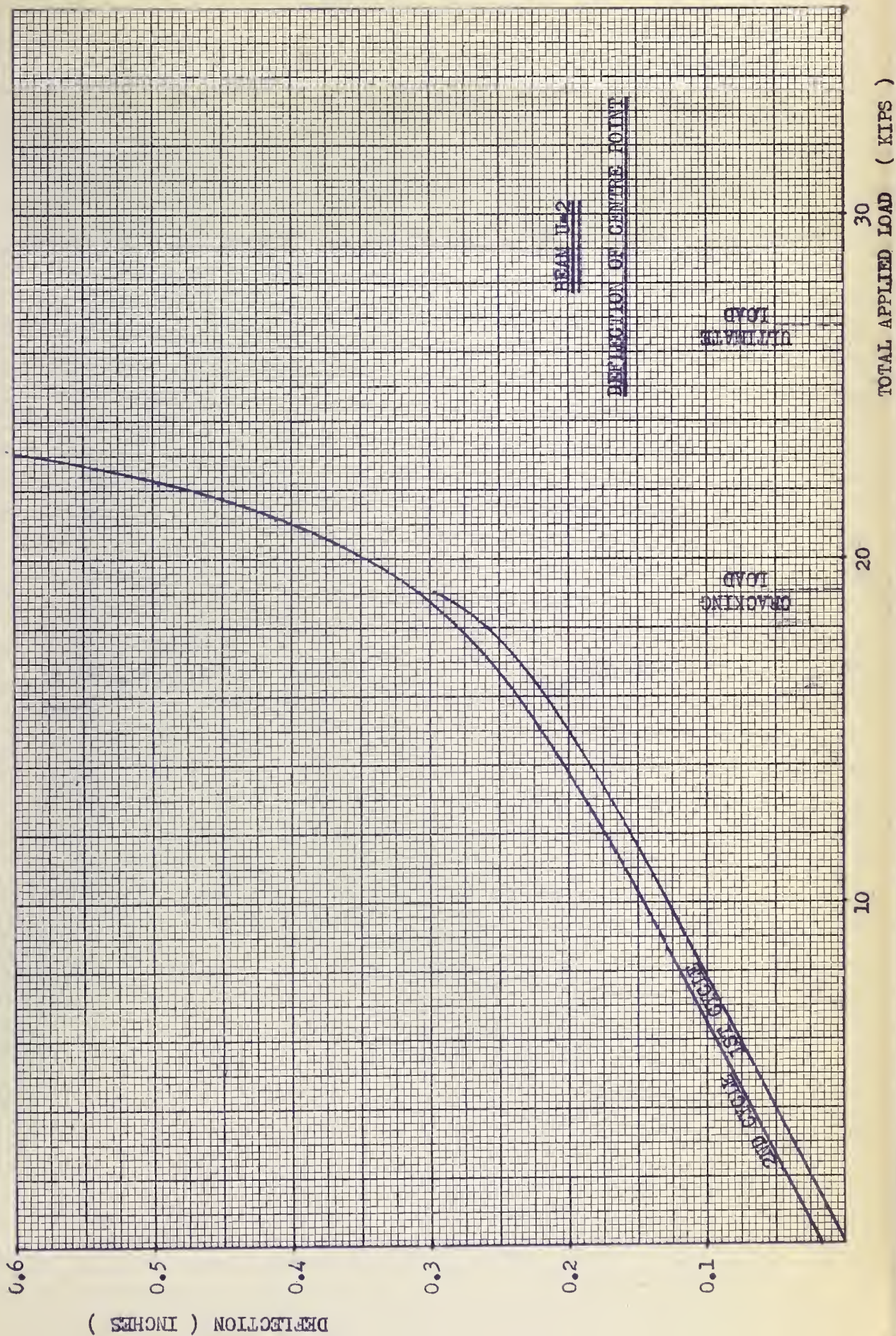


PLATE 9.



TOTAL APPLIED LOAD (KIPS)

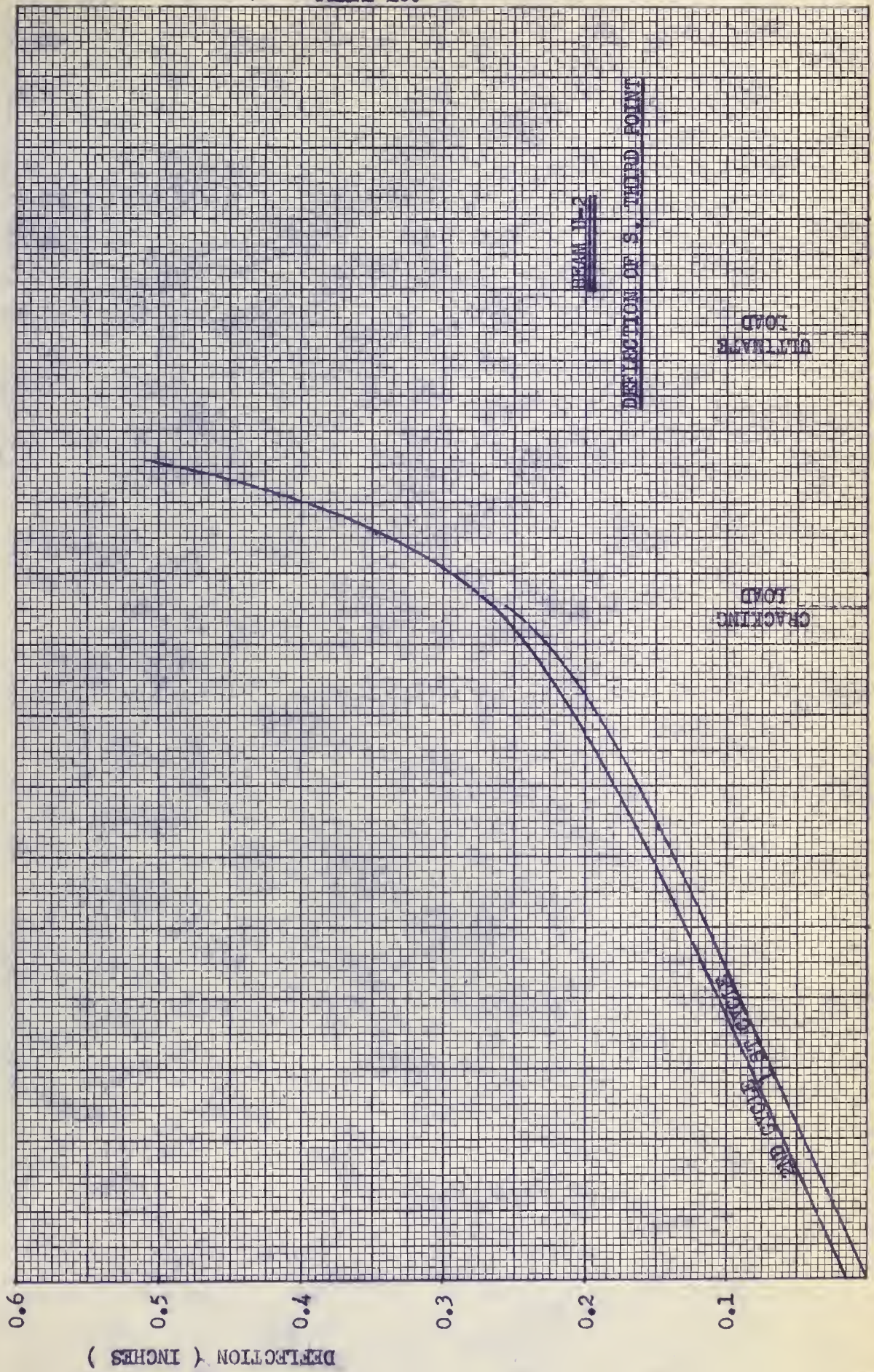
20

10

30

34

PLATE 10.



BEAM ID-2

DEFLECTION OF S. THIRD POINT

CRACKING
LOAD

ULTIMATE
LOAD

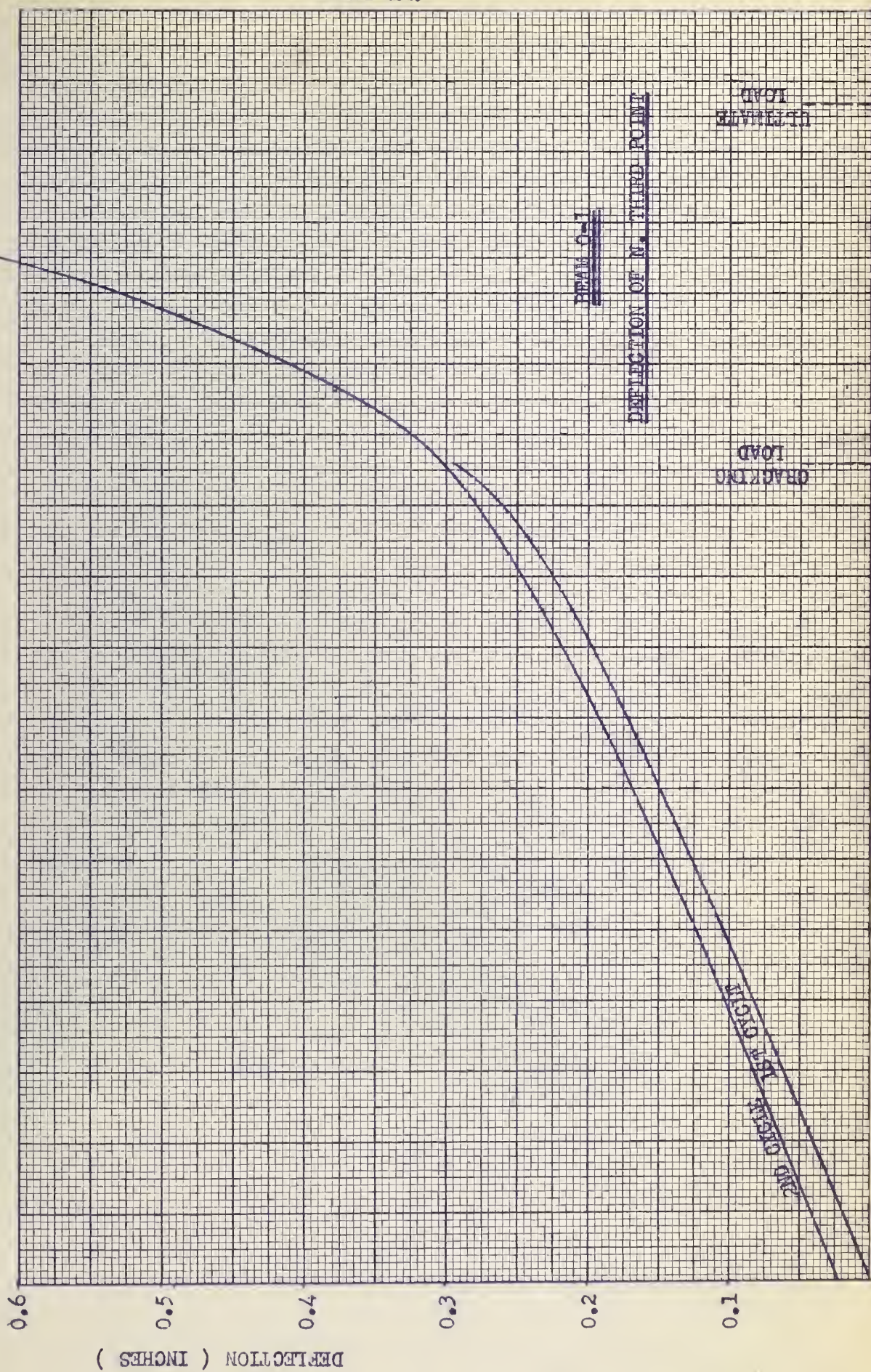
10

20

30

TOTAL APPLIED LOAD (KIPTS)

PLATE 11.



TOTAL APPLIED LOAD (WT)

20

10

30

PLATE 12 .

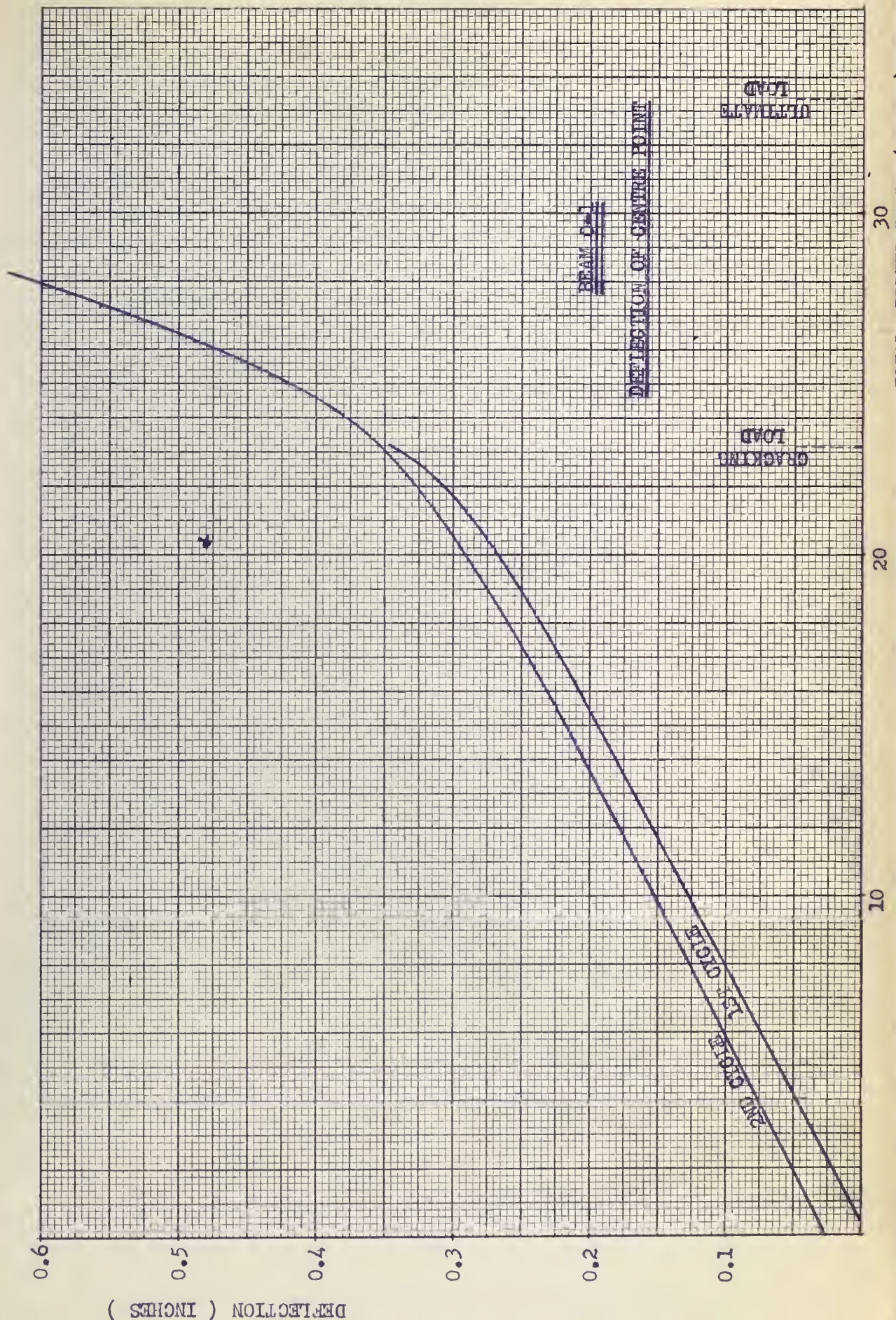


PLATE 13.

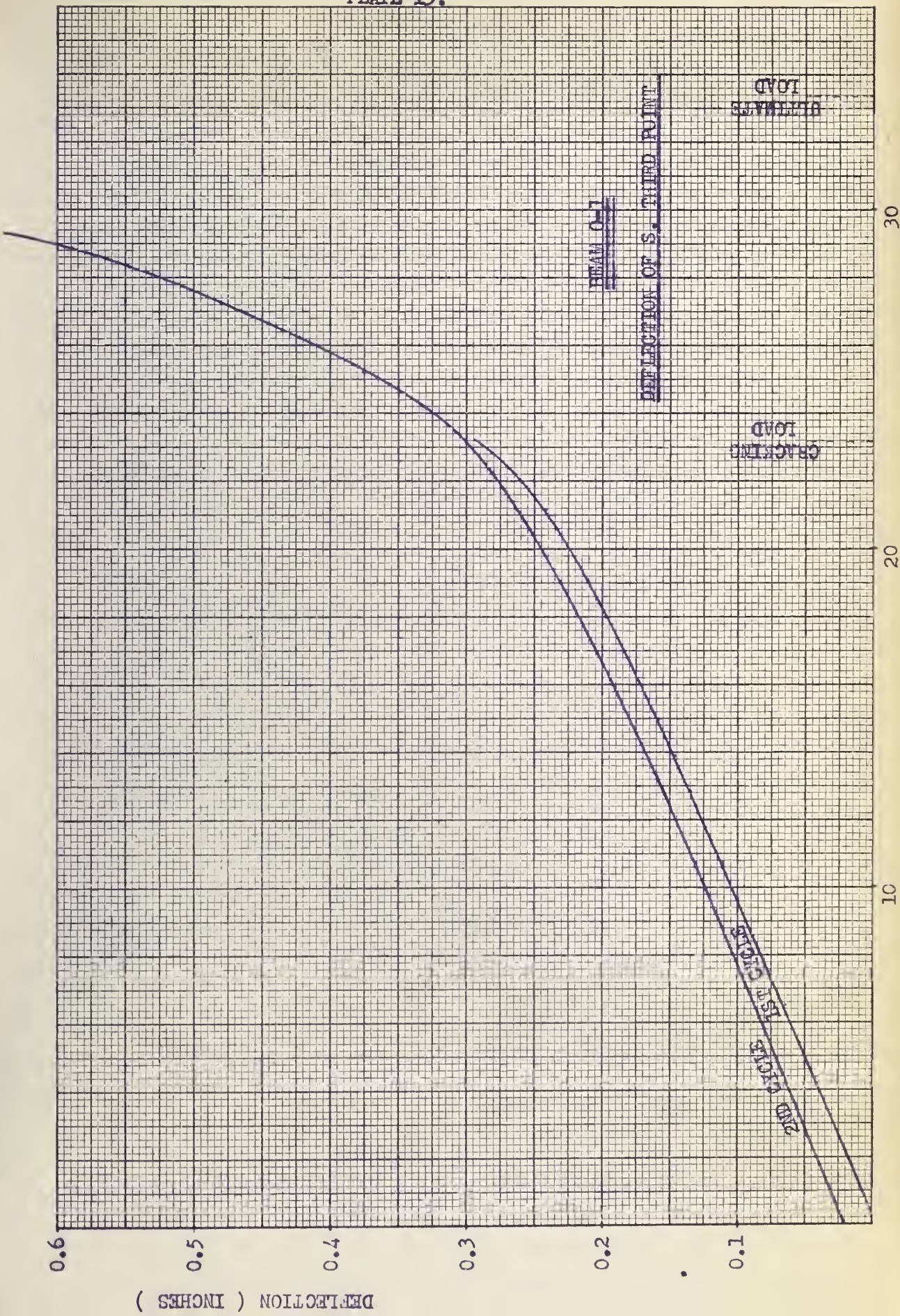


PLATE 14.

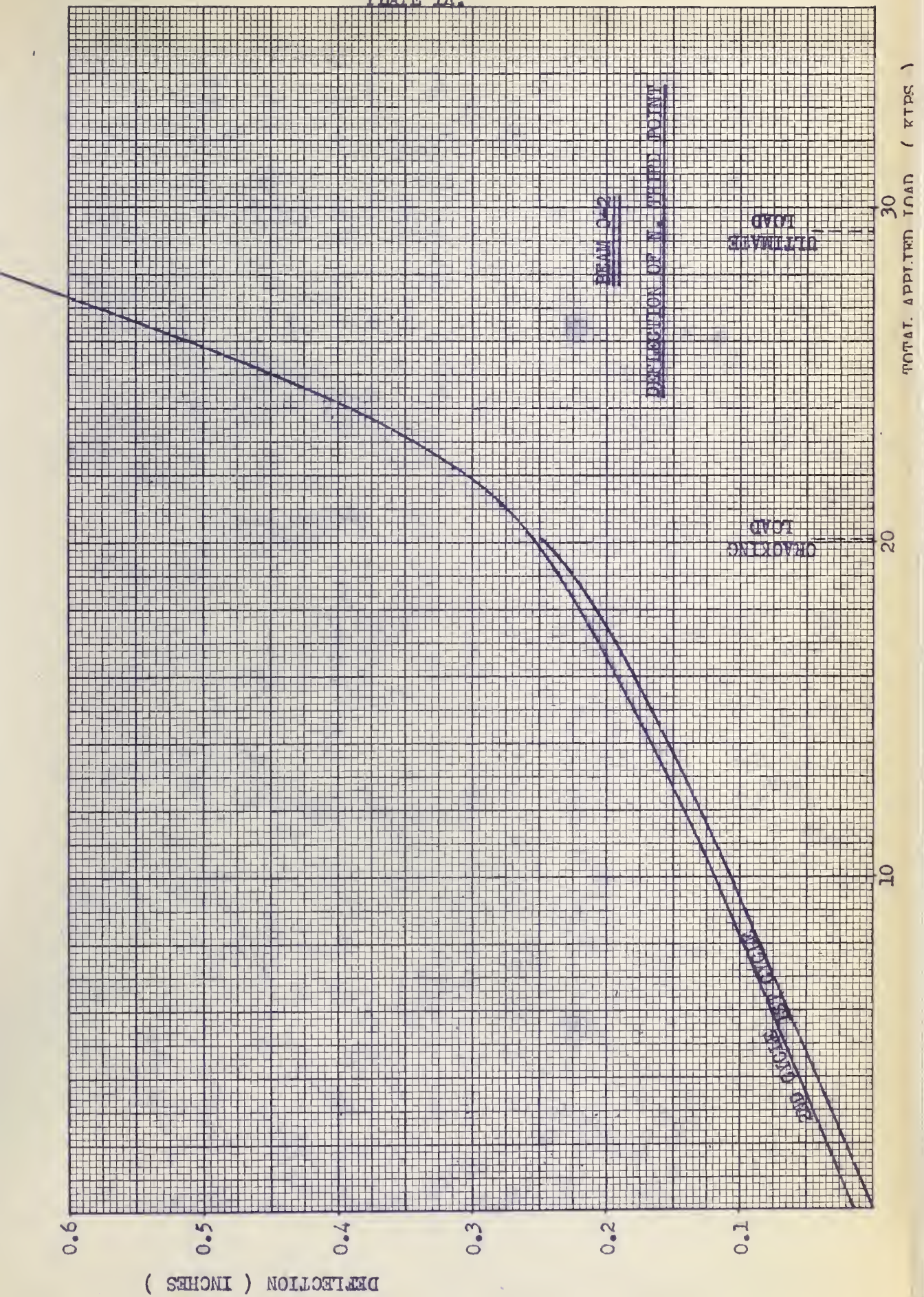


PLATE 15.

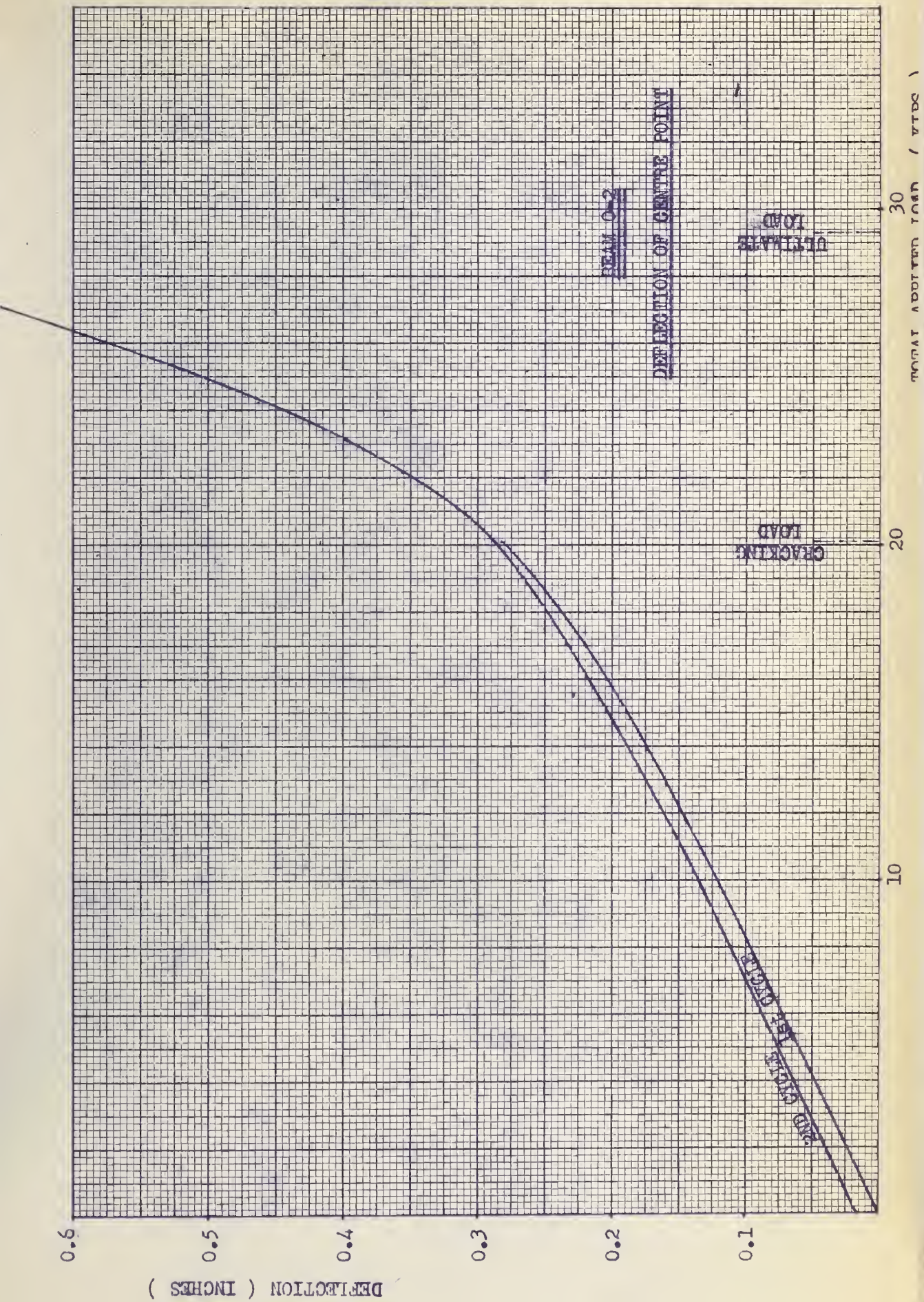


PLATE 16.

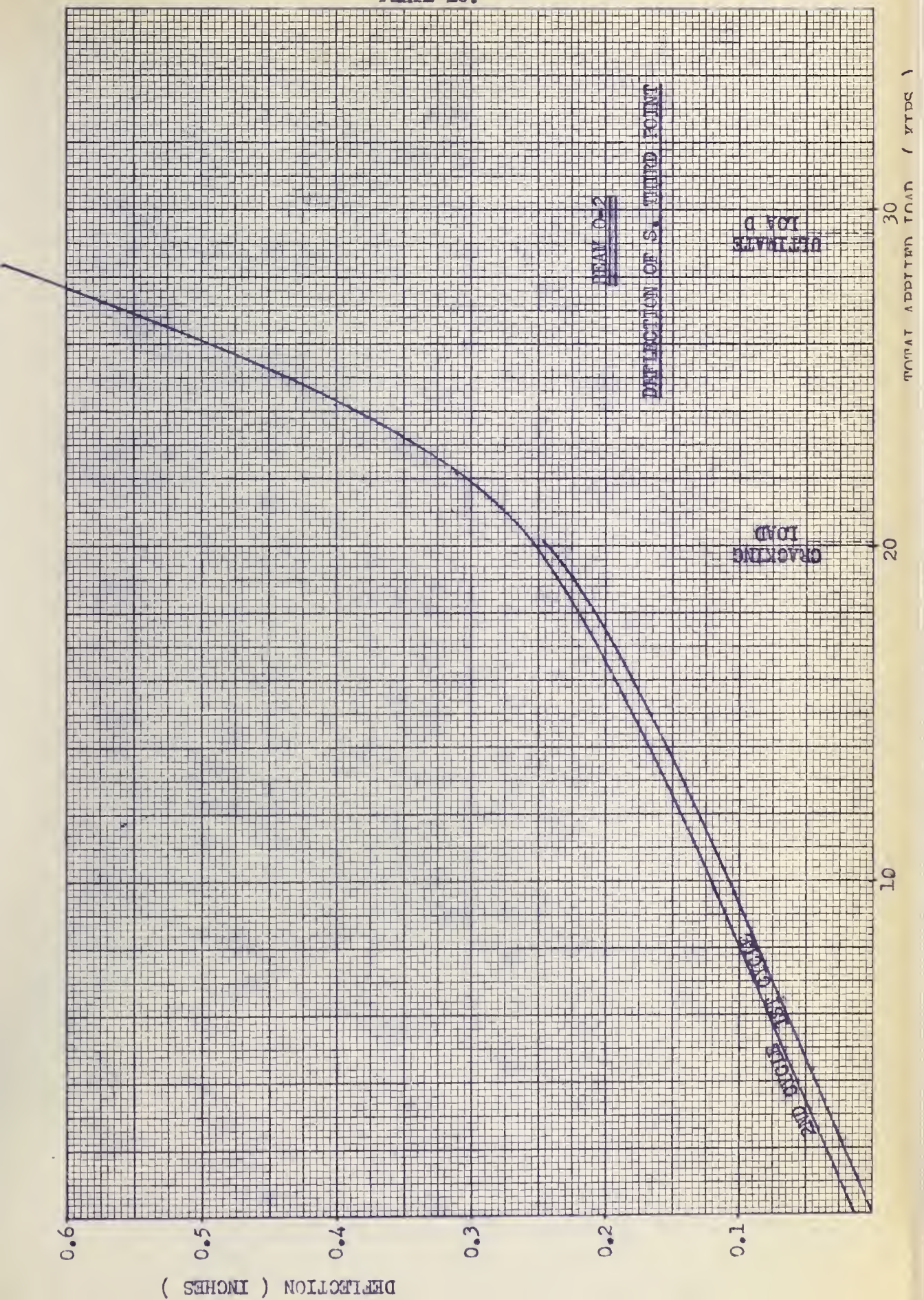


PLATE 17.

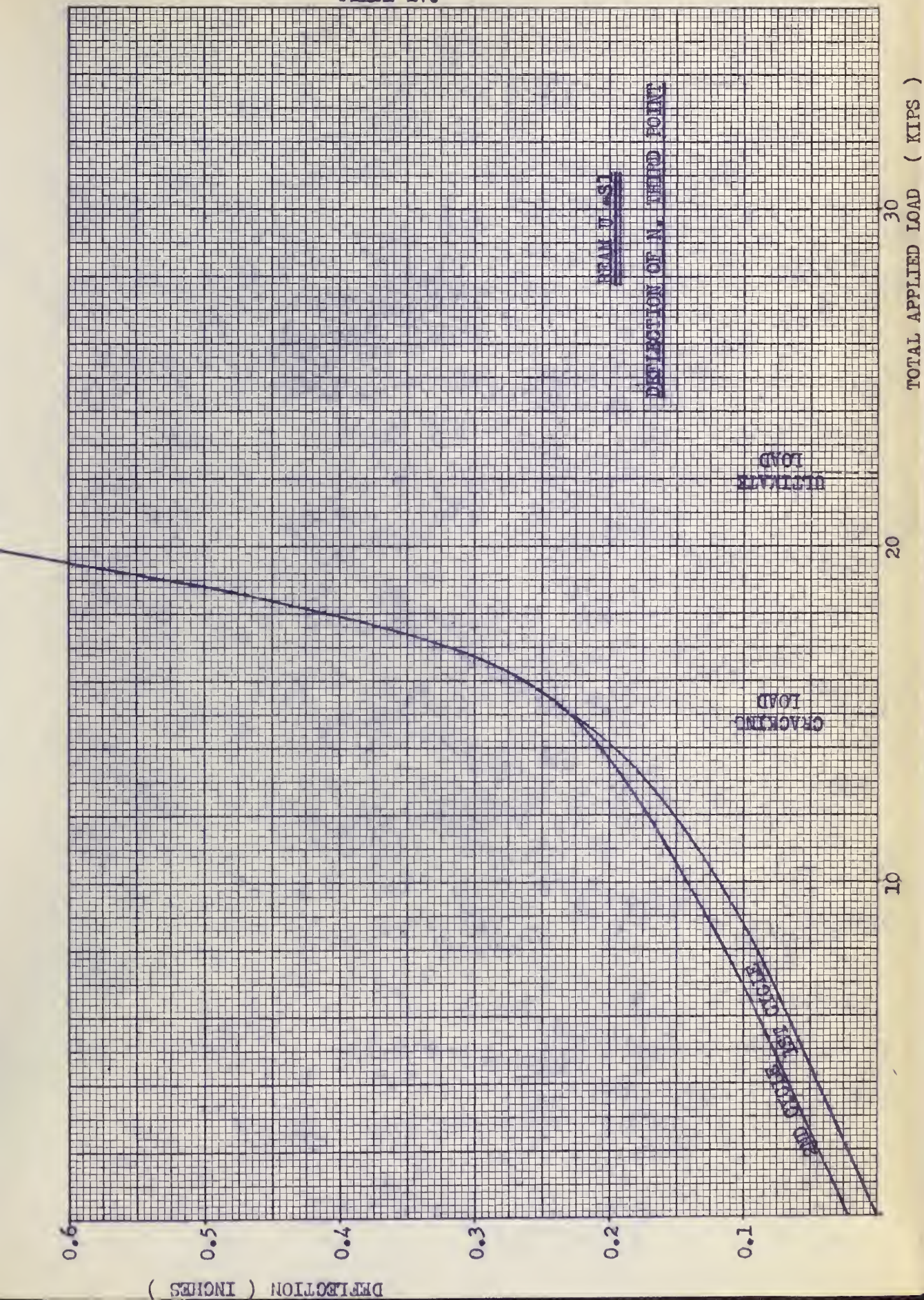


PLATE 18.

TOTAL APPLIED LOAD (KIPS)

30

20

10

BEAM 3-52

DEFLECTION OF CENTER POINT

ULTIMATE
LOAD

CRACKING
LOAD

2ND CRACK
15-35T
10-12 35T

DEFLECTION (INCHES)

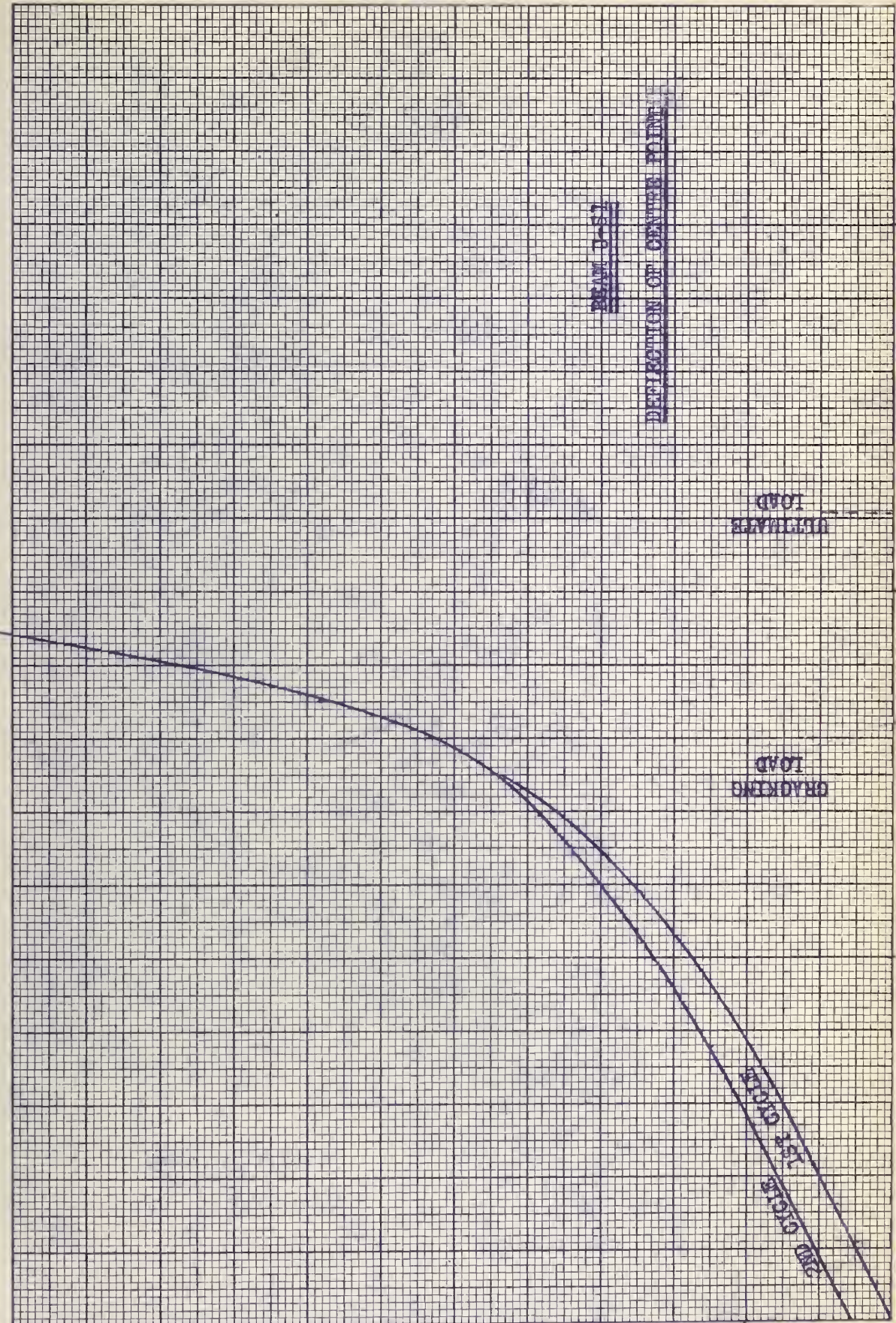
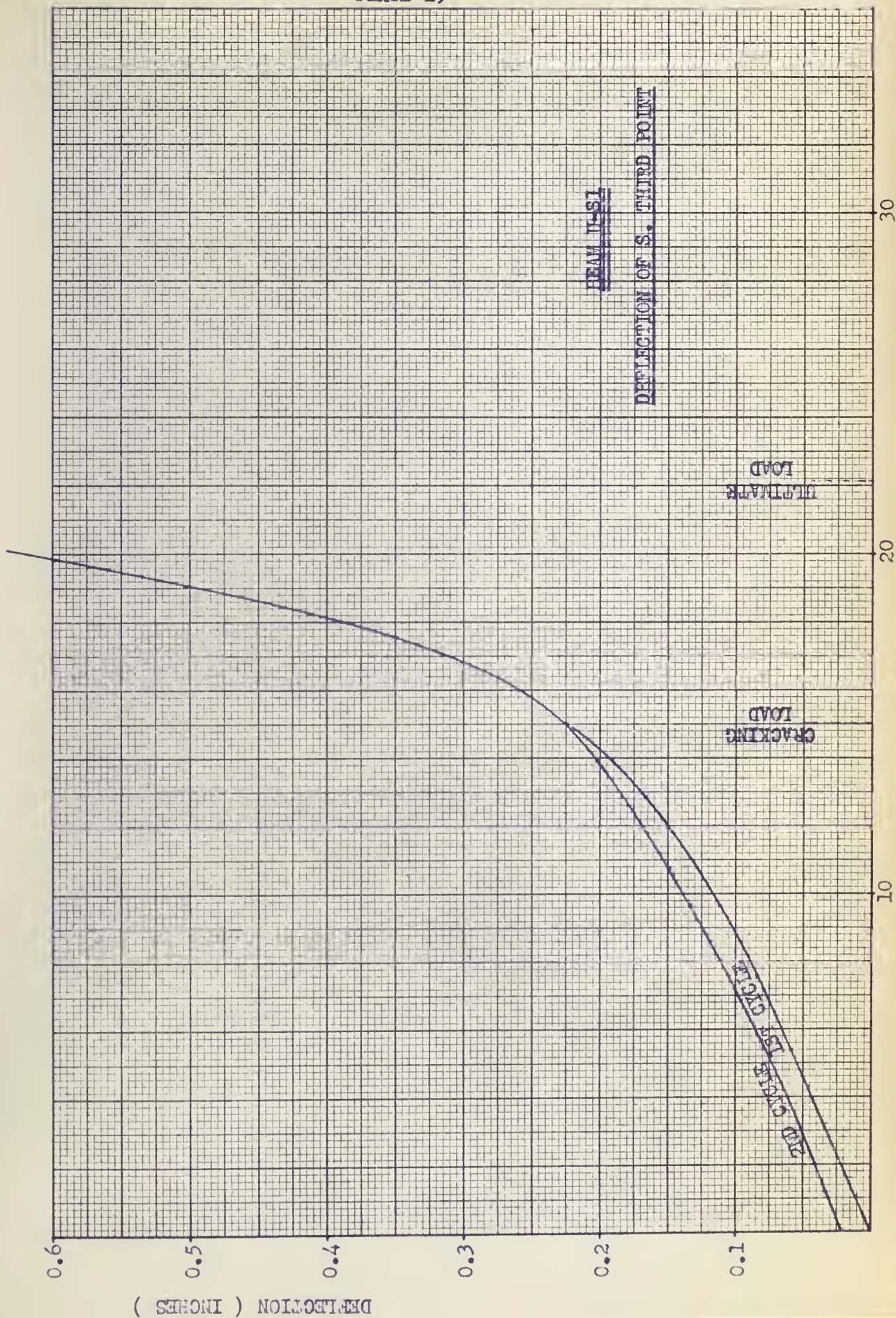


PLATE 19



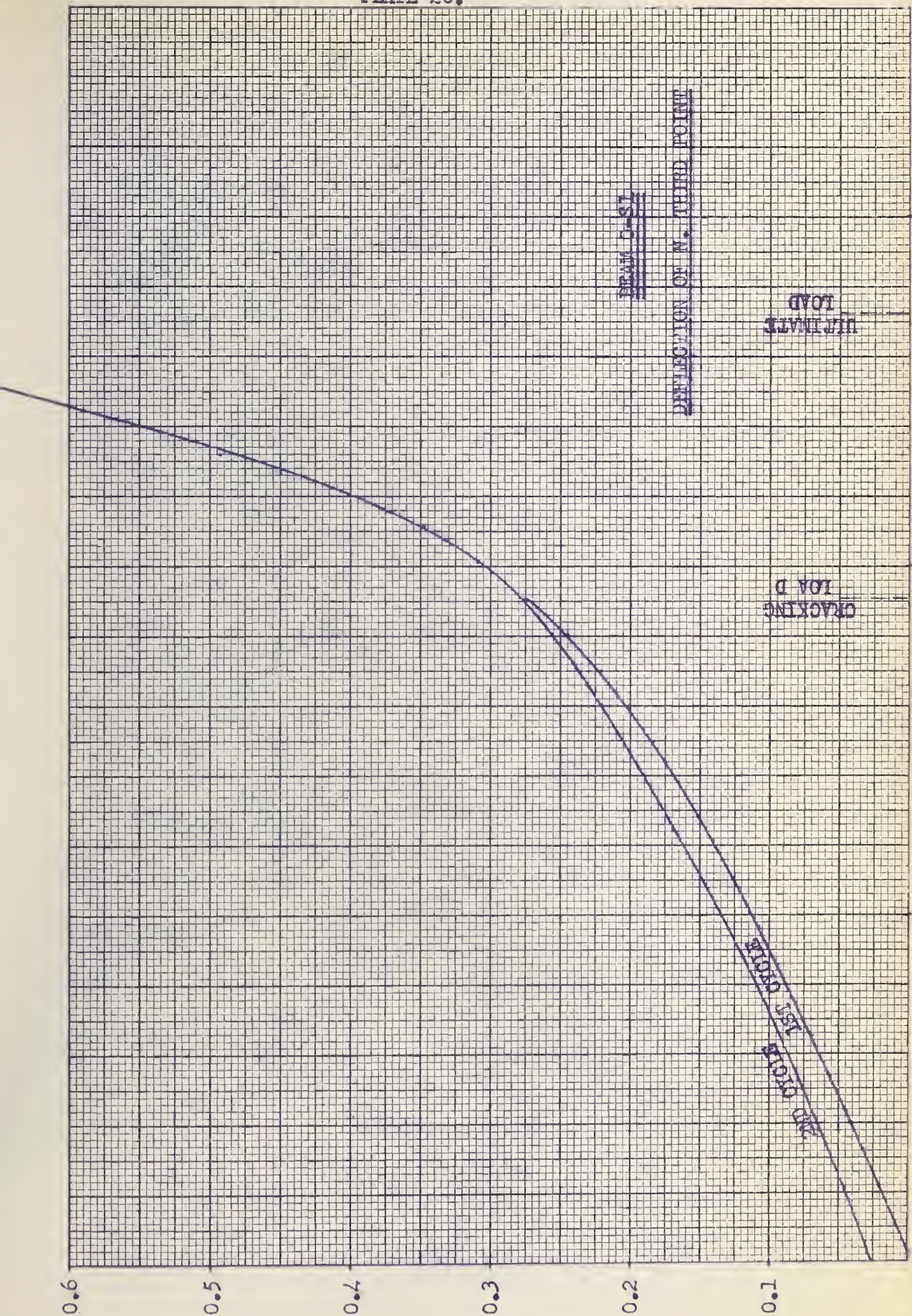
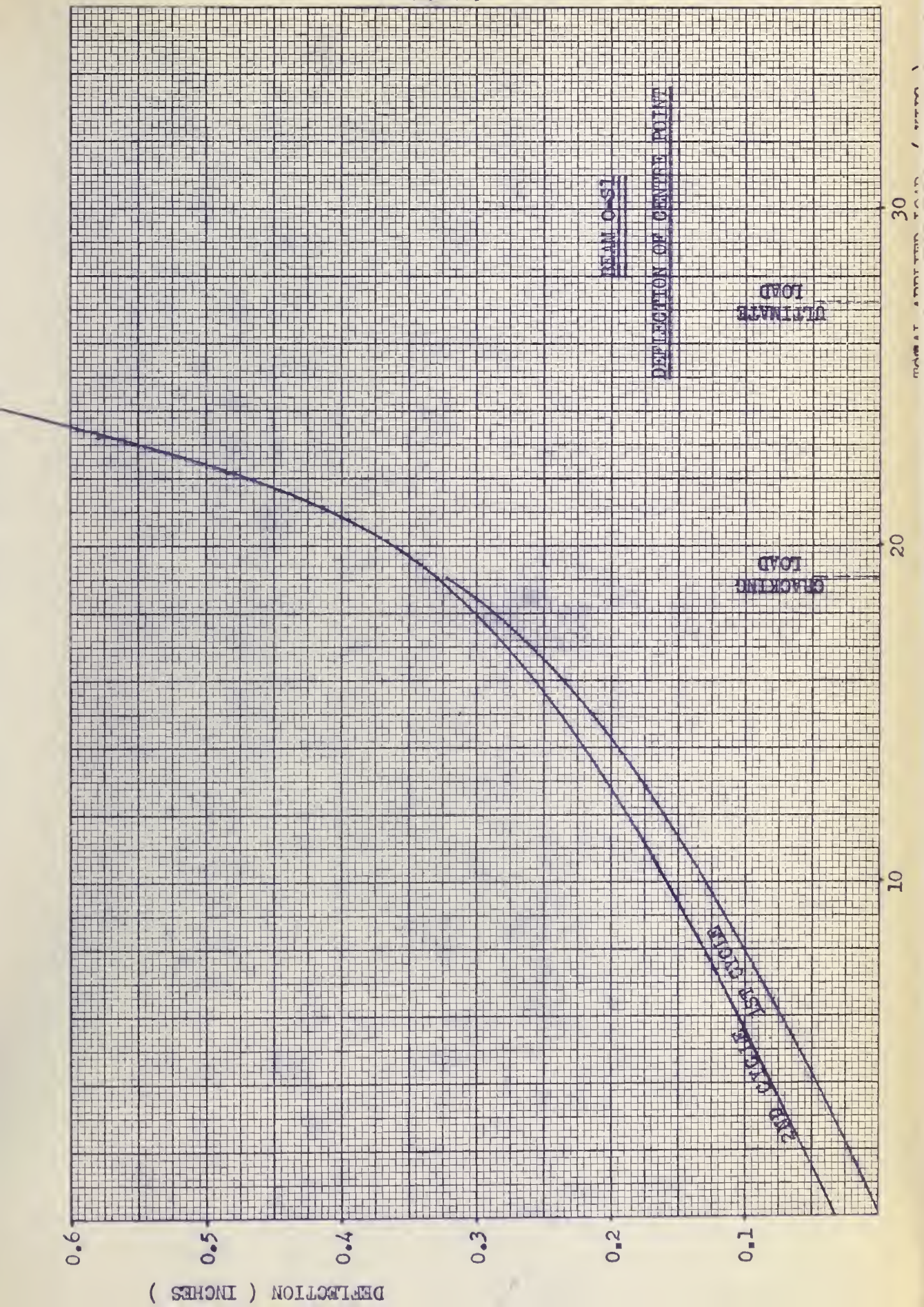
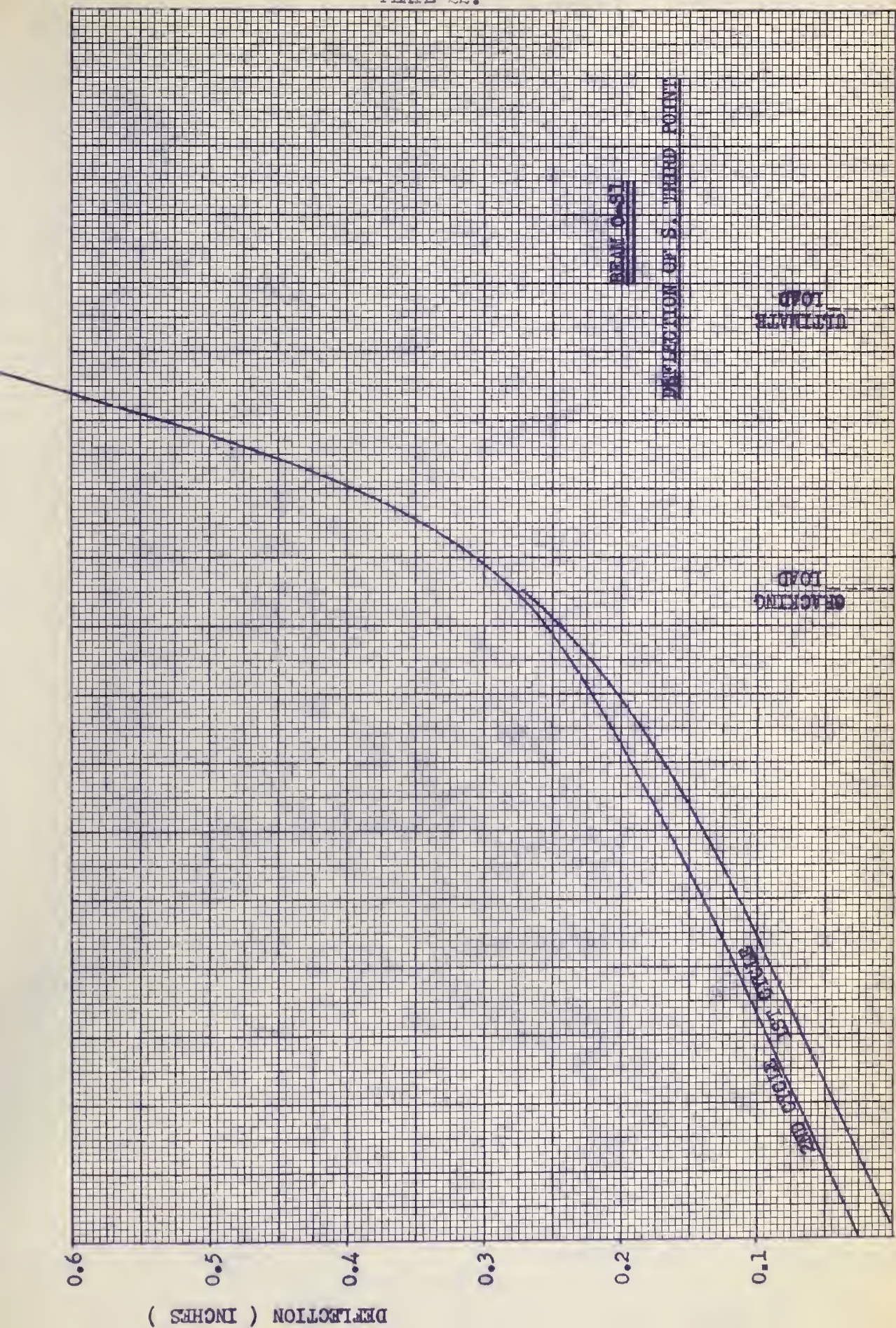
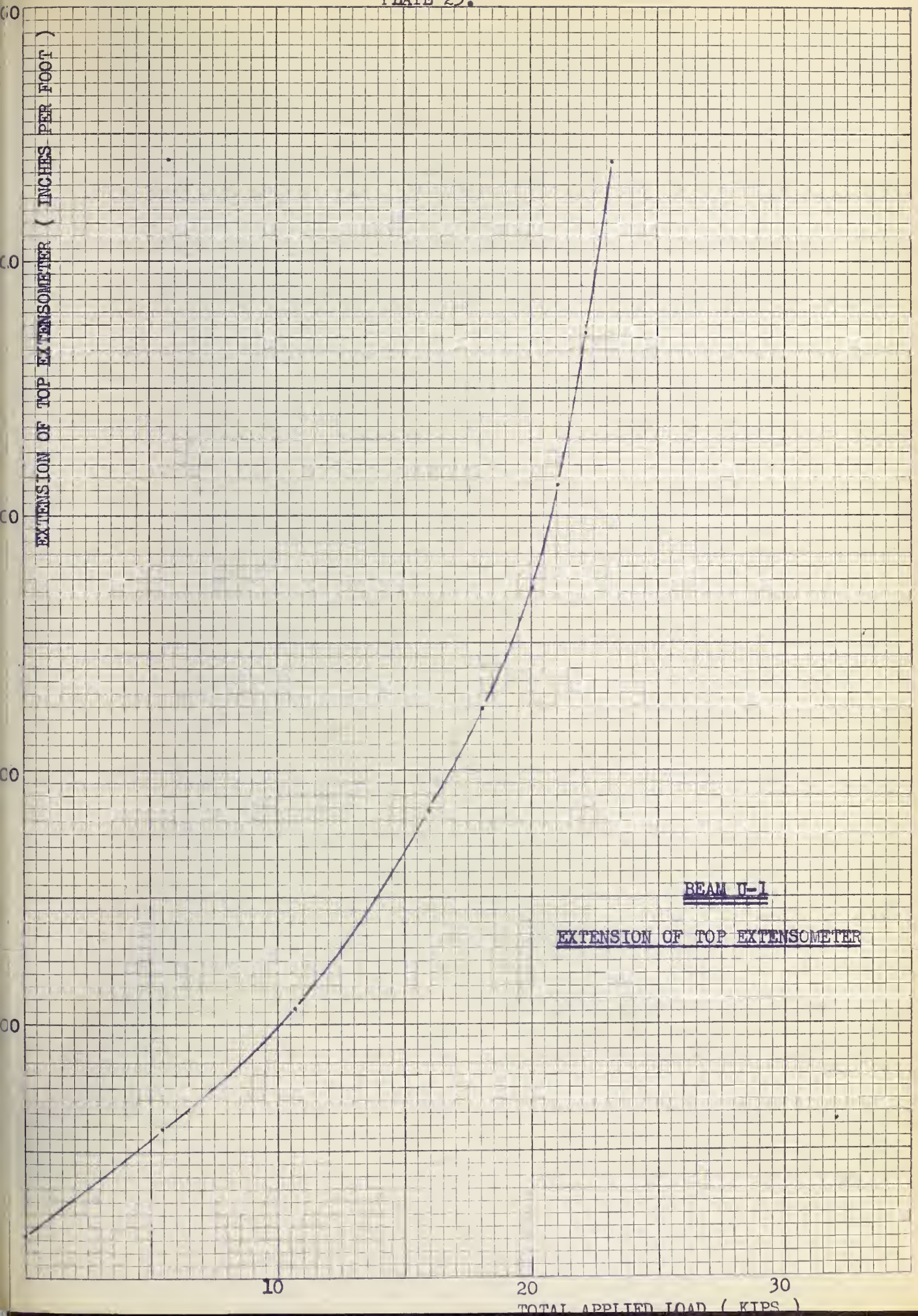


PLATE 21.



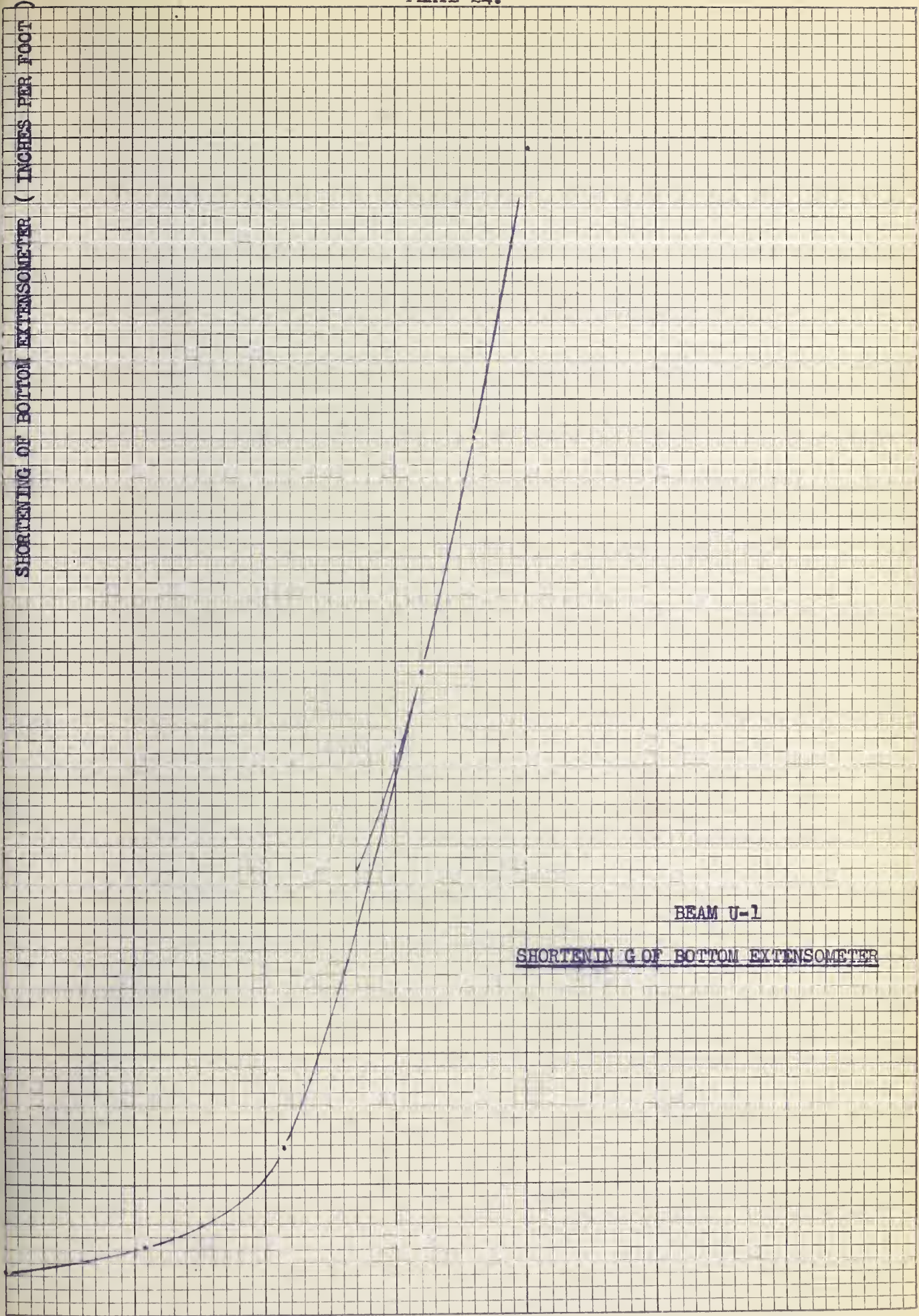




BEAM U-1

EXTENSION OF TOP EXTENSOMETER

SHORTENING OF BOTTOM EXTENSOMETER (INCHES PER FOOT)



BEAM U-1

SHORTENING OF BOTTOM EXTENSOMETER

10

20

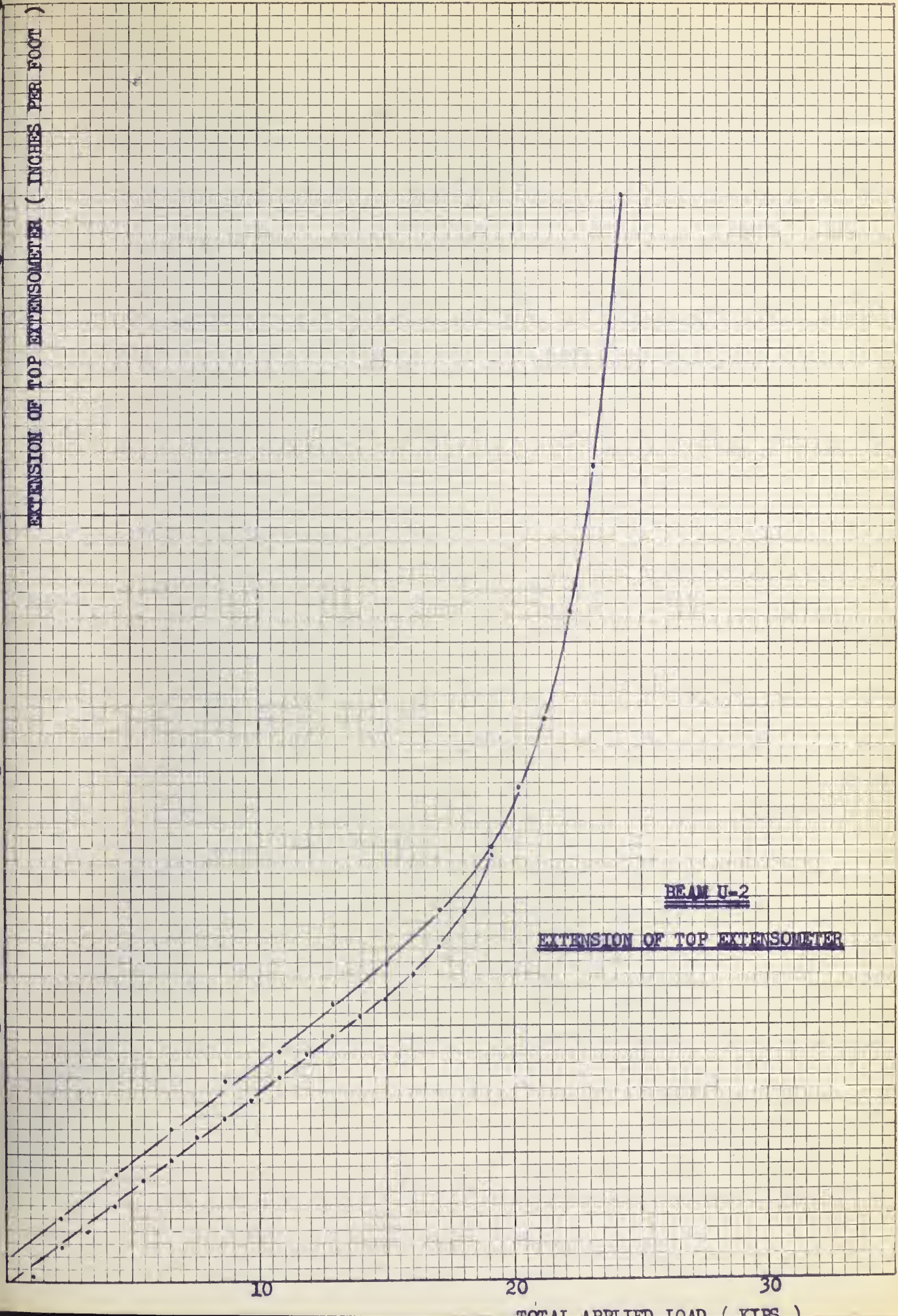
30

TOTAL APPLIED LOAD (KIIPS)

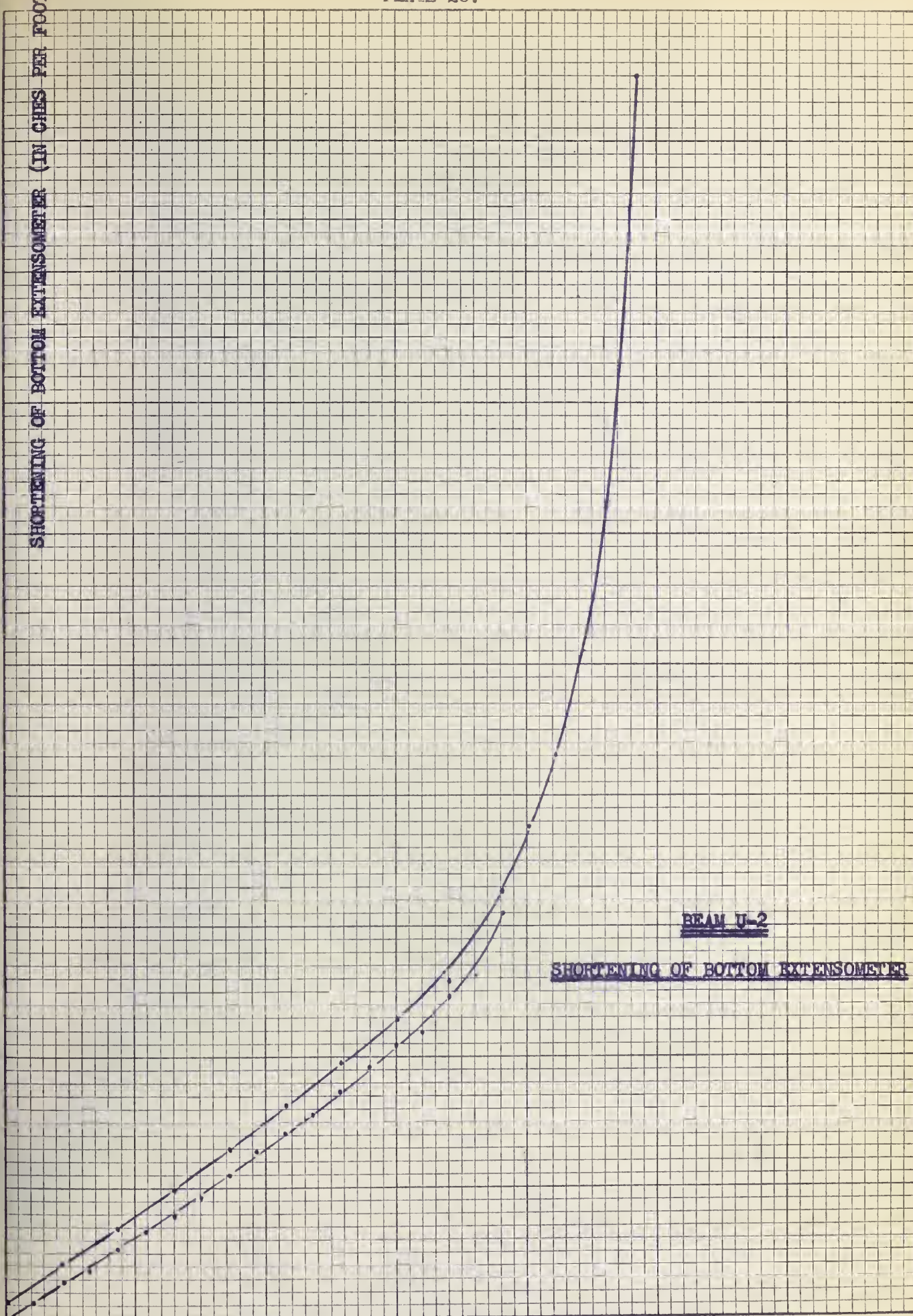
EXTENSION OF TOP EXTENSOMETER (INCHES PER FOOT)

BEAM U-2

EXTENSION OF TOP EXTENSOMETER



SHORTENING OF BOTTOM EXTENSOMETER (IN CHES PER FOOT)



BEAM U-2

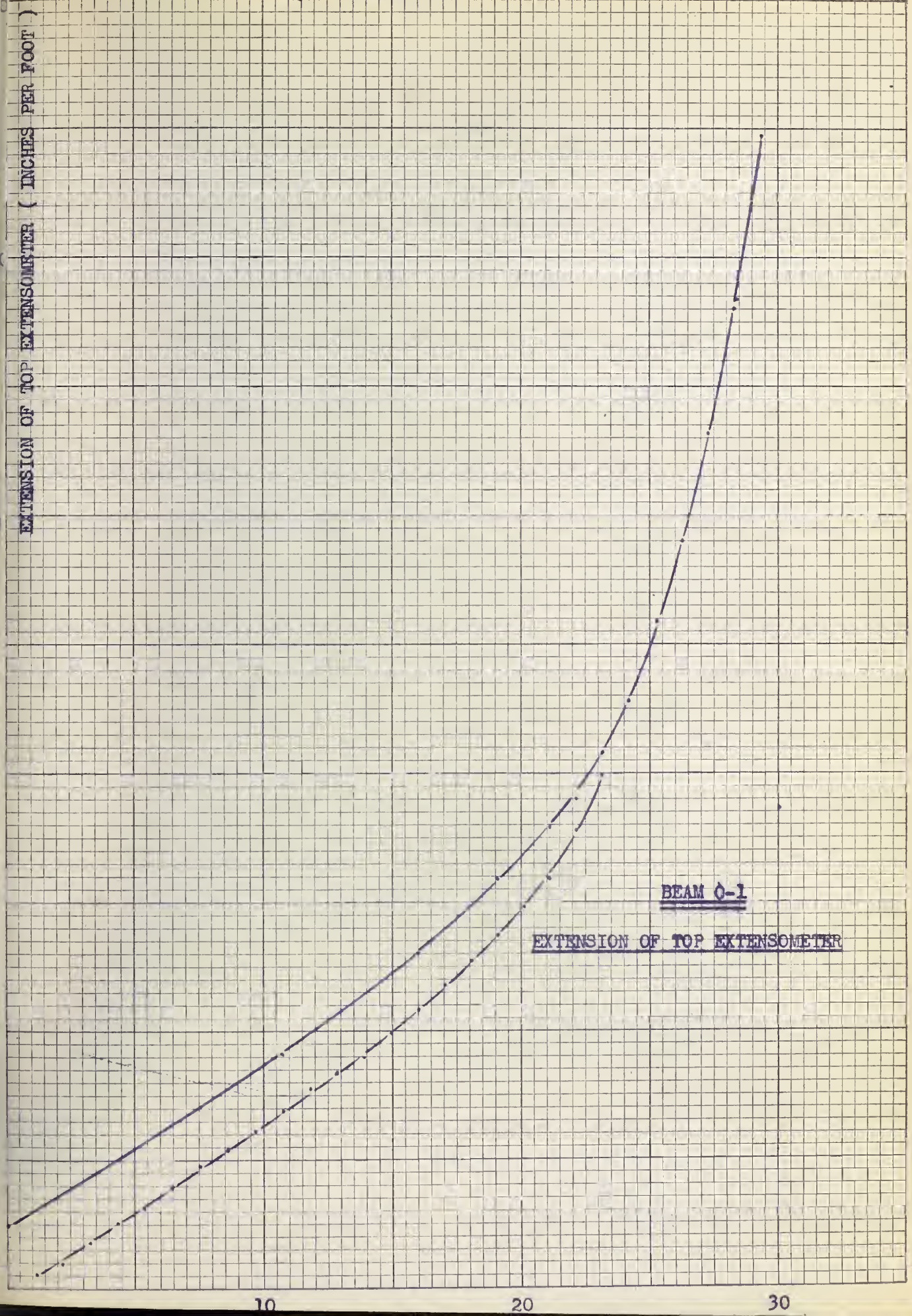
SHORTENING OF BOTTOM EXTENSOMETER

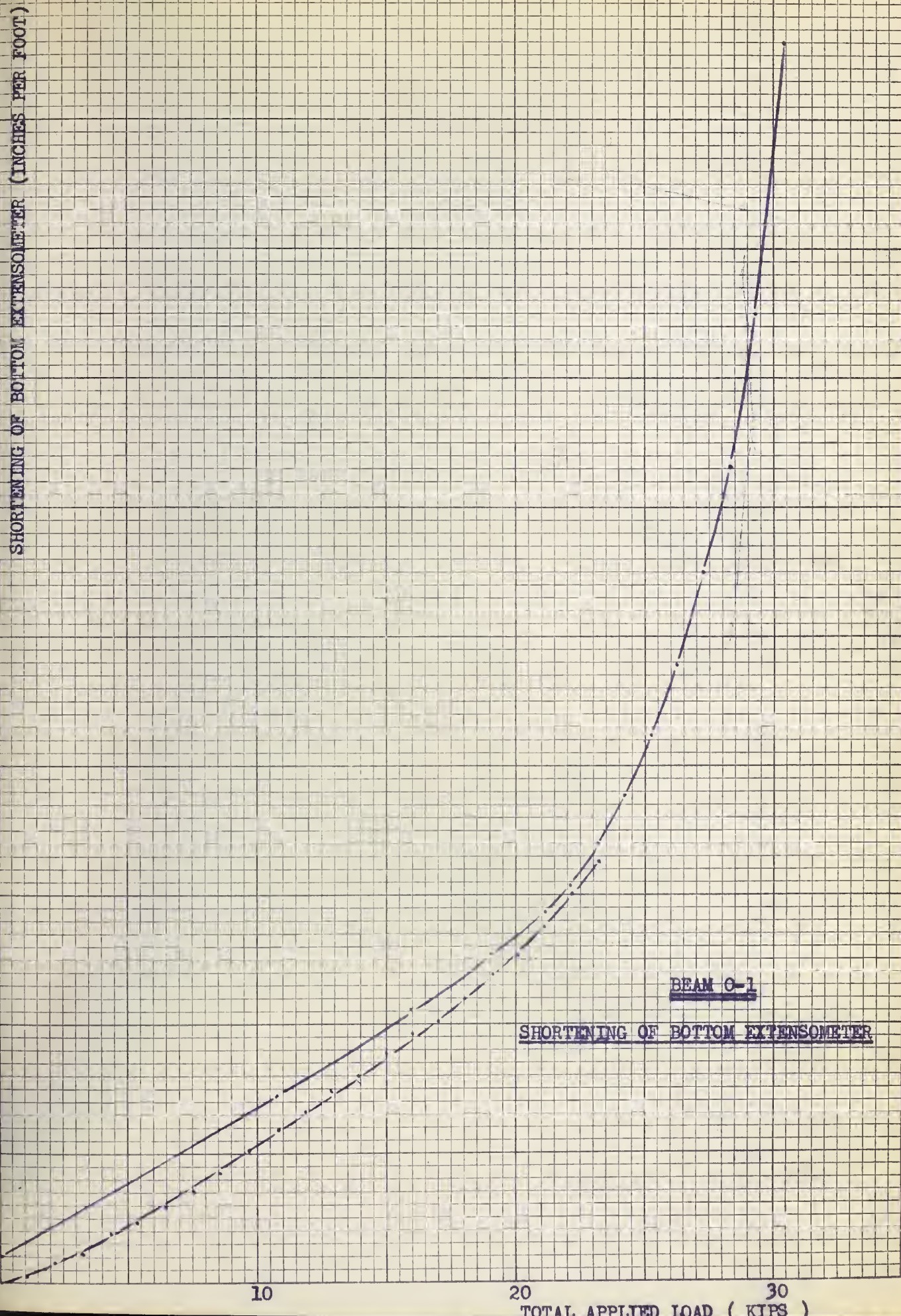
10

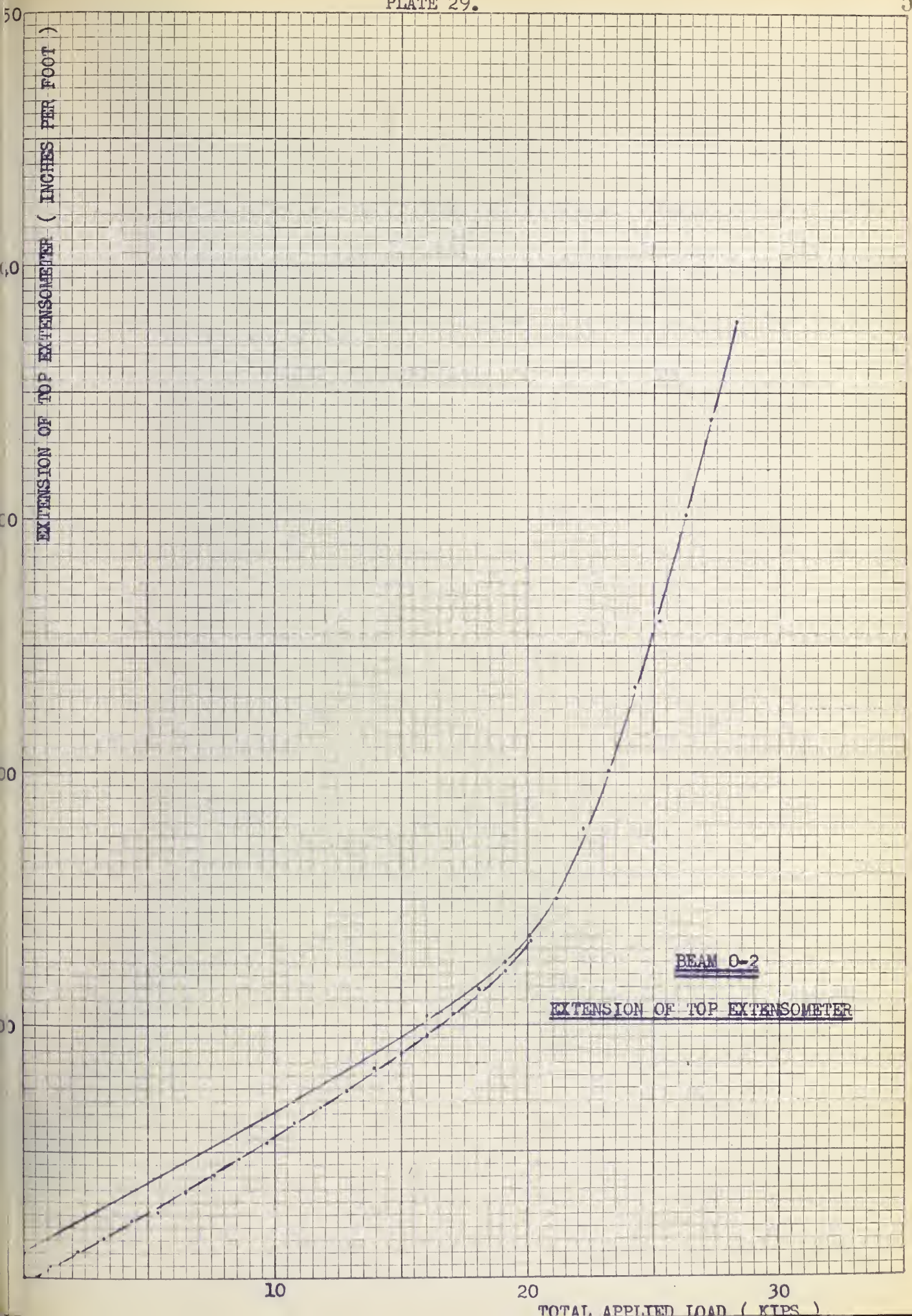
20

30

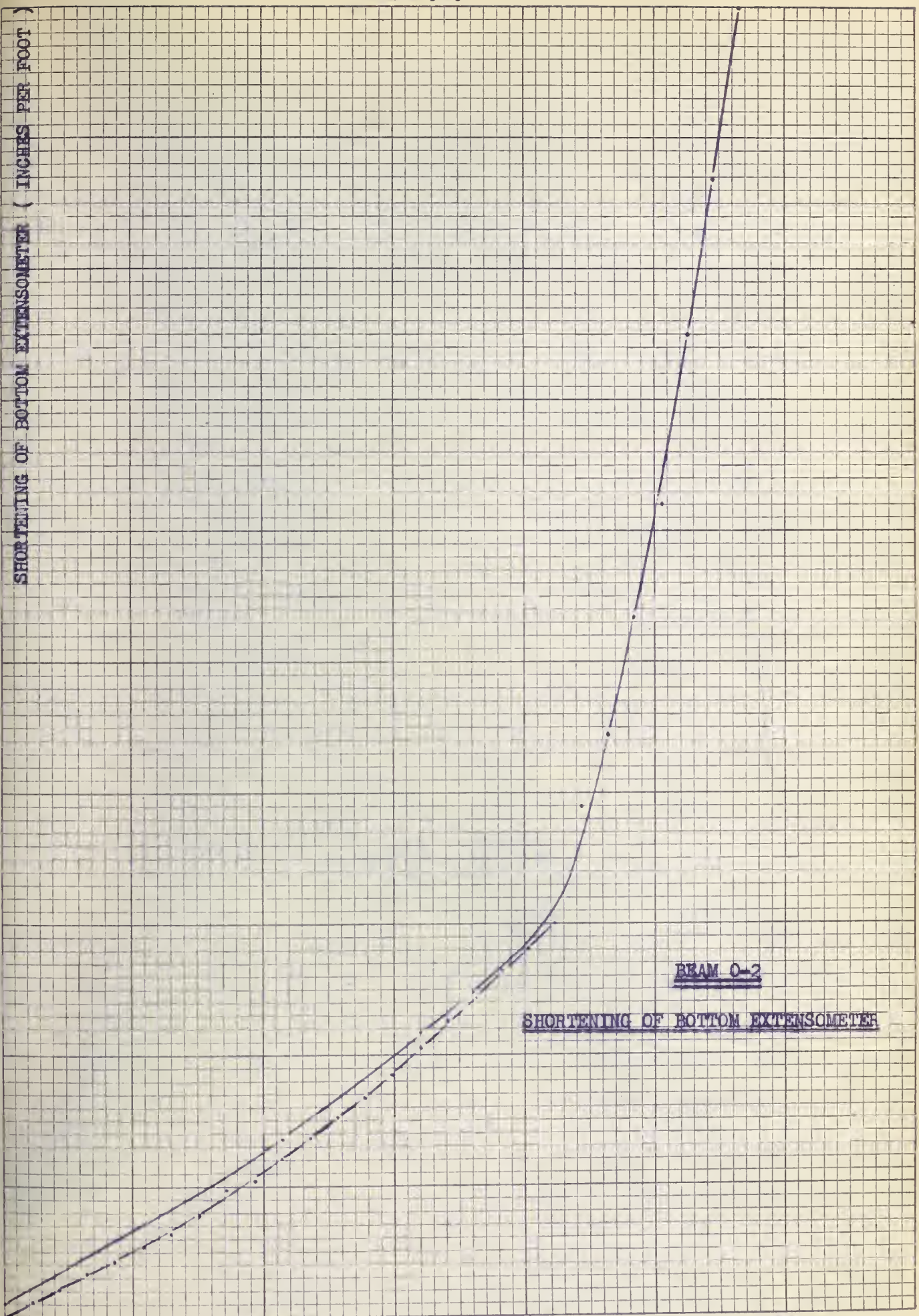
TOTAL APPLIED LOAD (KIPS)







SHORTENING OF BOTTOM EXTENSOMETER (INCHES PER FOOT)



BEAM 0-2

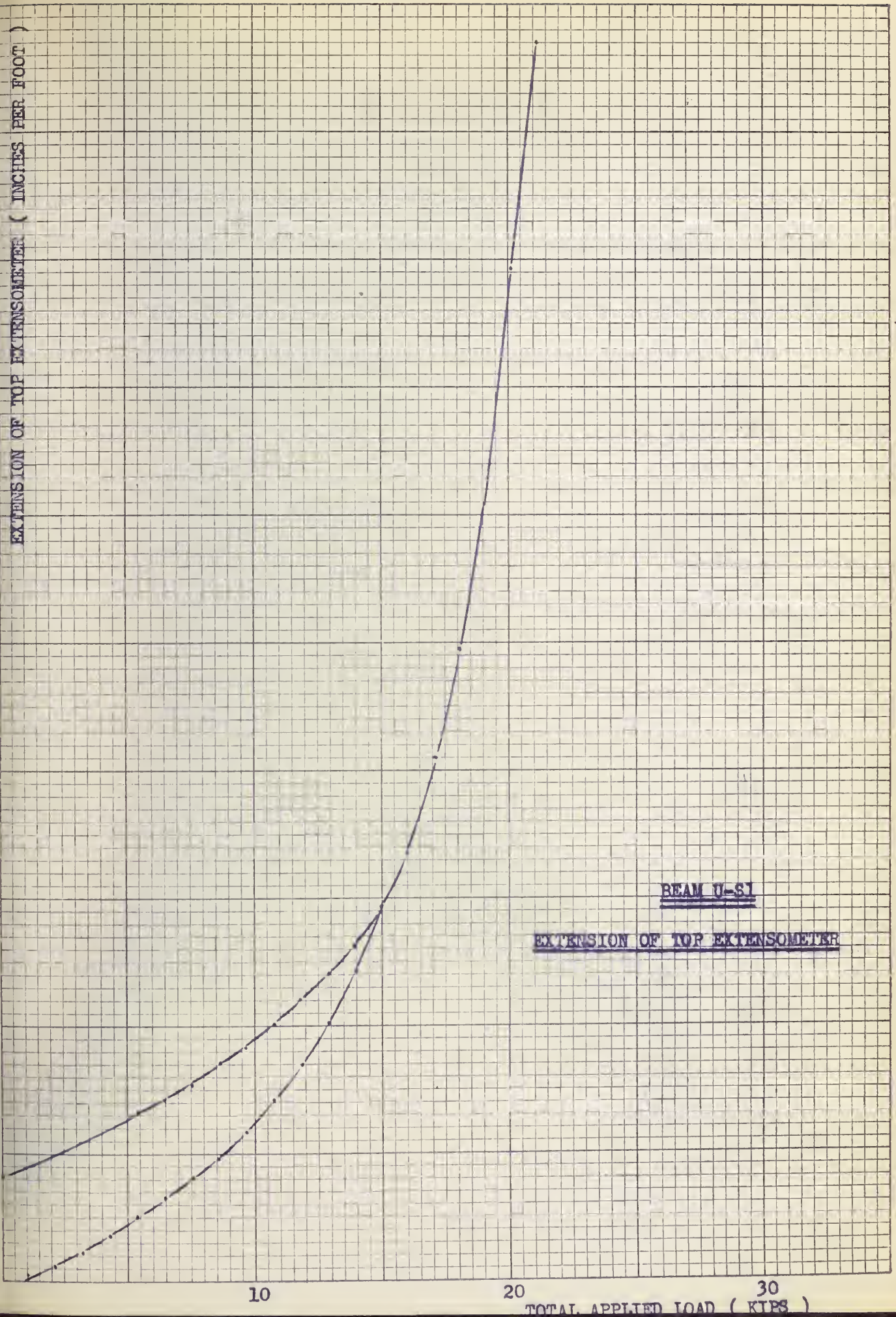
SHORTENING OF BOTTOM EXTENSOMETER

10

20

30

TOTAL APPLIED LOAD (KIPS)



BEAM U-61

EXTENSION OF TOP EXTENSOMETER

10

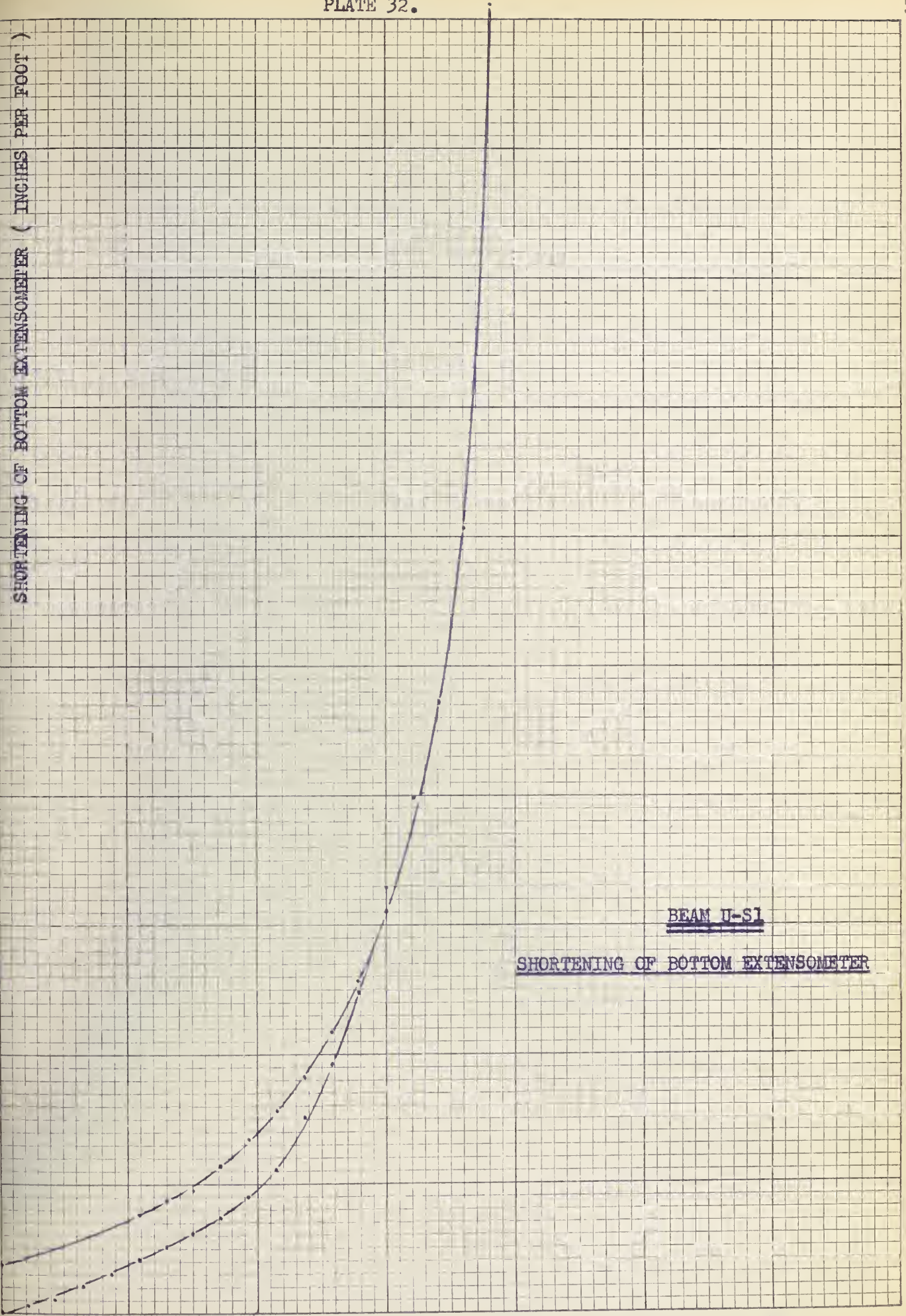
20

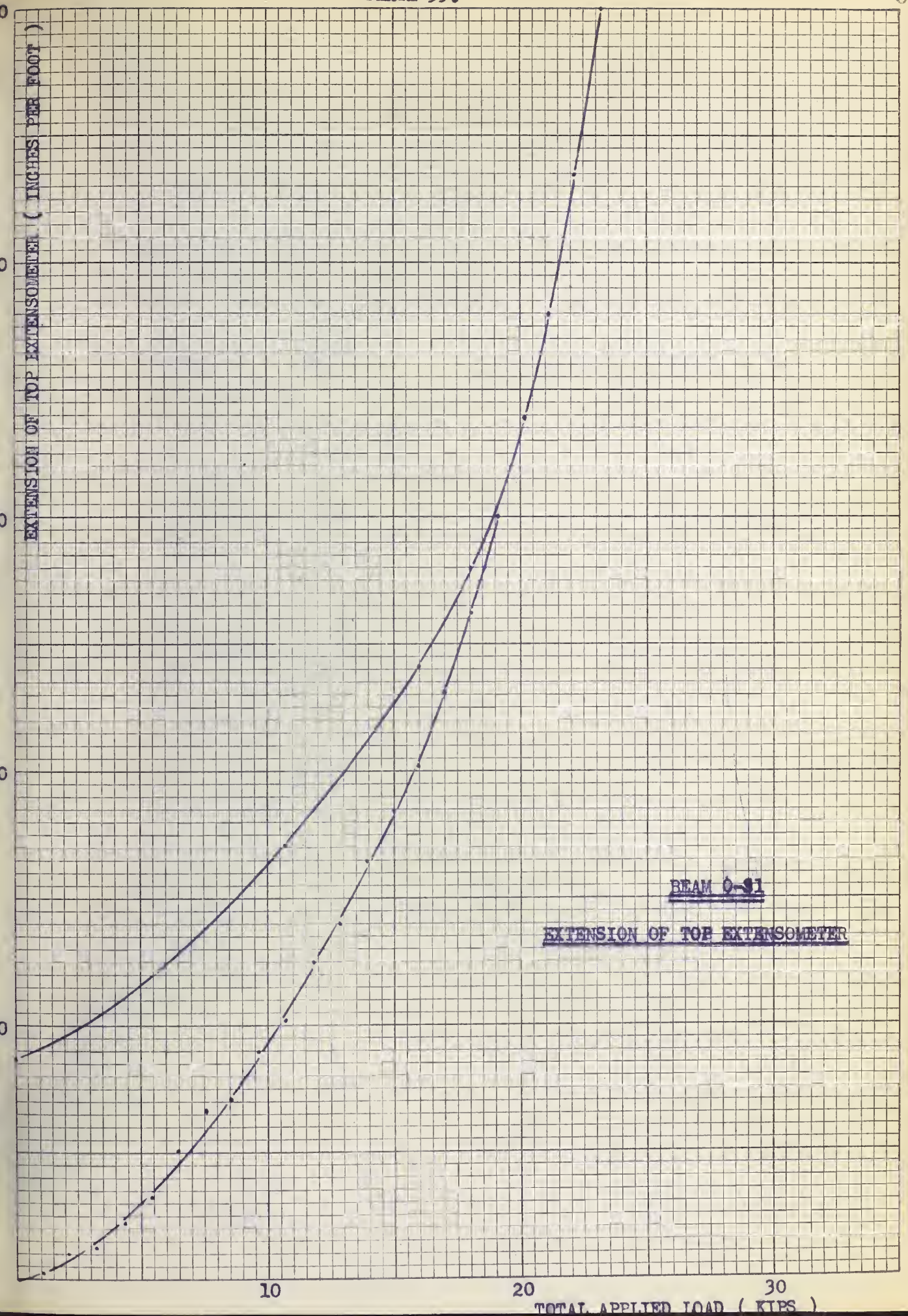
30

TOTAL APPLIED LOAD (KIPS)

SHORTENING OF BOTTOM EXTENSOMETER (INCHES PER FOOT)

BEAM U-S1
SHORTENING OF BOTTOM EXTENSOMETER





SHORTENING OF BOTTOM EXTENSOMETER (INCHES PER FOOT)

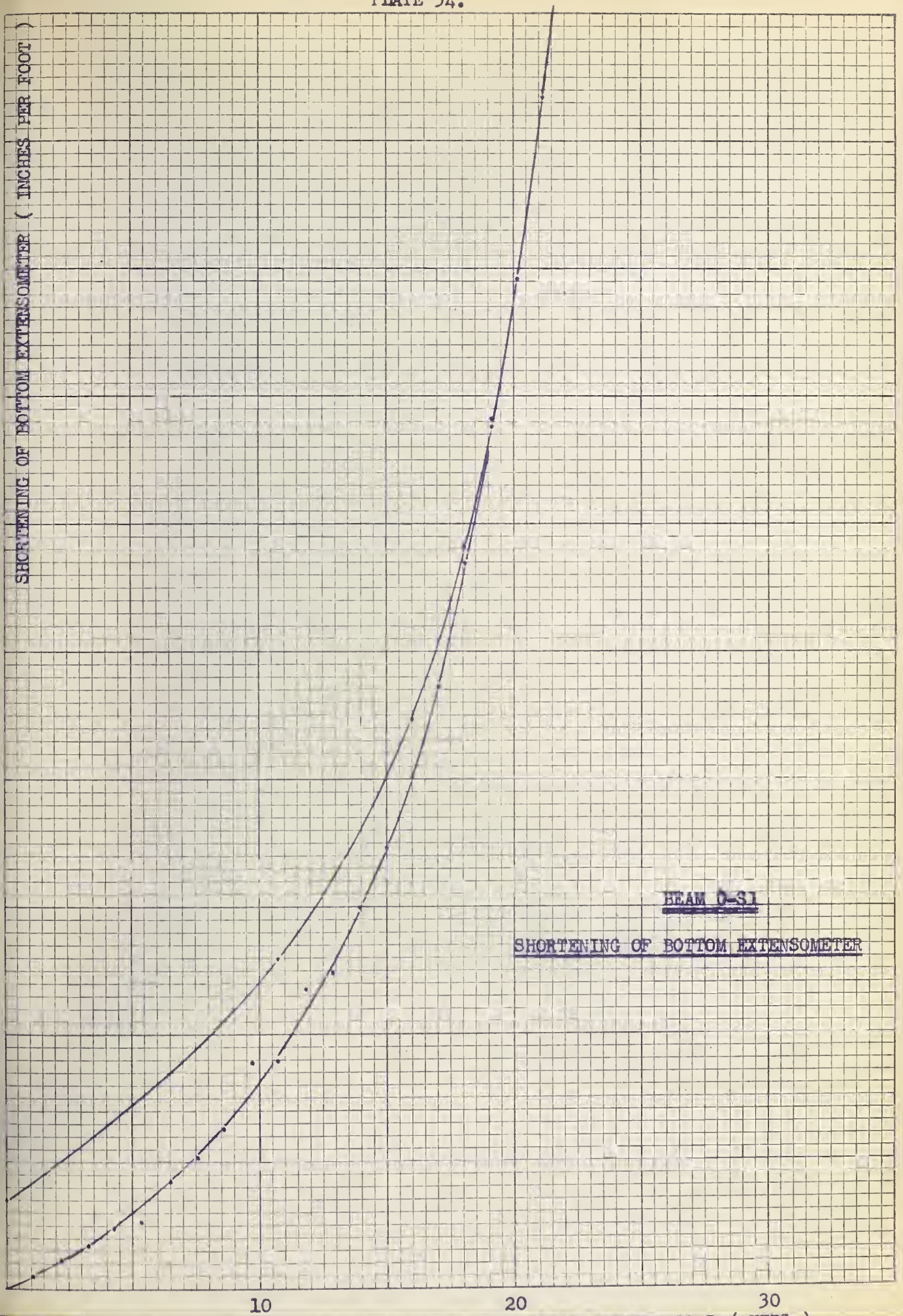
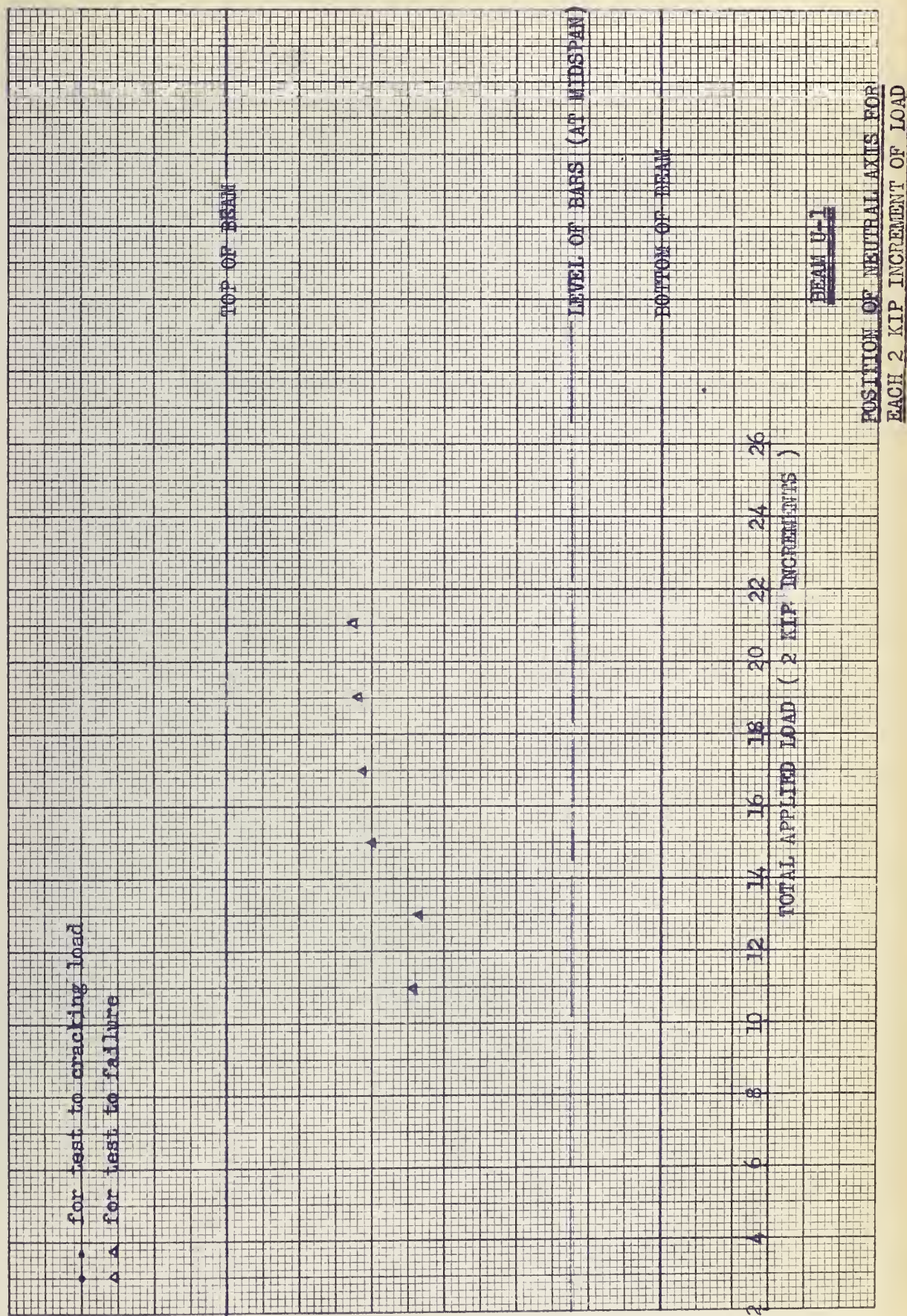


PLATE 35.



12"

PLATE 36.

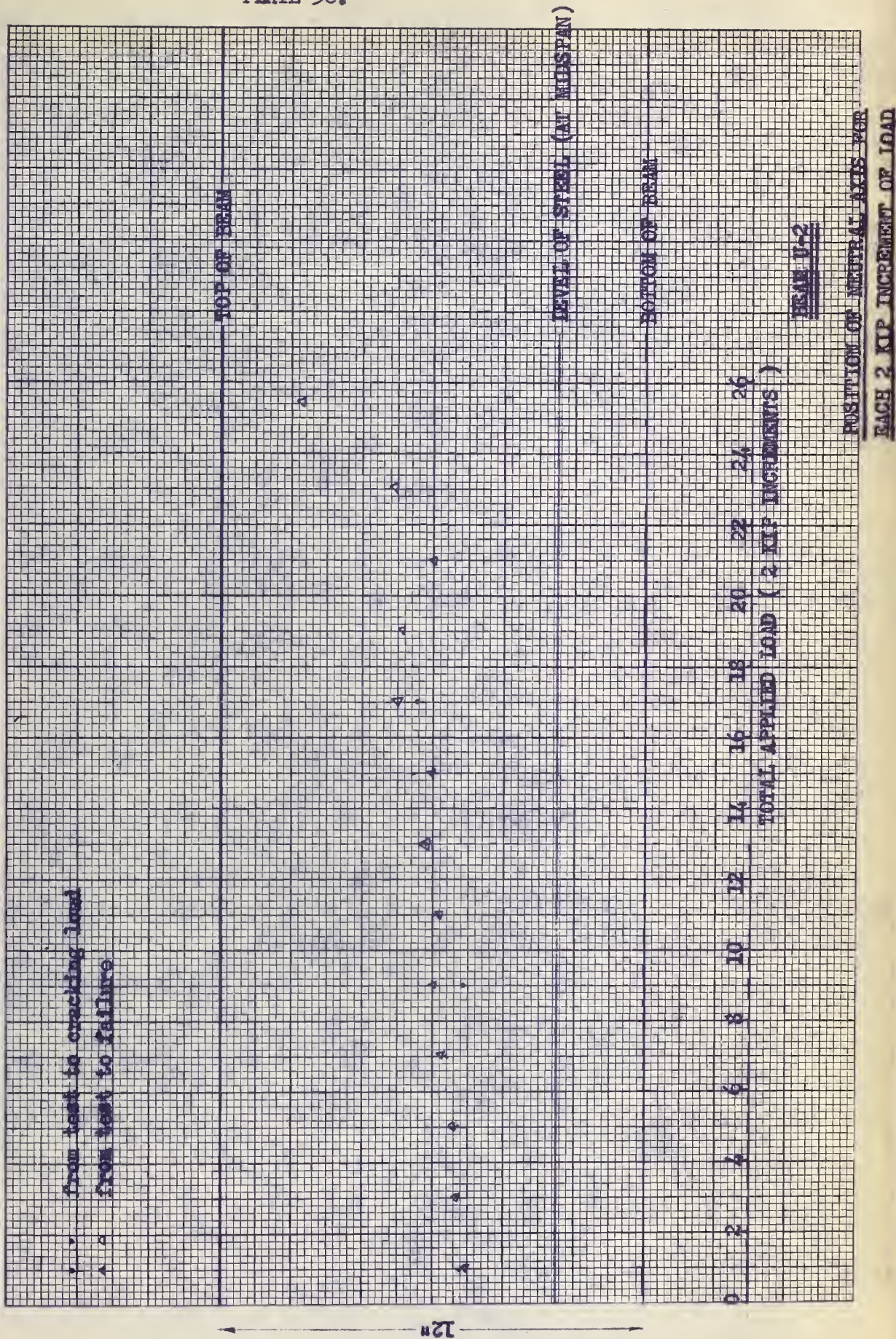
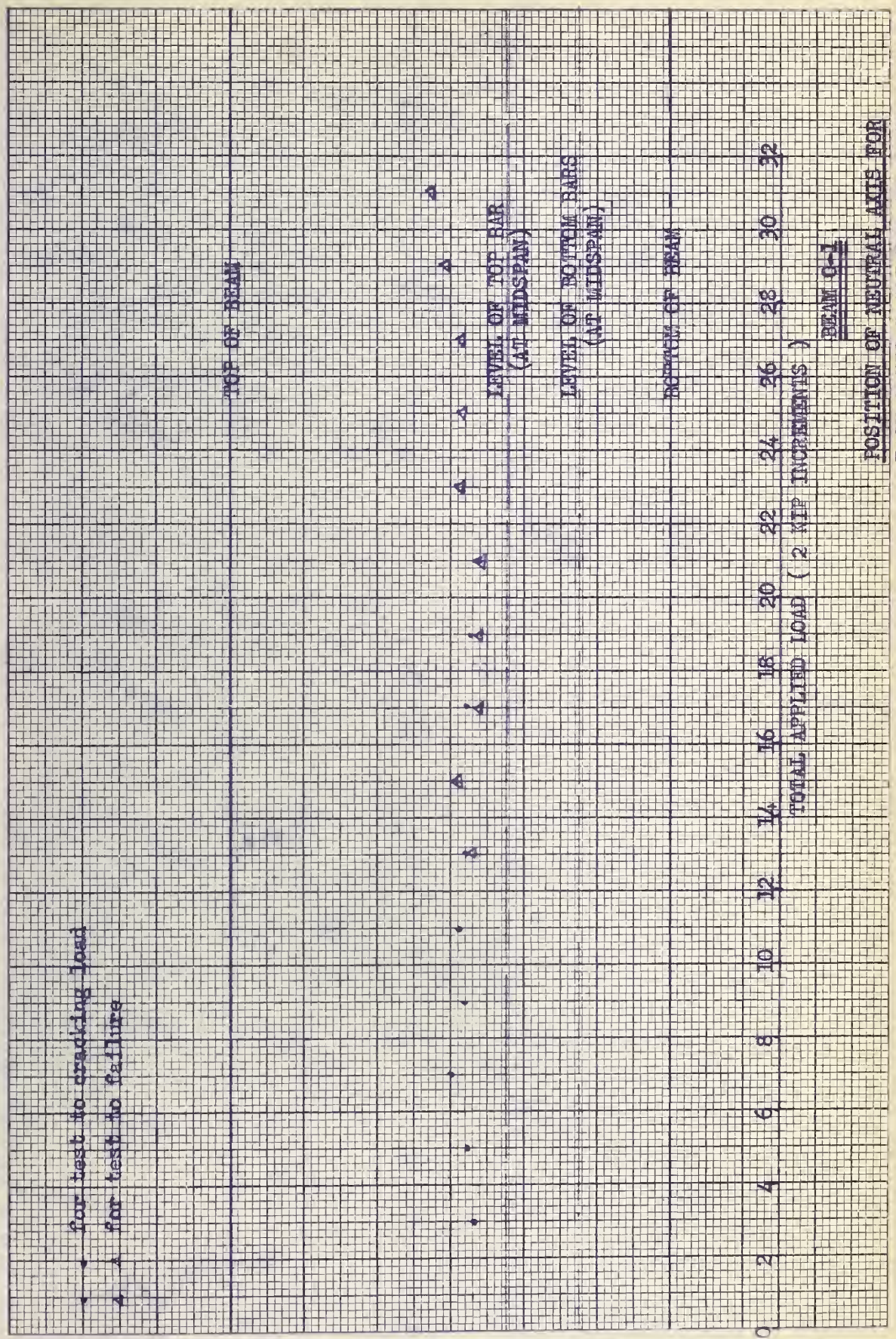
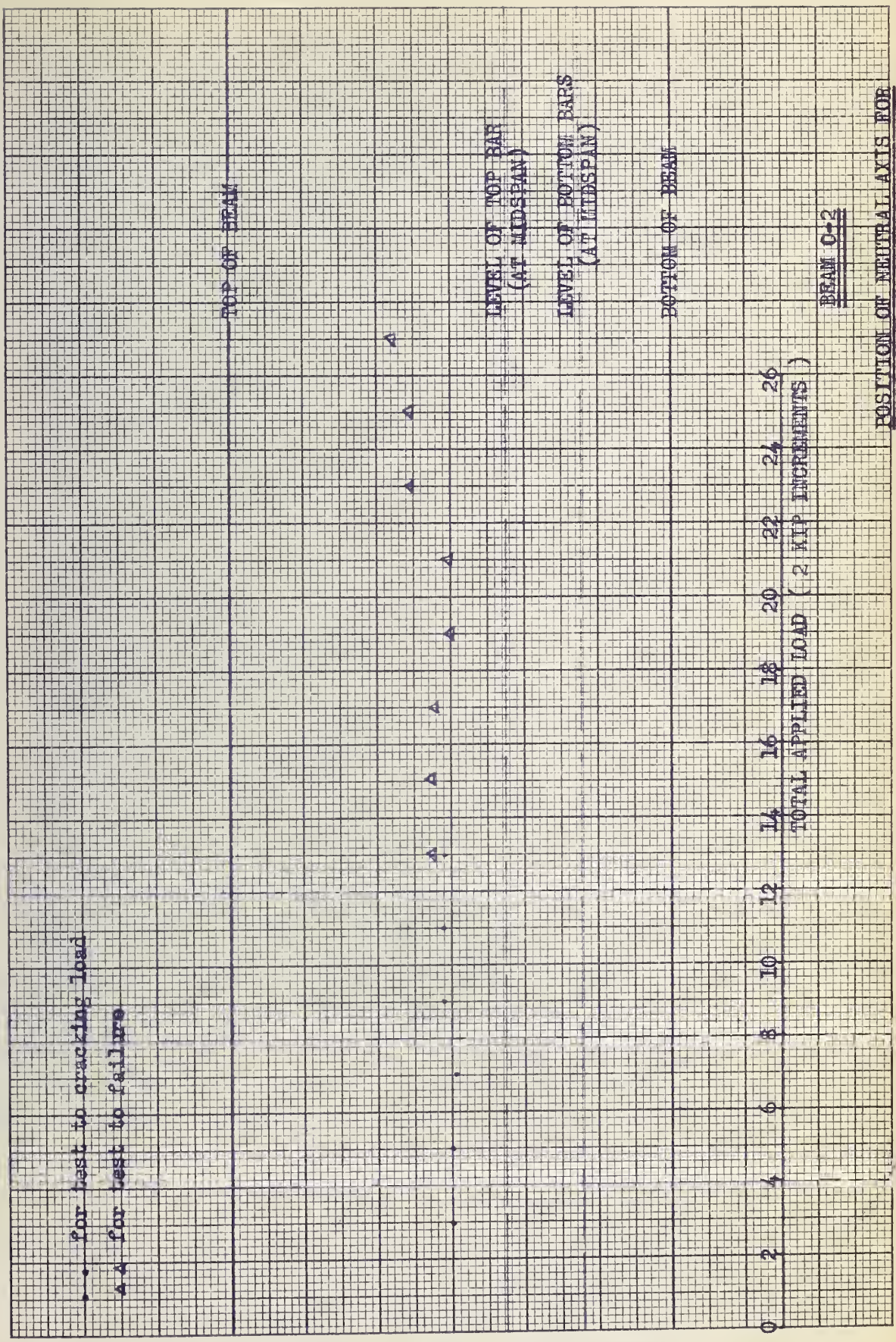


PLATE 37.



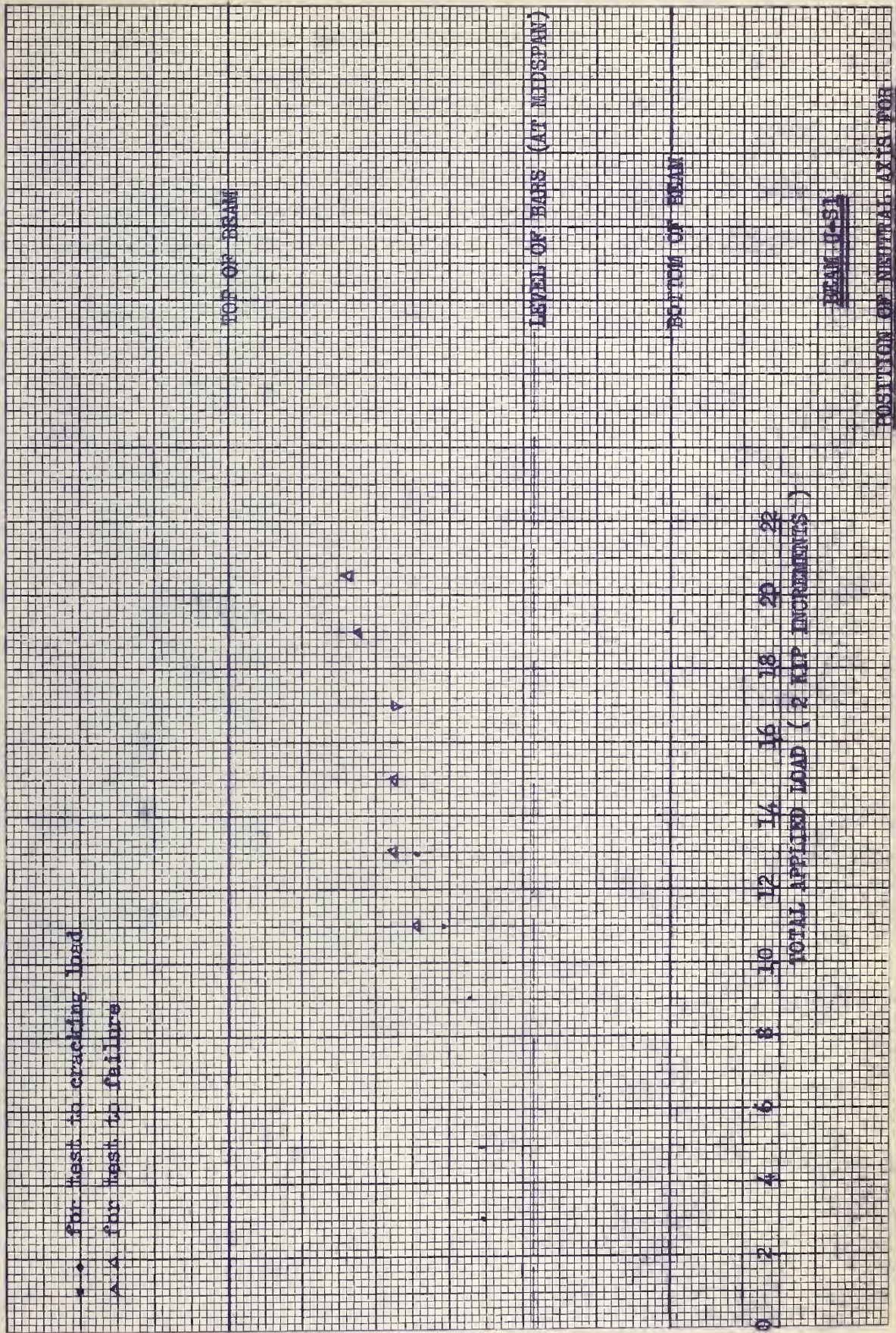
12"

PLATE 38.



12"

PLATE 39.



12"

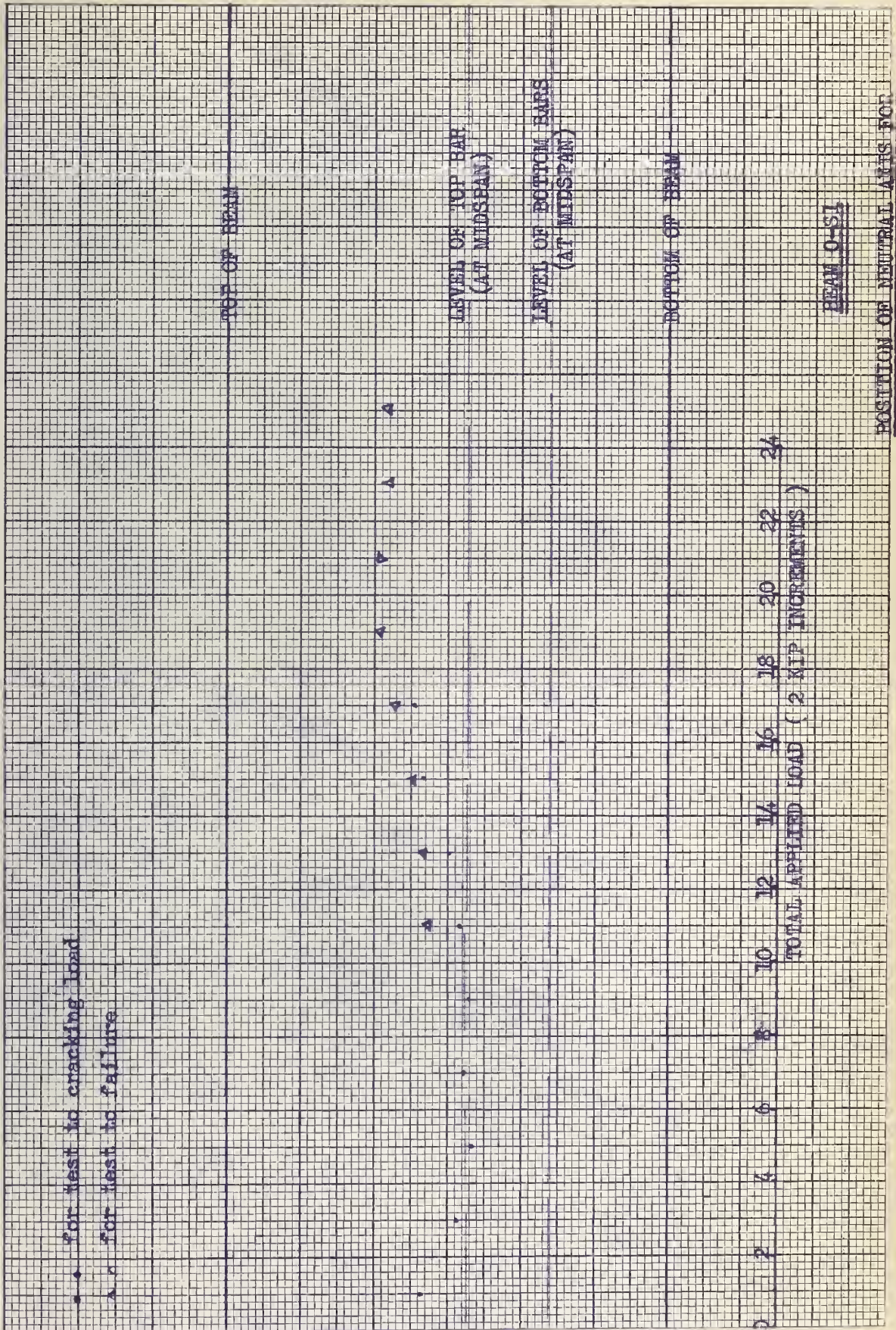


PLATE 41.

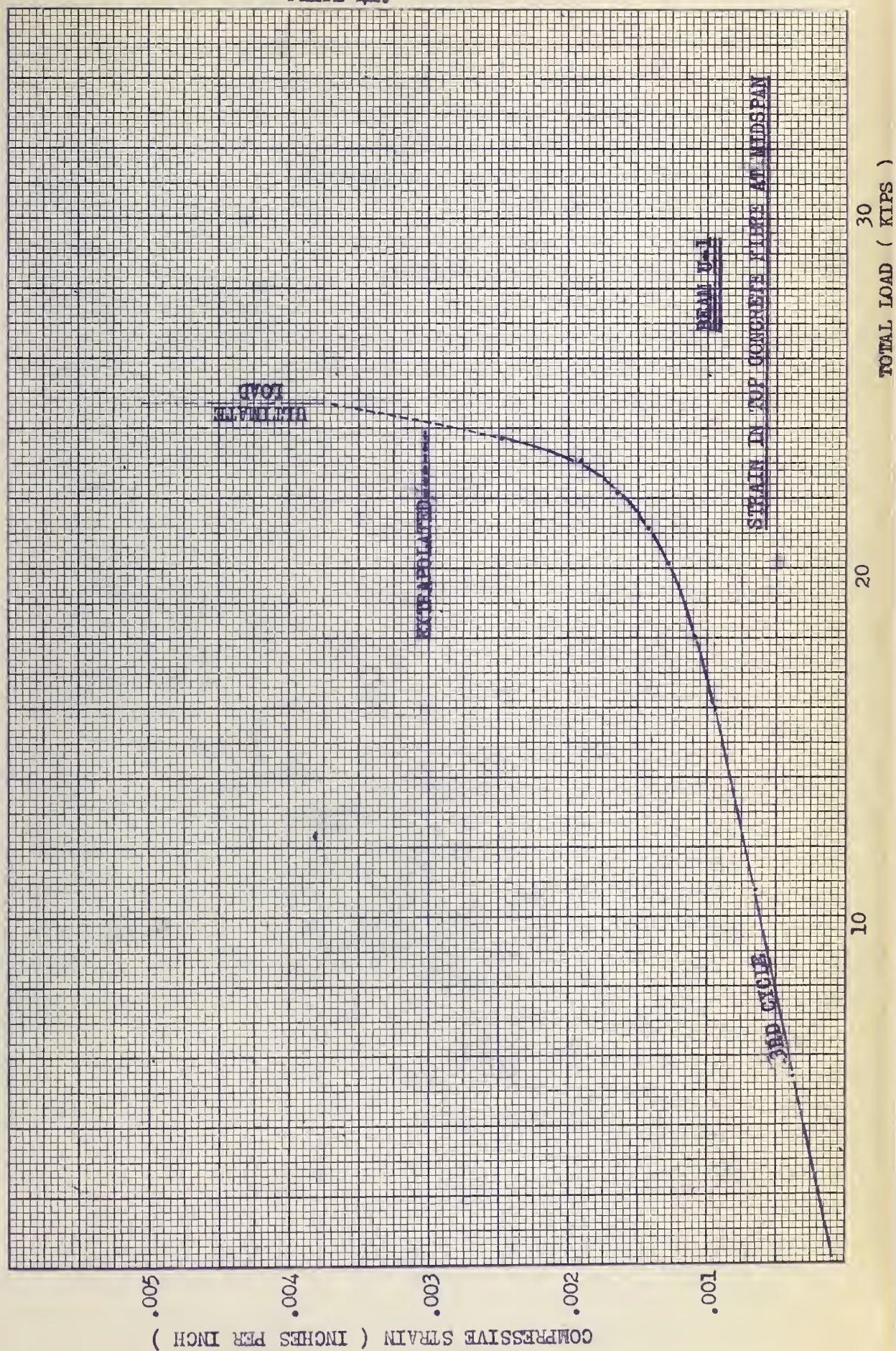


PLATE 42.

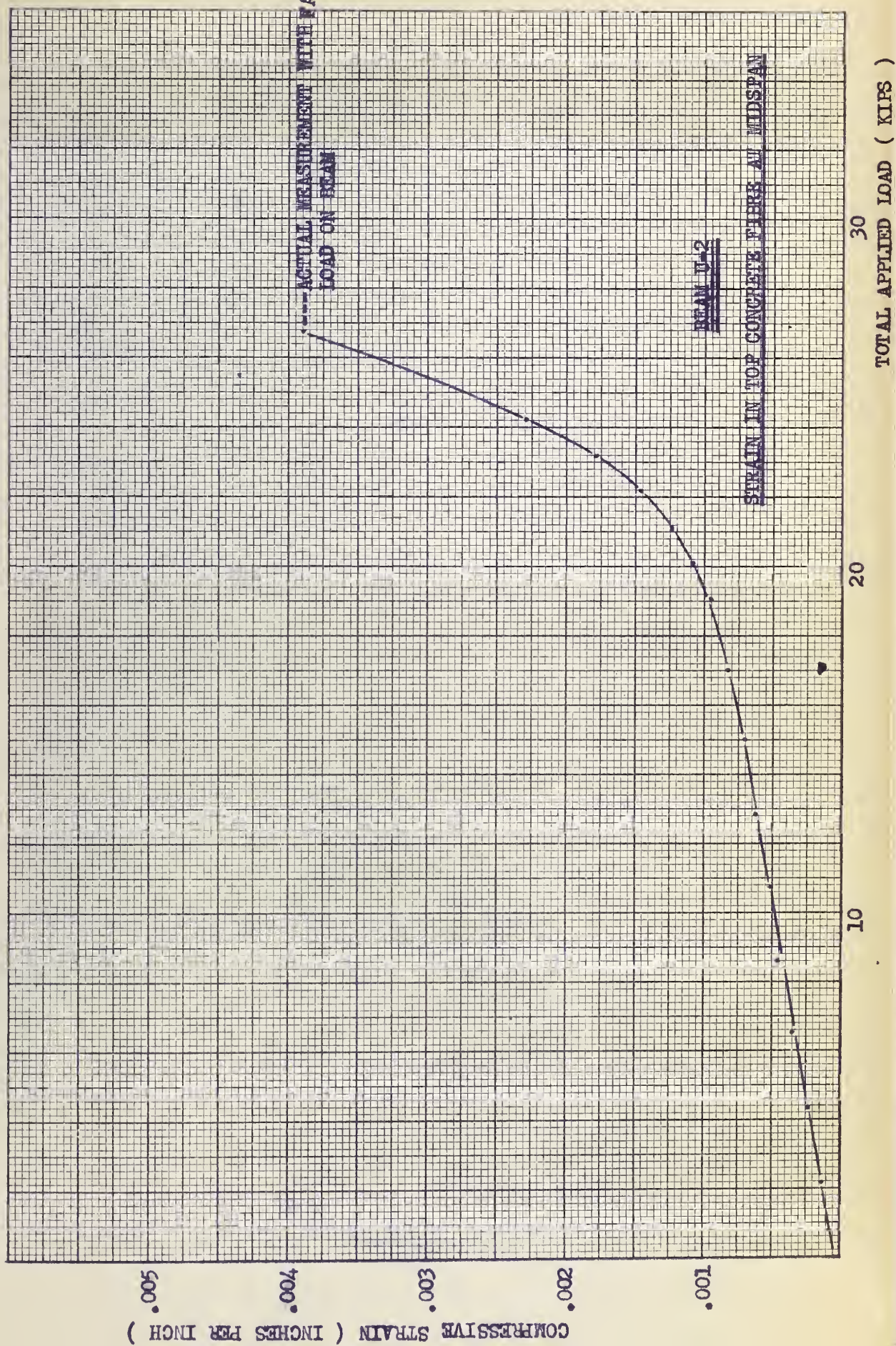
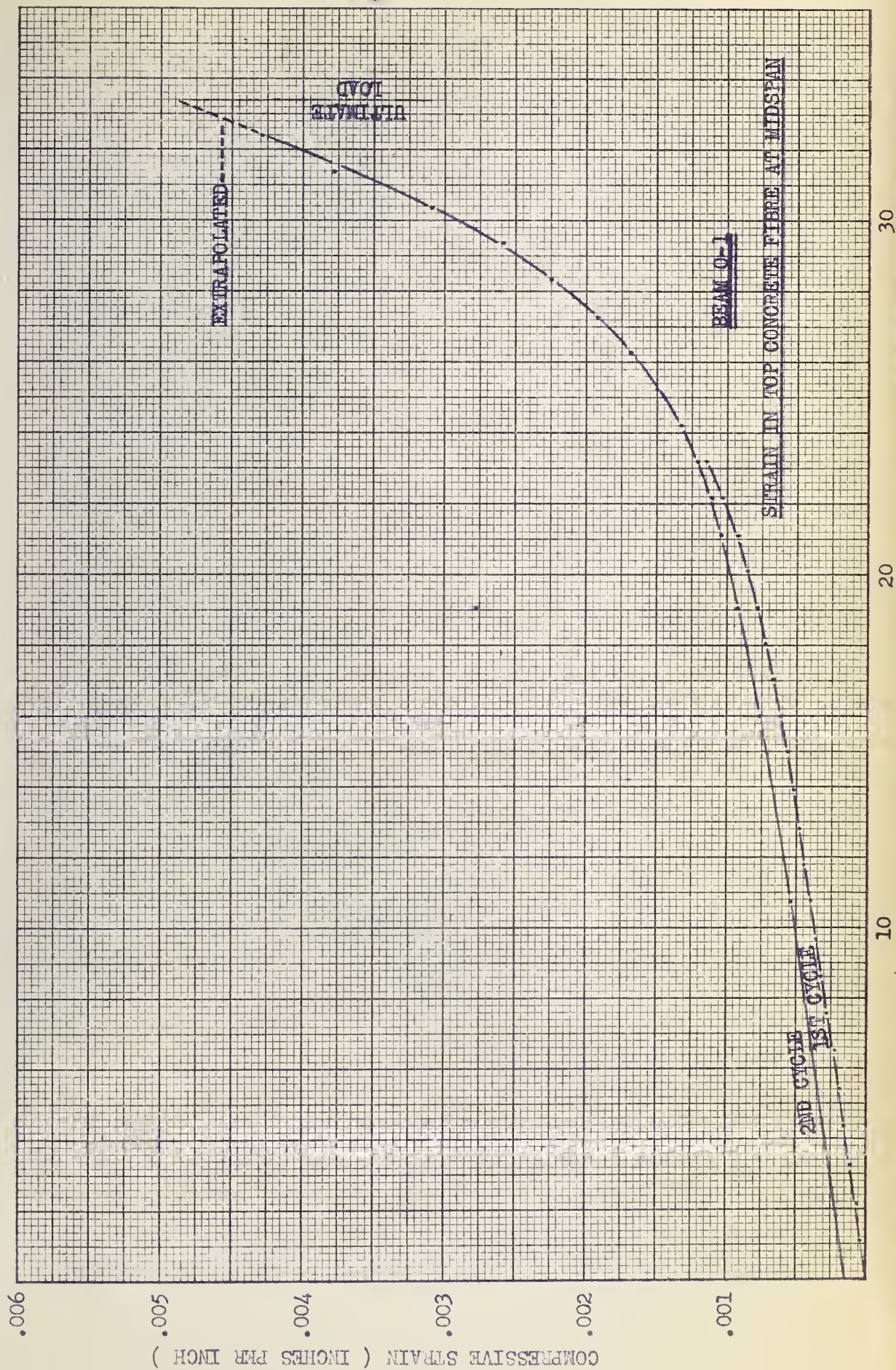


PLATE 43.



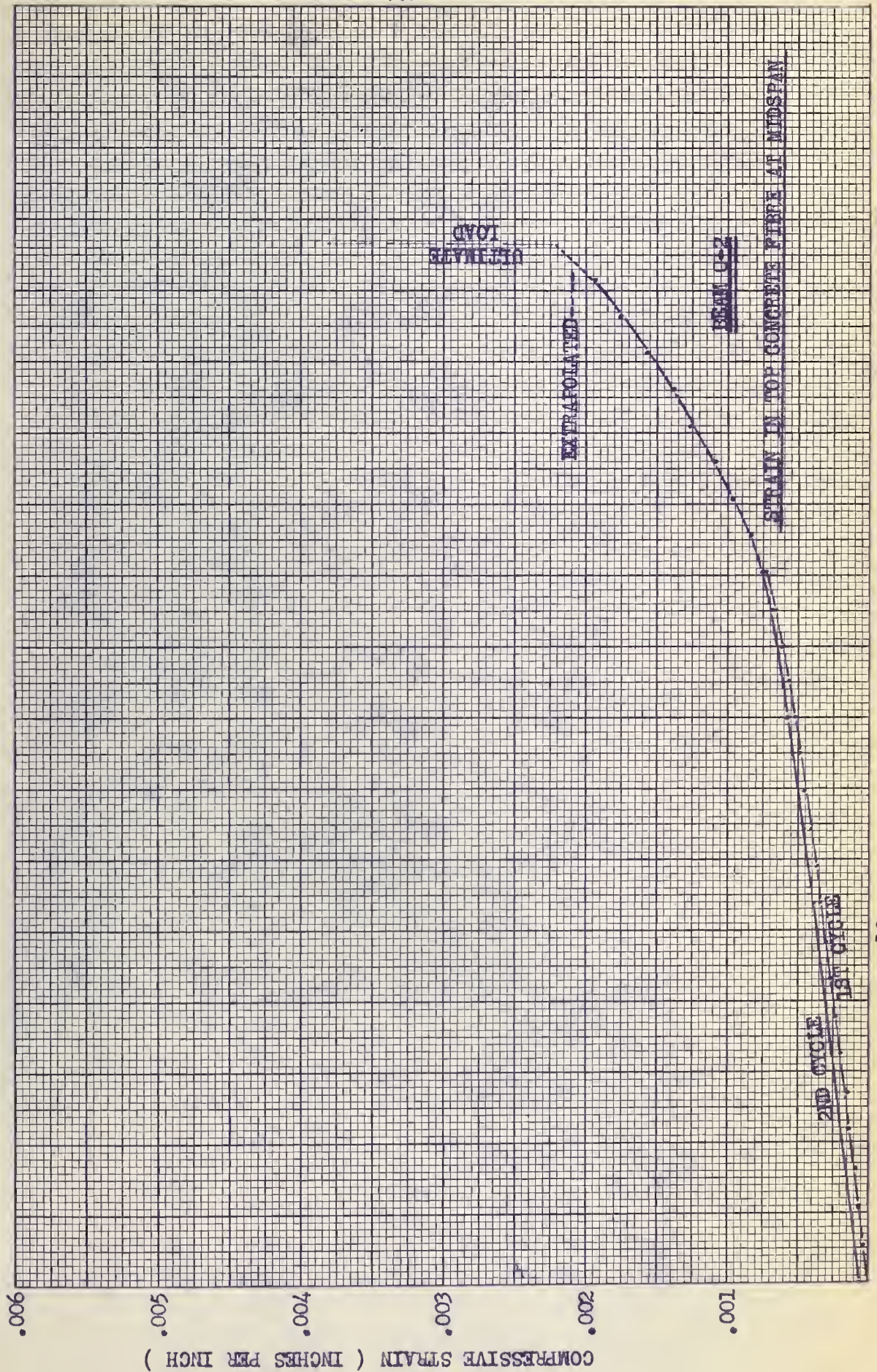
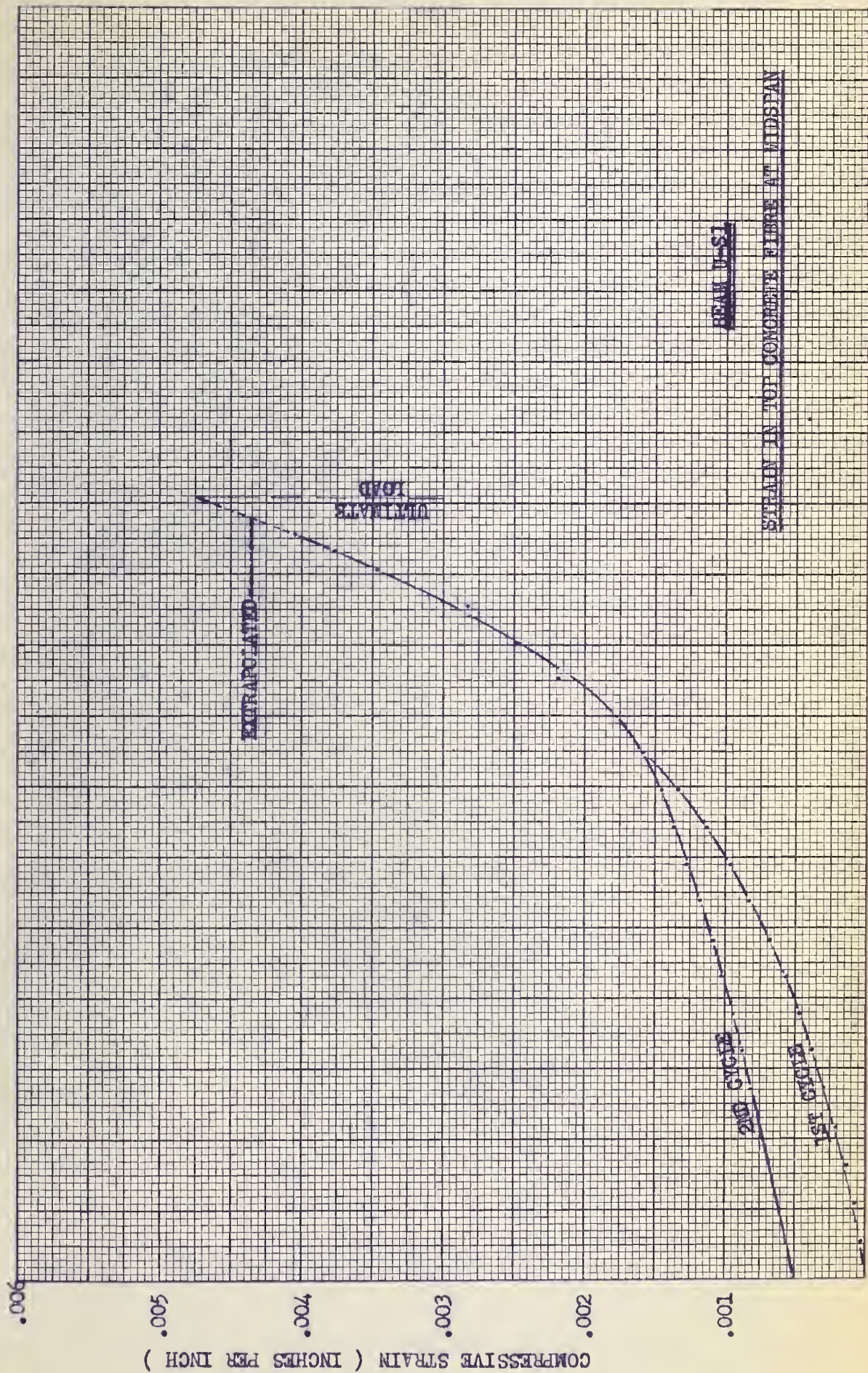


PLATE 45.



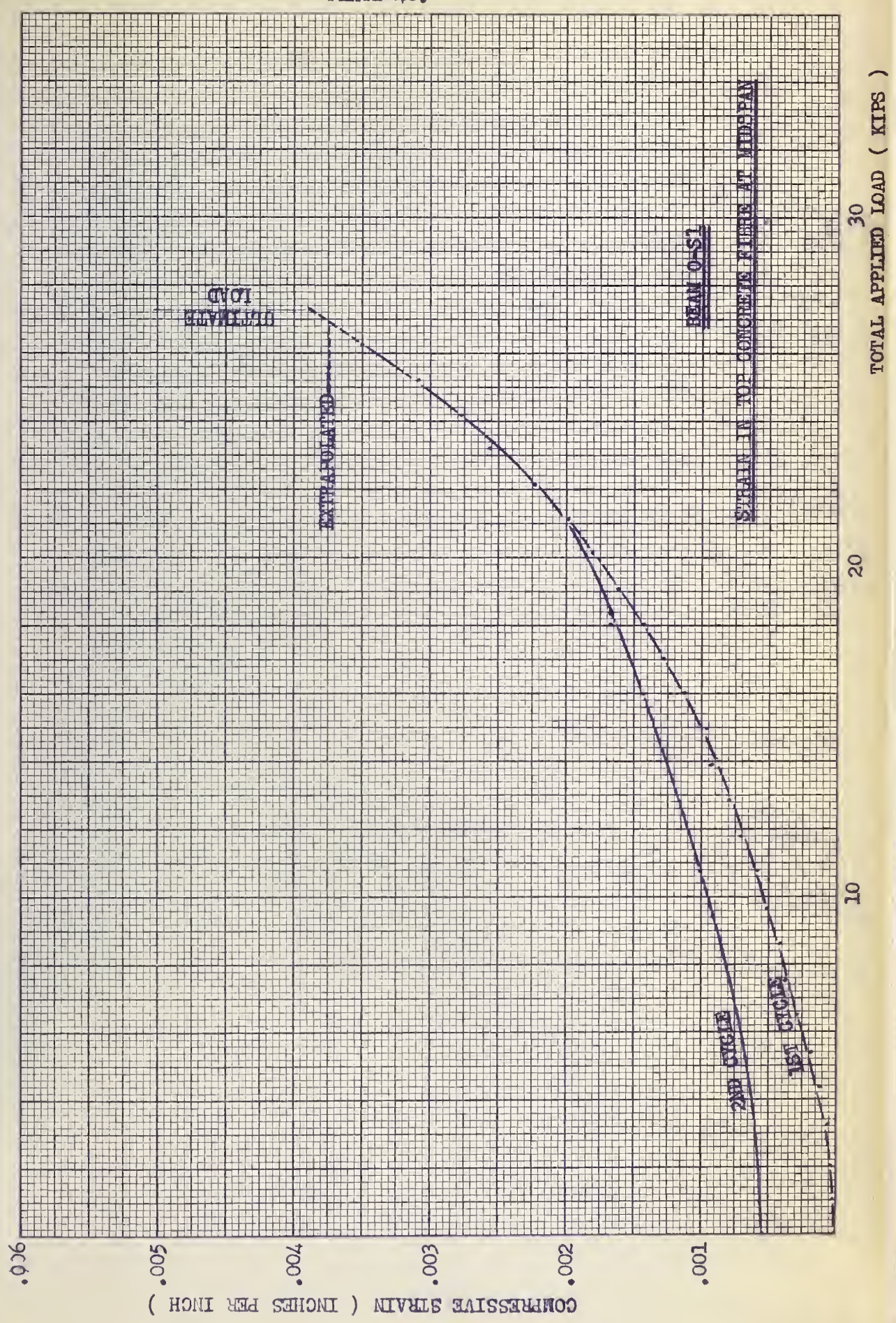
TOTAL APPLIED LOAD (KIIPS)

30

20

10

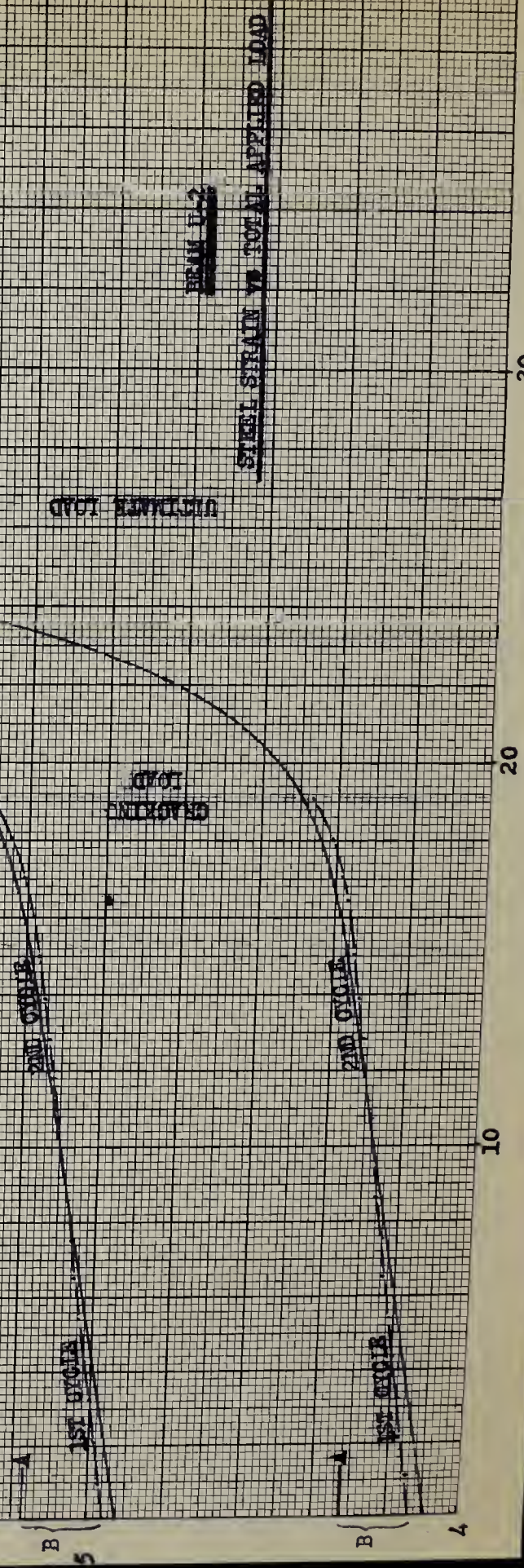
PLATE 46.



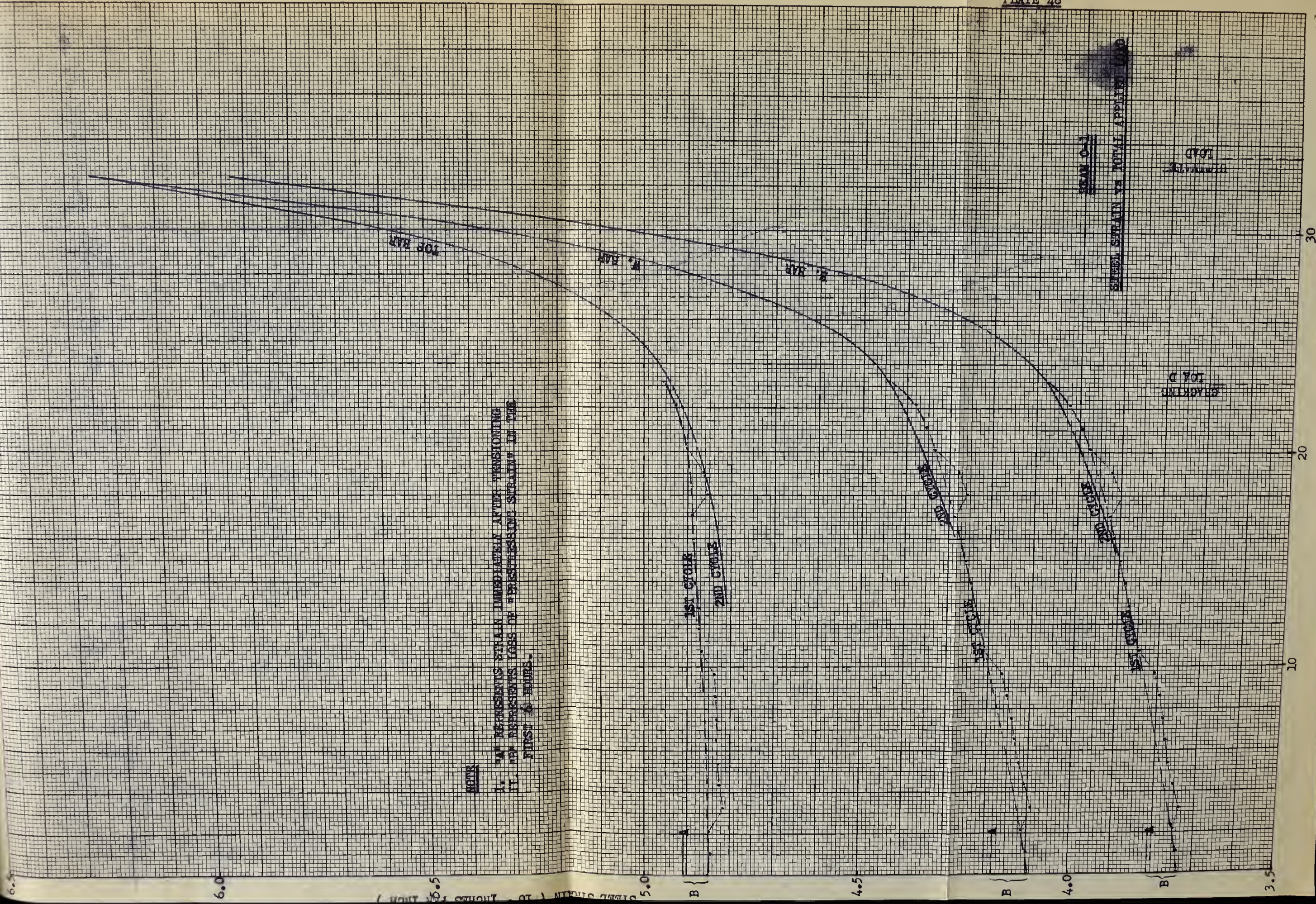
STEEL STRAIN (10⁻³ INCHES PER INCH)

NOTE

- I. "A" REPRESENTS STRAIN IMMEDIATELY AFTER TENSIONING
- II. "B" REPRESENTS LOSS OF PRESTRESSING STRAIN IN THE FIRST 20 HOURS.



TOTAL APPLIED LOAD (KIPS)



NOTE

- I. "M" REPRESENTS STRAIN IMMEDIATELY AFTER TENSIONING
- II. "M" REPRESENTS LOSS OF "PRESTRESSING STRAIN" IN THE FIRST 6 HOURS.

NOTE
I. "A" REPRESENTS STRAIN IMMEDIATELY AFTER TENSIONING
II. "B" REPRESENTS LOSS OF PRESTRESSING STRAIN IN THE
FIRST 20 HOURS.

K. BAR
JOF BAR
F. BAR

FAILURE

100 BAR

2ND CYCLE

1ST CYCLE

1ST CYCLE

2ND CYCLE

2ND CYCLE

1ST CYCLE

PEAK 0-2

STEEL STRAIN VS TOTAL APPLIED LOAD

CRACKING
LOAD

CRACKING
LOAD

20

10

30

TOTAL APPLIED LOAD (KIPS)

3.0

4.0

4.5

5.0

5.5

FAILURE

FROM 1-51

STEEL STRAIN VS TOTAL APPLIED LOAD

30
TOTAL APPLIED LOAD (KIPS)

NOTE

- I. "A" REPRESENTS STRAIN IMMEDIATELY AFTER TENSIONING.
- II. "B" REPRESENTS LOSS OF "PRESSTRESSING STRAIN" IN THE FIRST 28 HOURS.

W. BAR
E. BAR

2ND CYCLE

1ST CYCLE

1ST CYCLE

B

CRACKING
LOAD

ULTIMATE
LOAD

STEEL STRAIN (10³ INCHES PER INCH)

10

20

30

40

50

60

70

80

90

100

110

120

130

140

150

160

170

180

190

200

210

220

230

240

250

260

270

280

290

300

310

320

330

340

350

360

370

380

390

400

410

420

430

440

450

460

470

480

490

500

510

520

530

540

550

560

570

580

590

600

610

620

630

640

650

660

670

680

690

700

710

720

730

740

750

760

770

780

790

800

810

820

830

840

850

860

870

880

890

900

910

920

930

940

950

960

970

980

990

1000

1010

1020

1030

1040

1050

1060

1070

1080

1090

1100

1110

1120

1130

1140

1150

1160

1170

1180

1190

1200

1210

1220

1230

1240

1250

1260

1270

1280

1290

1300

1310

1320

1330

1340

1350

1360

1370

1380

1390

1400

1410

1420

1430

1440

1450

1460

1470

1480

1490

1500

1510

1520

1530

1540

1550

1560

1570

1580

1590

1600

1610

1620

1630

1640

1650

1660

1670

1680

1690

1700

1710

1720

1730

1740

1750

1760

1770

1780

1790

1800

1810

1820

1830

1840

1850

1860

1870

1880

1890

1900

1910

1920

1930

1940

1950

1960

1970

1980

1990

2000

2010

2020

2030

2040

2050

2060

2070

2080

2090

2100

2110

2120

2130

2140

2150

2160

2170

2180

2190

2200

2210

2220

2230

2240

2250

2260

2270

2280

2290

2300

2310

2320

2330

2340

2350

2360

2370

2380

2390

2400

2410

2420

2430

2440

2450

2460

2470

2480

2490

2500

2510

2520

2530

2540

2550

2560

2570

2580

2590

2600

2610

2620

2630

2640

2650

2660

2670

2680

2690

2700

2710

2720

2730

2740

2750

2760

2770

2780

2790

2800

2810

2820

2830

2840

2850

2860

2870

2880

2890

2900

2910

2920

2930

2940

2950

2960

2970

2980

2990

3000

3010

3020

3030

3040

3050

3060

3070

3080

3090

3100

3110

3120

3130

3140

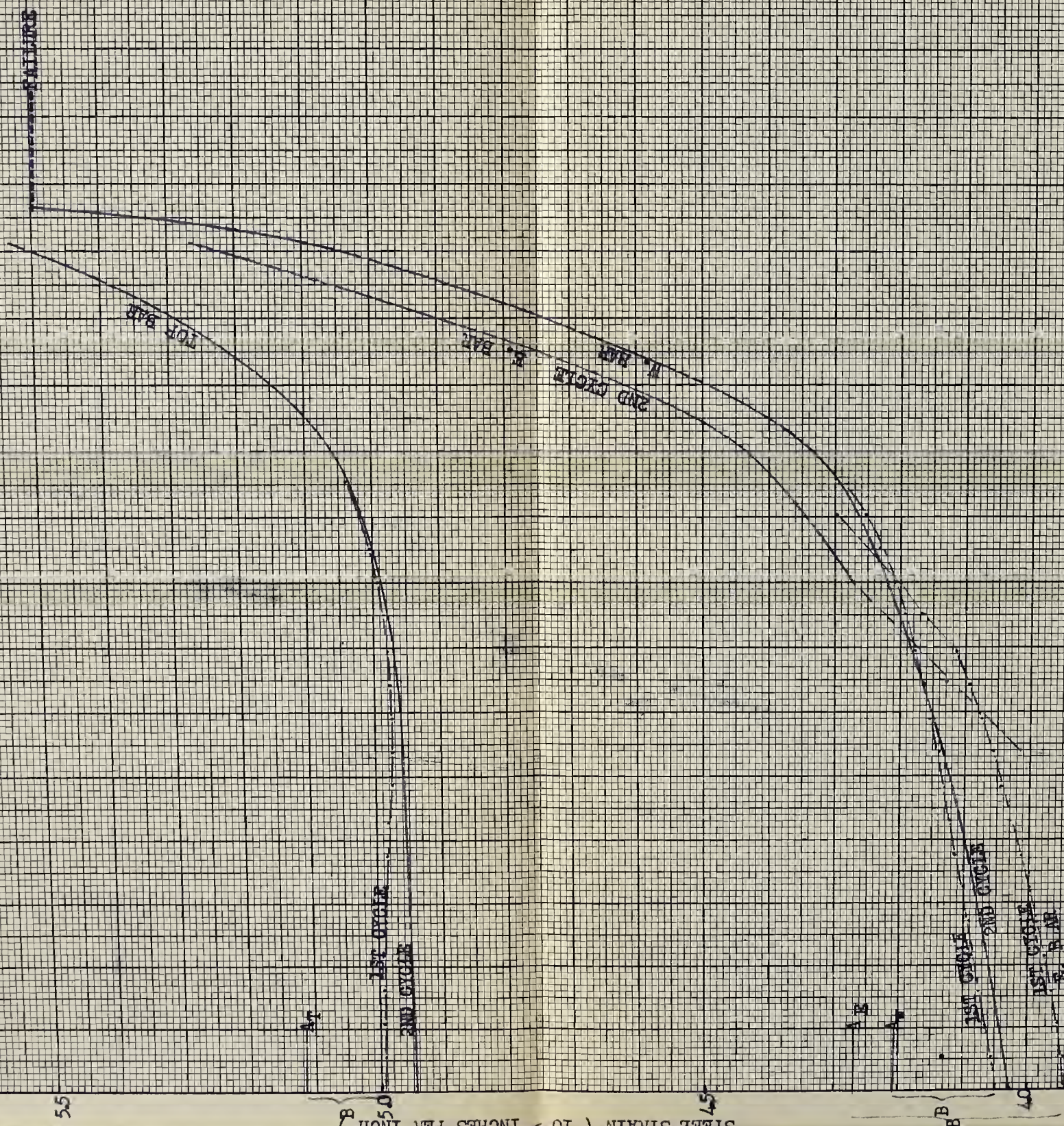
3150

3160

3170

3180

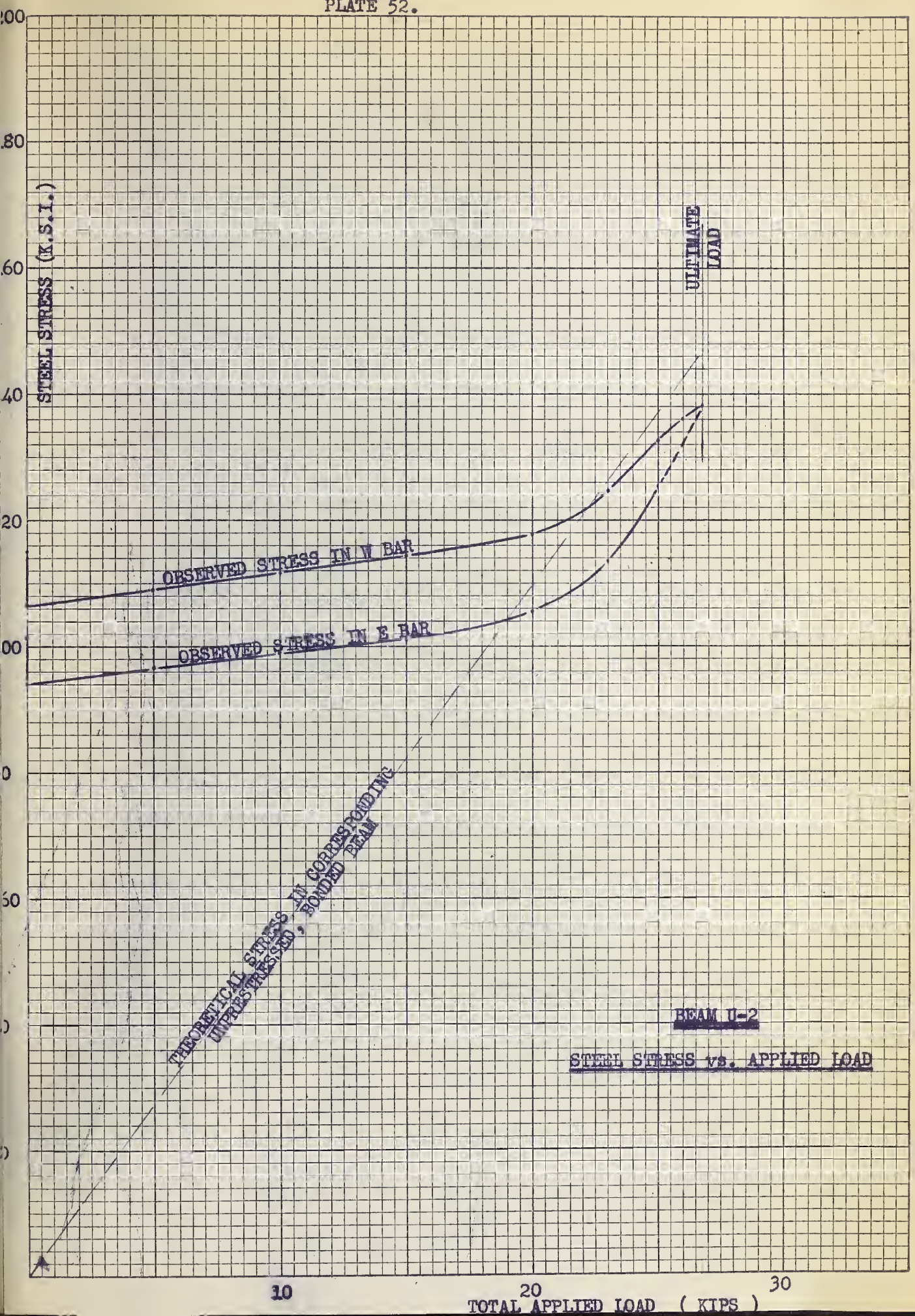
3190

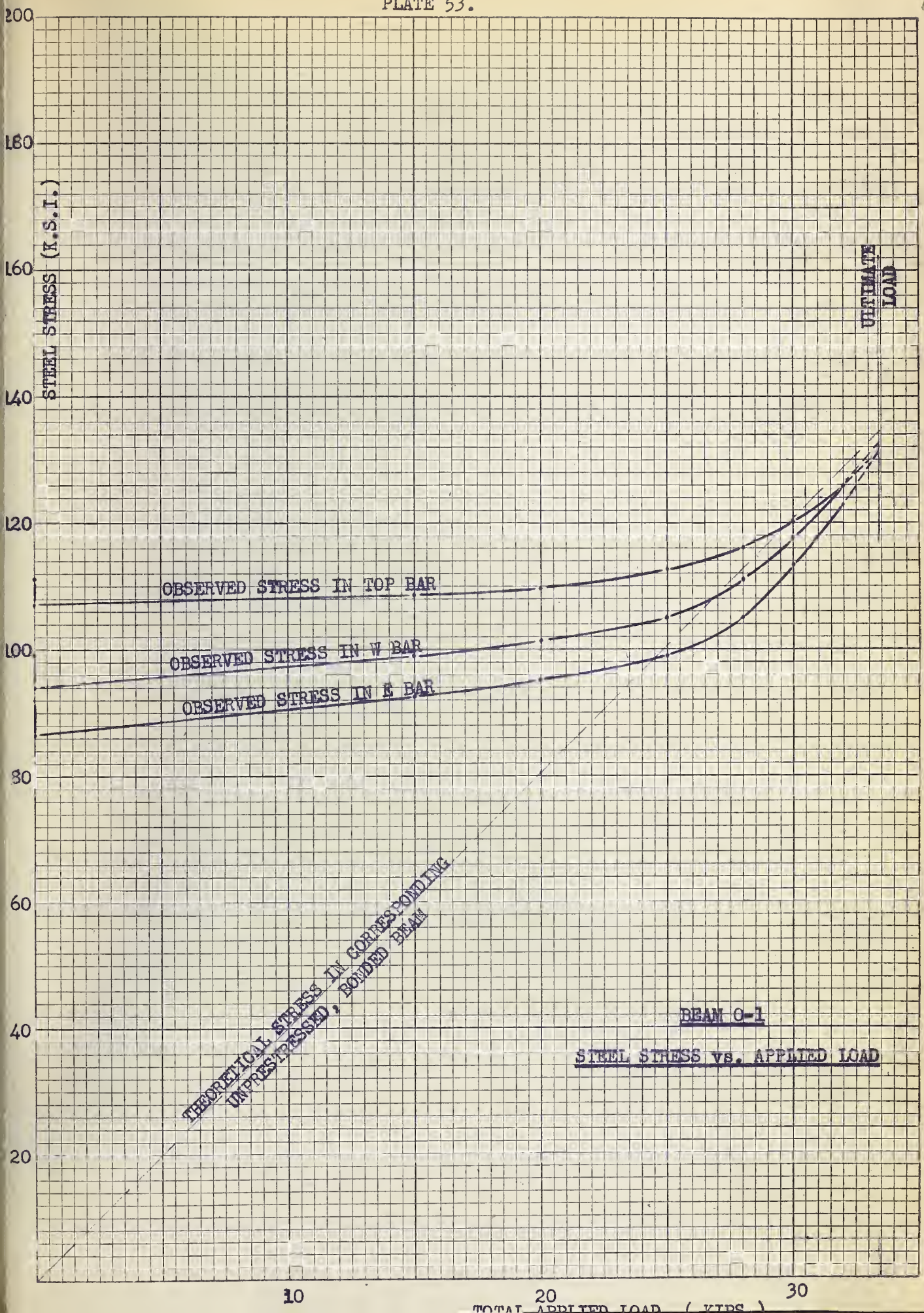


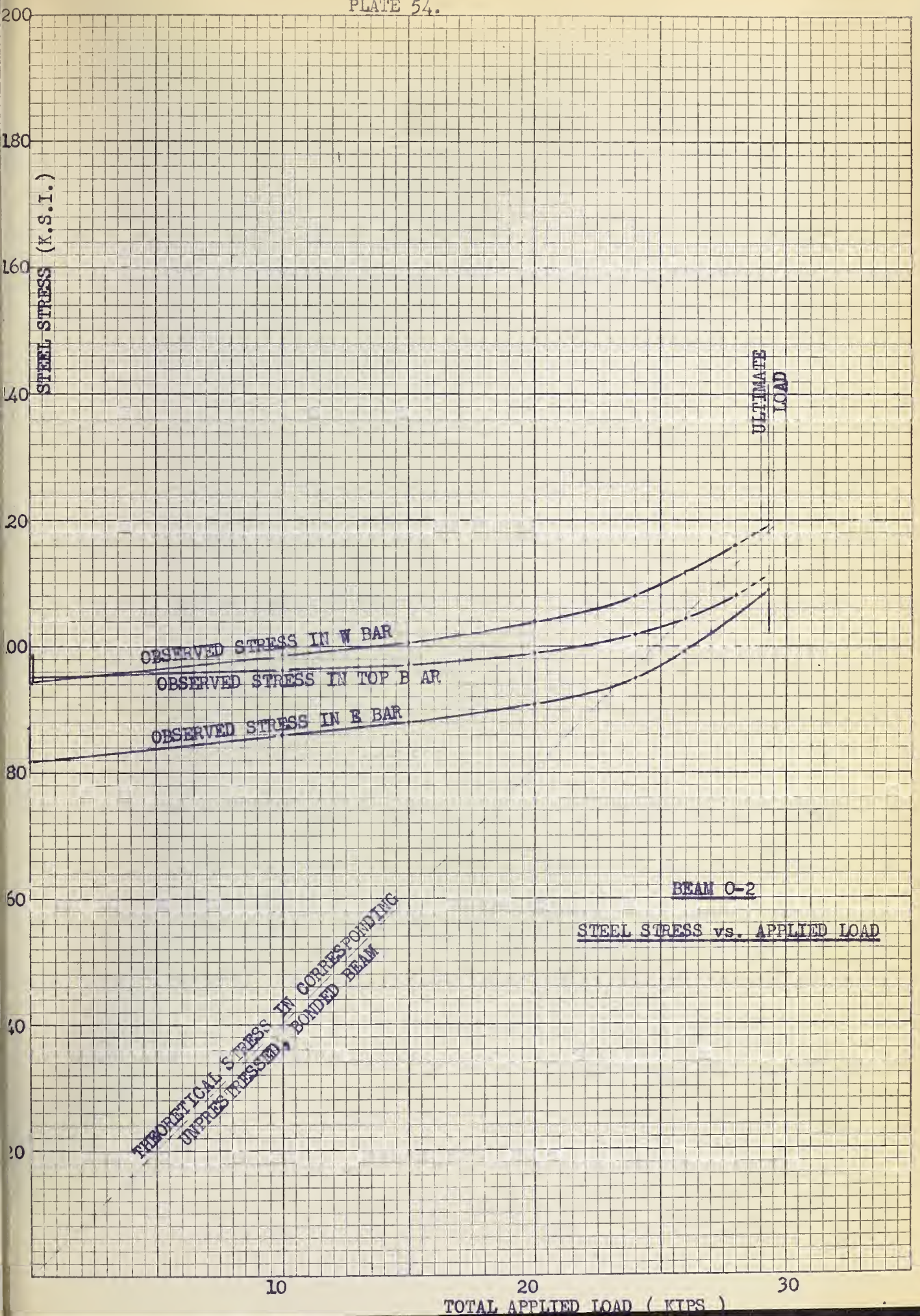
NOTE

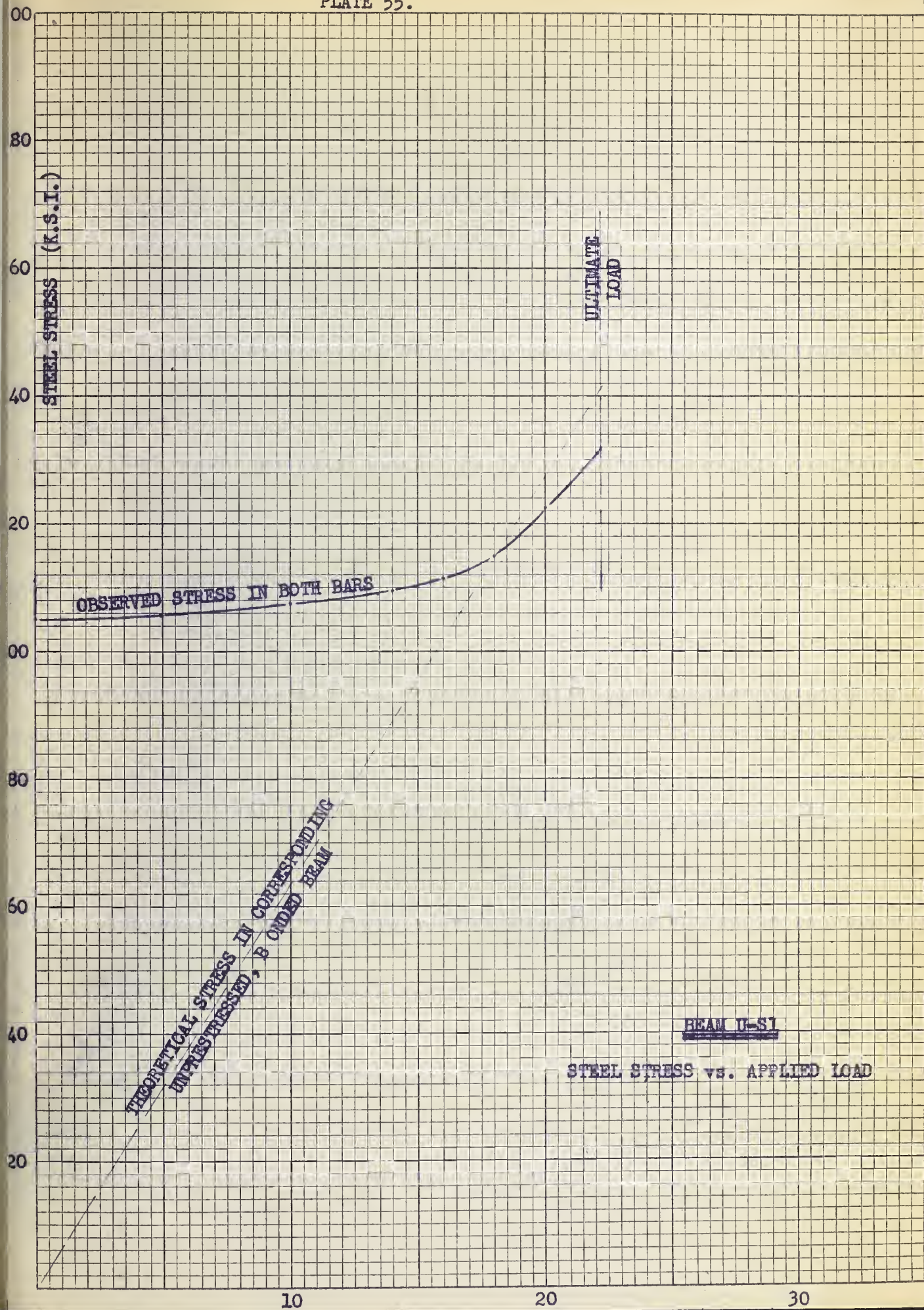
I. "A" REPRESENTS STRAIN IMMEDIATELY AFTER FINISHING

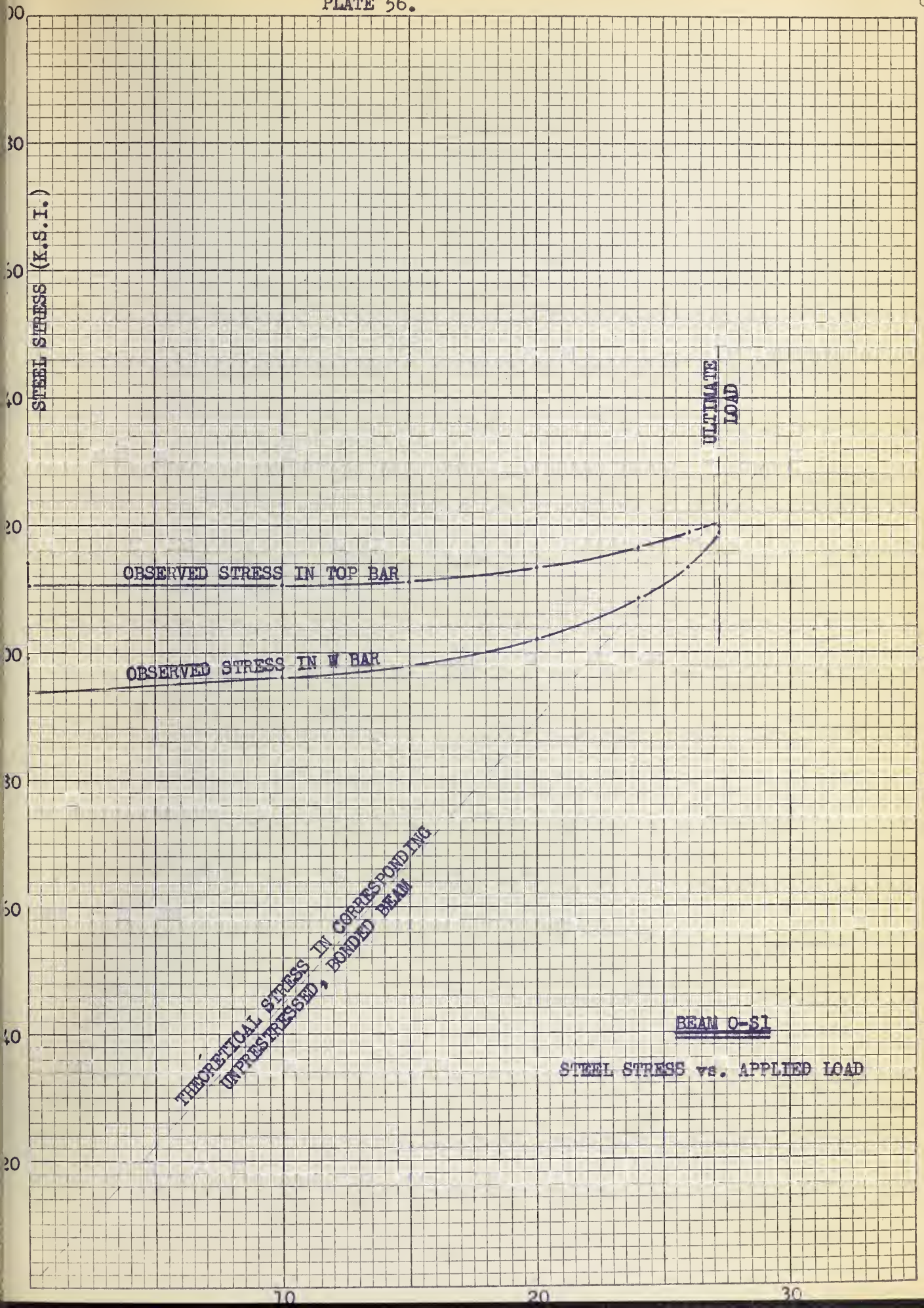
II. "B" REPRESENTS LOSS OF "PRESTRESSING STRAIN" IN THE FIRST 2.0 HOURS.











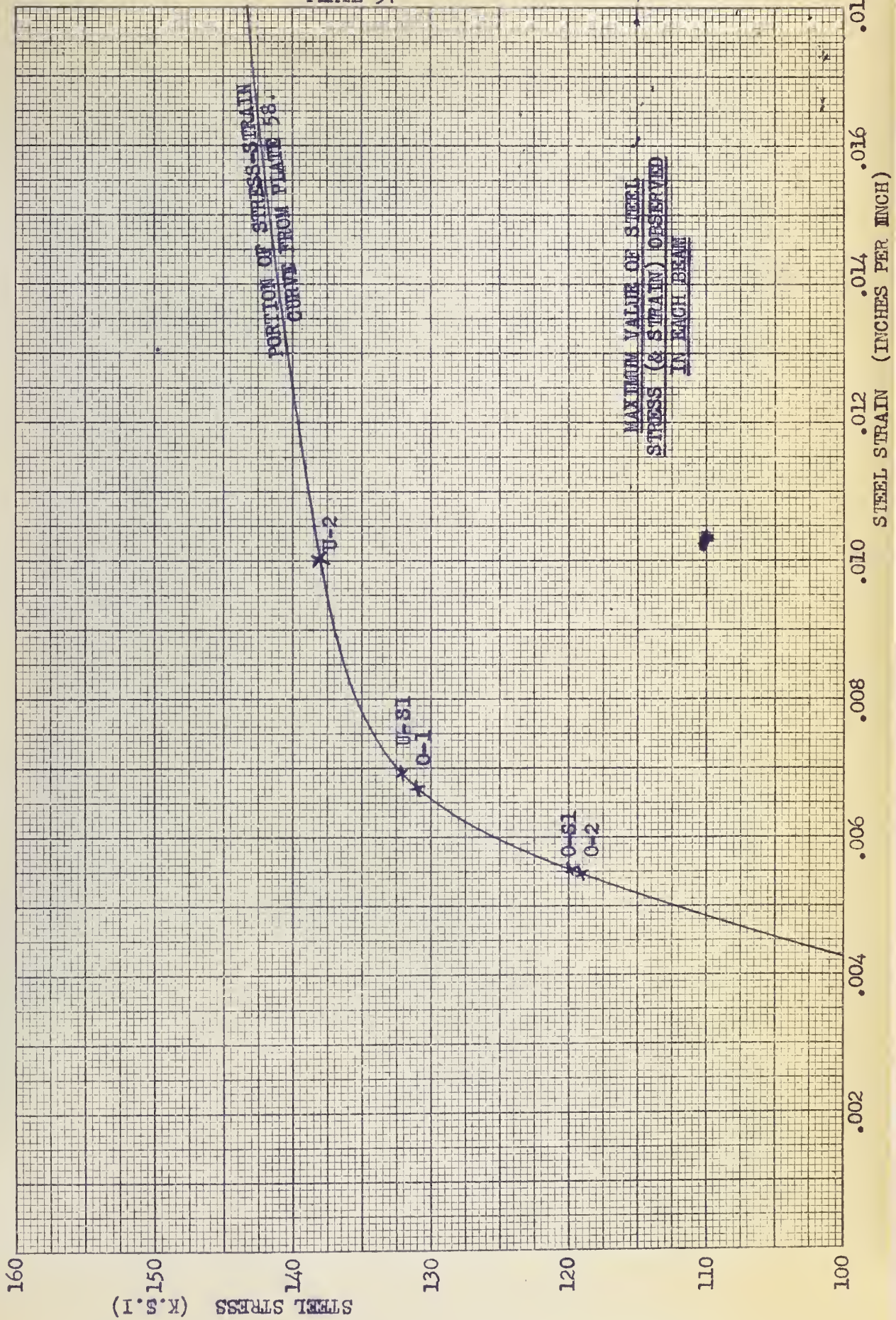


TABLE I - OTHER DATA

BEAM	CYLINDER STRENGTH f'_c p.s.i.	CRACKING (dead wt. not included)		ULTIMATE (dead wt. not included)		ACTUAL PRESTRESSING FORCES (kips)		OBSERVED MAX. STEEL STRAIN (Under external load).
		LOAD kips.	MOMENT ft.kips	LOAD kips	MOMENT ft.kips	BOTTOM BAR	TOP BAR	
U-1	4700	17.0	28.4	24.7	41.2	not measured.		
	4000							
	3700							
	3900							
U-2	6100	19.1	31.8	26.8	44.7	42.3	<u>none</u>	.0052 in./in. (bottom bars)
	6300							
	5400							
	5800							
O-1	5550	23.2	38.7	33.4	55.7	38.5	22.3	.0025 in./in. (bottom bars)
	5760							
	5650							
	6200							
O-2	5300	20.1	33.5	29.3	48.9	37.3	19.8	.0013 in./in. (bottom bars)
	5730							
	5830							
	4740							
U-S1	5800	14.9	24.9	22.2	37.0	43.4	<u>none</u>	.0022 in./in.
	5510							
	5900							
	5630							
O-S1	5510	19.1	31.8	27.3	45.5	38.5	22.9	.00135 in./in. (bottom bars)
	4420							
	5020							
	5480							

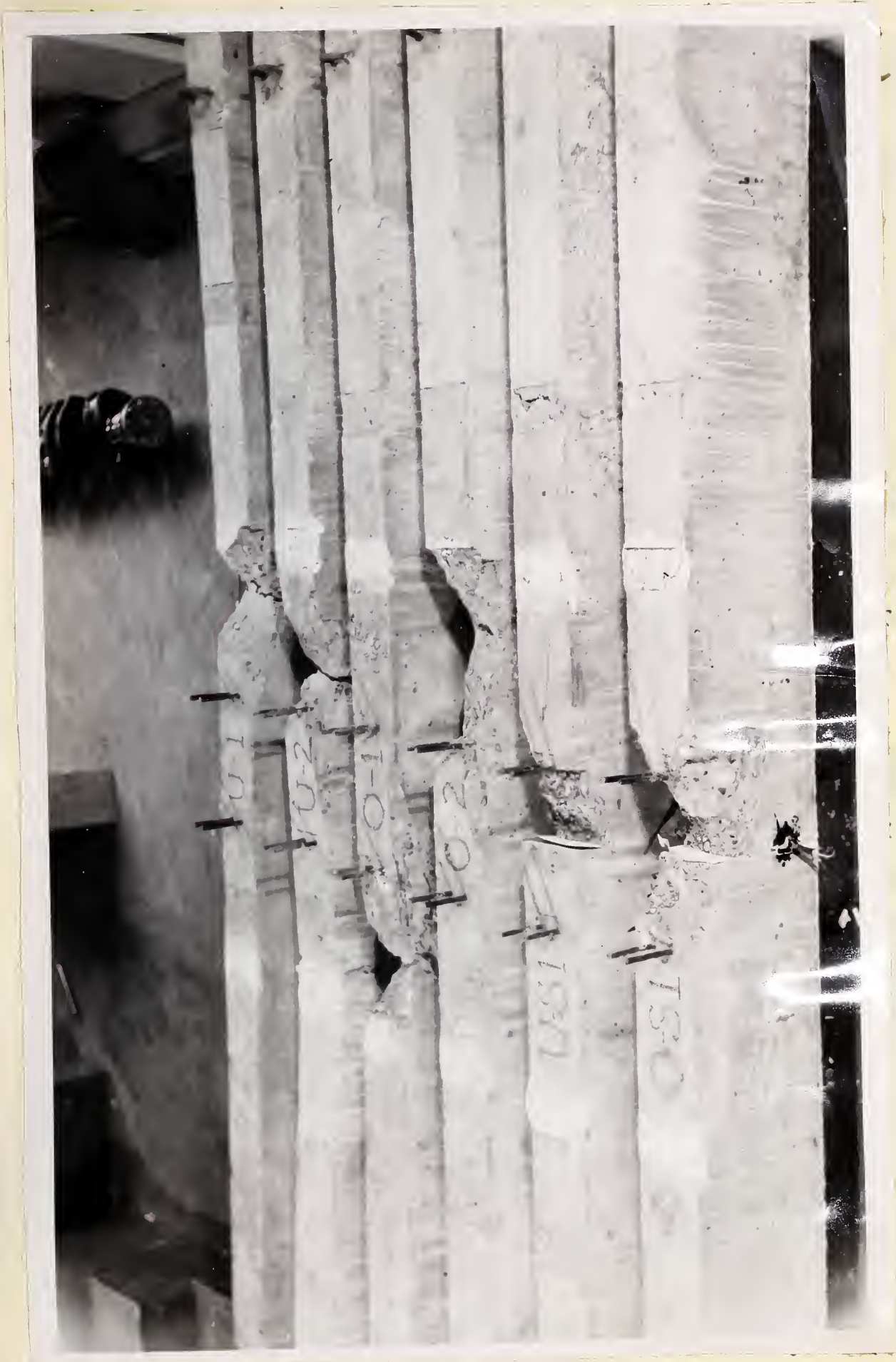


Figure 7. The physical characteristics of the various failures.

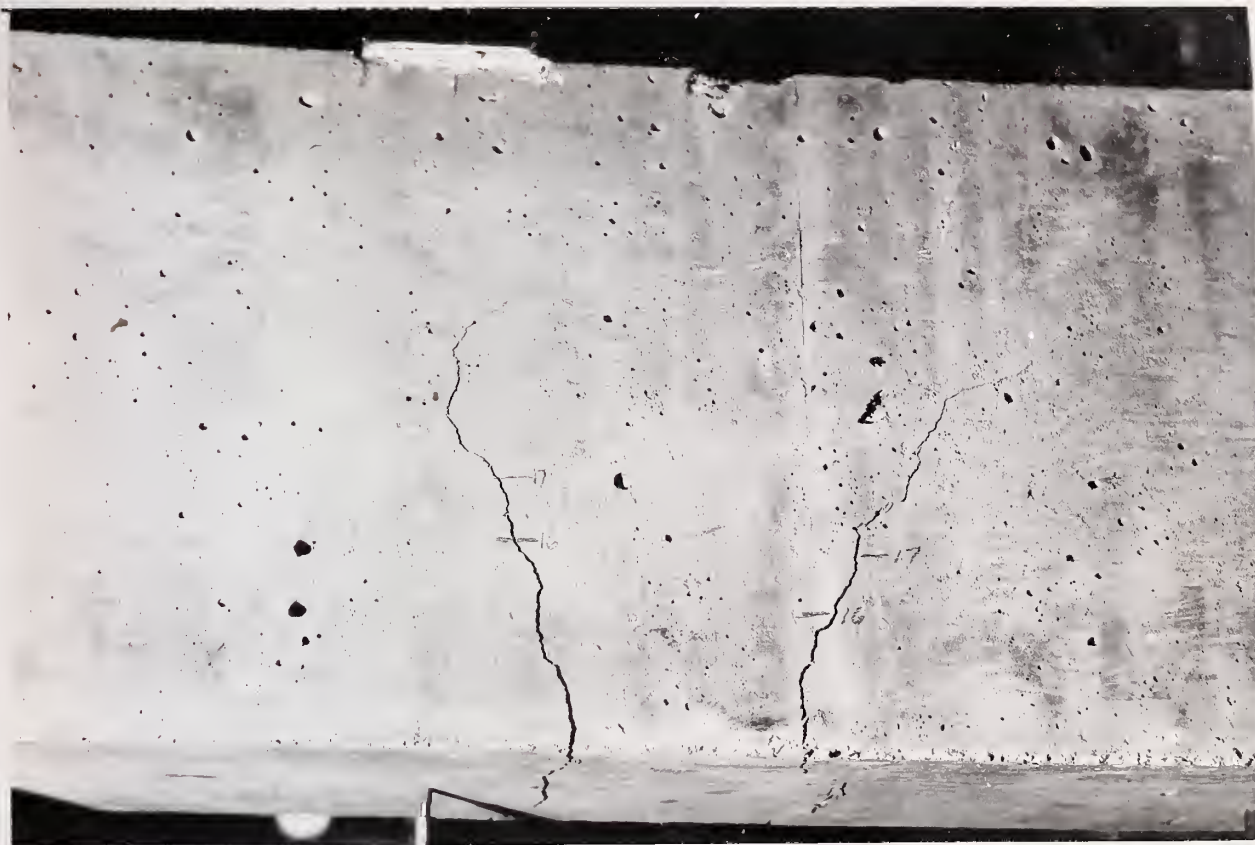


Figure 8. Failure zone of Beam U-1 as the cracks were beginning to develop. (load 22 kips)

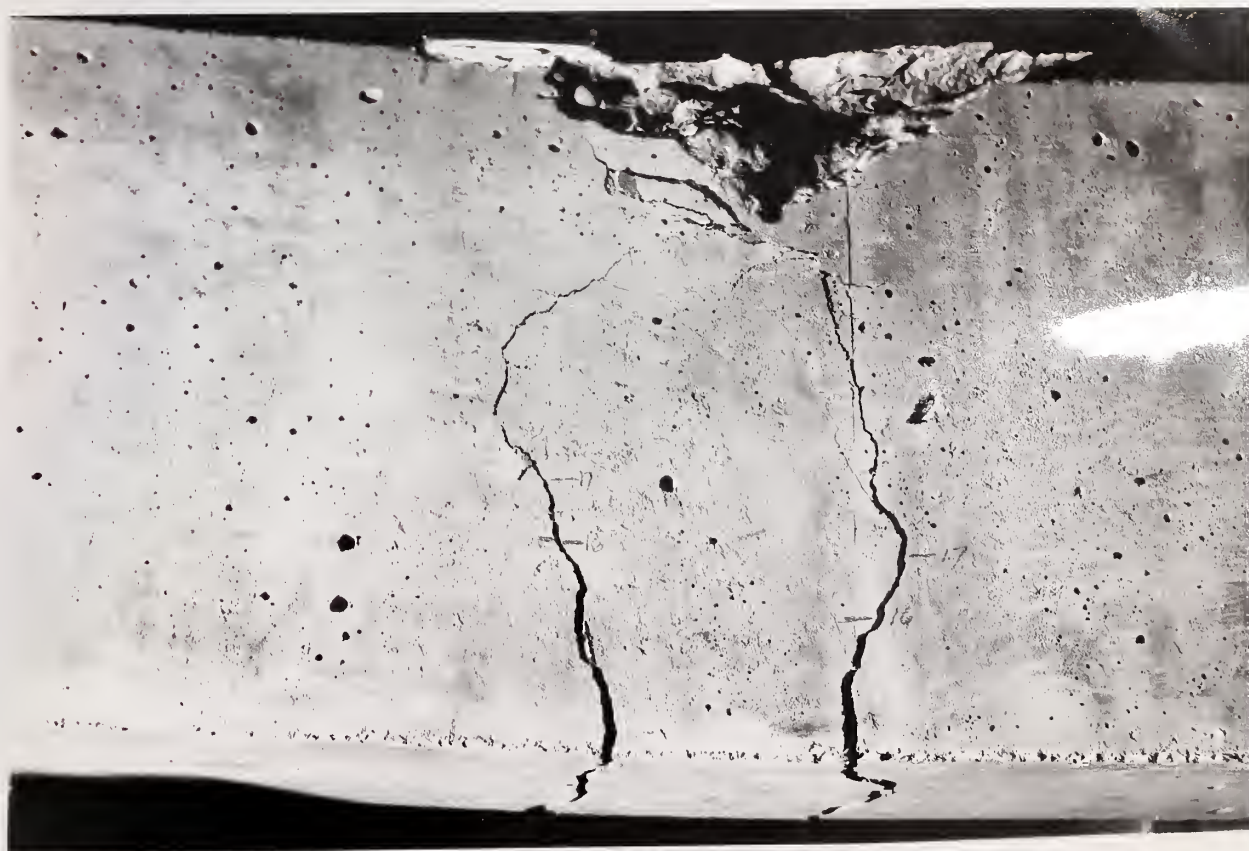


Figure 9. A closeup of the failure in Beam U-1. (load 24.7 kips)

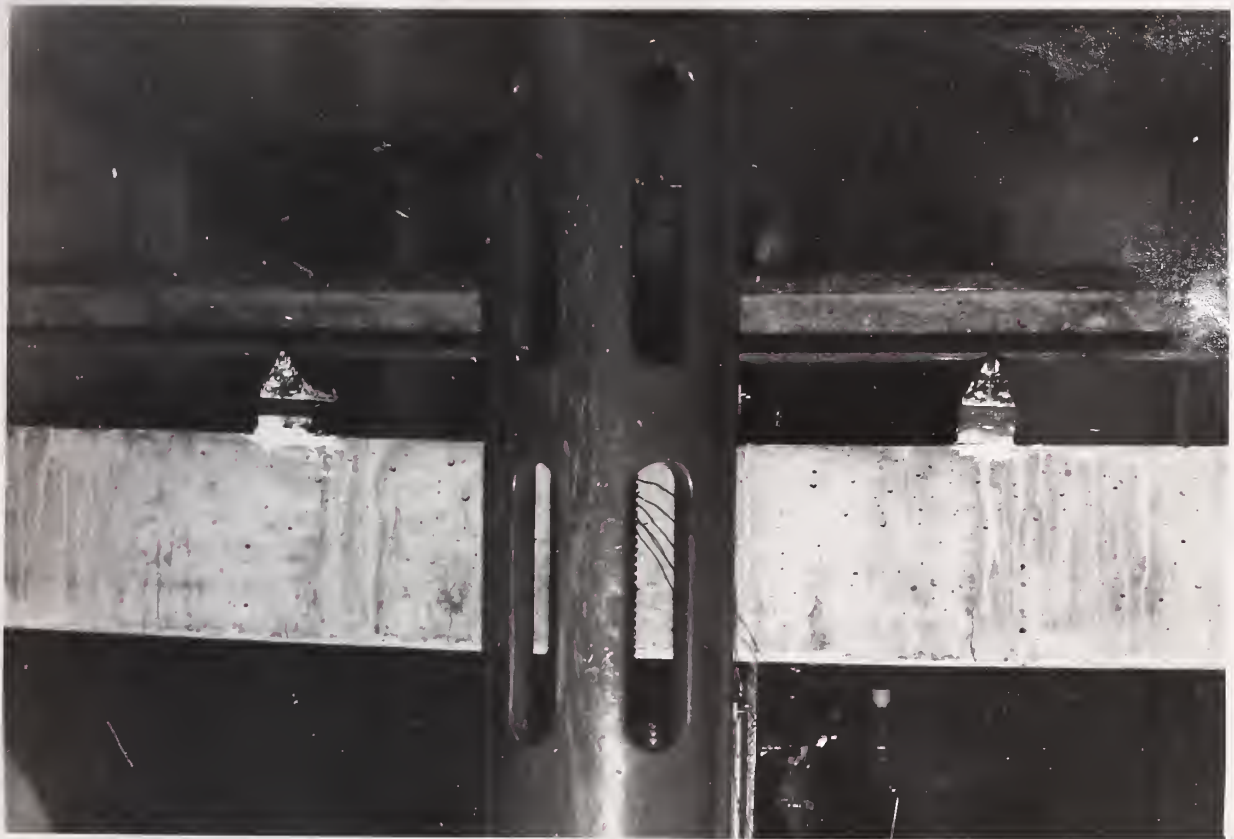


Figure 10. Beam 0-1 under a load of 31.5 kips.



Figure 11. The horizontal cracks obtained with Beam U-S1.
(load 20 kips)

VII DISCUSSION OF RESULTS

1. Load-Deflection Characteristics

The Load-Deflection curves all have the same general shape. During the initial stages of loading deflections are very nearly proportional to the applied loads. There is little deviation from the straight line at loads which are 70% of the cracking load or less. At about 90% of the cracking load there is a marked change in slope. Following cracking the rate of change of deflection with respect to applied load continues to increase till the ultimate load is reached.

All beams showed a residual deflection of at least 0.02 in. after being subjected to loads which caused cracking. However, Beams U-S1 and O-S1 had 50% greater residual deflections than did the other beams.

2. The Axis about which Sections Rotate

The points plotted in Plates 35 to 40 are somewhat scattered, yet they do give some general indications of the position of the axis about which plane sections rotate during bending. Hognestad's work⁷ points out that plane sections do remain plane during bending.

In Beams U-2, O-2, U-S1, and O-S1 the axis of rotation rose noticeably before the cracking load was reached. During the early stages of loading the axis of rotation in Beams U-2, O-1, U-S1 and O-S1 was between $\frac{1}{2}$ in. and 1 in. lower than the centre of gravity axis. It would appear from these results that, even during the early stages of loading, sections do not rotate about the centre of gravity axis which

is indicated by the elastic theory. Since sections apparently rotate about an axis which is lower than the centre of gravity axis before cracking occurs, the actual change in stresses in the bottom fibres under an external load is somewhat less (in the top fibres it is more) than the elastic theory would indicate. This could be partly the reason why the observed cracking loads are larger than the computed ones.

3. Concrete Strains (in the top fibre)

The curves in Plates 41 to 46 indicate that the compressive strain in the top concrete fibre is very nearly proportional to the total applied load for loads up to the cracking load.

The average ultimate compressive strain in the concrete was found to be 0.0039 ins./in. The method used here to arrive at this value (by extrapolation of a load-strain curve) is the same as that used by Hognestad. The value he obtained, from tests on 100 columns, was 0.0038 in./in.. Chambaud, in France, has suggested a value of 0.0036 in./in., but it is not known how he arrived at his figure.

There are two factors which have not been considered in these results and which could influence the value of 0.0039 in./in. Firstly, no account was taken of the initial tensile strains which occurred in the top fibre under the prestressing force. Secondly, the measurements were not taken at the failure section. The first would cause the indicated value to be too high; the second would cause it to be too low.

4. The Cracking Loads

The observed and estimated cracking loads are compared in Table II. In the fourth column the estimated cracking load has been adjusted by the amount of over-stressing.

BEAM	CRACKING LOAD (KIPS)		
	Observed	Estimated	Adjusted
U-1	17.0	15.5	----
U-2	19.1	15.5	16.5
O-1	23.2	19	20
O-2	20.1	19	18.5
U-S1	14.9	13.2	14.0
O-S1	19.1	16.7	17.5

TABLE II

From Table II it is readily apparent that even when the exact prestressing force is taken into account the observed cracking loads are still 6% to 15% higher than the computed cracking loads. It should be realized that the computations are based on an assumed tensile strength for the concrete of 750 p.s.i. or $0.15f'_c$. That value might be too low. It is also possible that the first crack is not visible as soon as it forms. However, part of the 6% to 15% difference between observed and computed values for the cracking load is probably due to the fact that sections rotate about an axis which is lower than the elastic theory would indicate (discussed in part B).

5. Steel Stresses (& Strains)

The peculiar effects observed with Beam O-1 (Plate 48)

cannot be explained completely. The electric gauges were tested for short circuits several times and each time there was no indication of such. However, the sudden drop in steel strains which occurred in identical spots for all three bars points to two possible causes:

1. disturbance of the temperature compensation gauge,
2. a sudden draft of warm or cold air on the compensating gauge.

The inconsistent action of the gauge point on the east bar of Beam O-S1 was very likely the result of the difficulties experienced in post-tensioning that bar. The anchorage device slipped (by "stripping" the nut) after the jack had been released. The gauges could have been damaged by the sudden movement of the bar with respect to the concrete. On the other hand, the discontinuity of the strain curve for that bar may be due to a "tightening up" of the ten split washers that had to be used when the bar was re-tensioned.

With these two exceptions, the Steel Strain vs. Total Applied Load curves are typical:

1. They are very nearly straight lines initially.
2. They curve upwards just before the cracking load is reached.
3. They show a residual plastic strain in the steel after loading and unloading.

The curves indicate that there is a residual plastic strain in the steel of less than 0.00005 ins./in. after one cycle of loading up to the cracking load. This corresponds to a

loss in prestress of only 1.0 to 1.5 k.s.i. (or of the order of $1\frac{1}{2}\%$ of the initial prestressing force). The Steel-Stress vs. Total Applied Load curves show a loss in prestressing force of 6% to 7% during the first day and 4% to 5% during the first 6 hours.

The Stress-Load curves in plates 52 to 56 show that there is about 6% to 10% increase in steel stress when a beam is loaded to its cracking load. There will be an error (on the safe side) in the cracking load when it is computed on the basis that the area and moment of inertia in an unbonded beam are those for the concrete section alone. This is still another reason why the computed cracking load is less than the observed value. The theoretical curves which have been superimposed on the above plates have been computed on the assumption that $n = 5$ and using the standard elastic theory for composite sections. Thus they are somewhat simplified. The stress-strain moduli for the steel and concrete were obtained from plate 58 and reference 7, respectively.

6. Ultimate Loads

Table III presents the ultimate moments that were observed and the final values of j (the ratio of the moment arm to the effective depth) which were computed using the observed maximum steel stresses.

It is apparent from this table that the final value of j (just before failure occurred) was higher in the beams with two bars than in those with three bars, compare 0.98 vs. 0.95. Also, it can be seen that the final value of j

BEAM	ULTIMATE LOAD (kips)	ULTIMATE MOMENT (ft.-kips)	MAX. STEEL STRESS (k.s.i.)	MAX. FORCE IN STEEL (kips)	MOMENT ARM (ins.)	EFFECTIVE DEPTH, d (ins.)	$j = \frac{\text{MOMENT ARM}}{d}$
U-1	24.7	41.0	no steel strain observed				
U-2	26.7	44.5	137	57.5	9.3	9.5	0.98
O-1	33.5	55.5	131	82.0	8.2	8.83	0.93
O-2	29.3	49.0	112	70.0	8.4	8.83	0.95
U-S1	22.2	37.0	132	55.5	8.0	8.25	0.97
O-S1	27.3	45.5	120	75.0	7.3	8.00	0.91

TABLE III ULTIMATE MOMENTS & VALUE OF j AT FAILURE

was reduced by 1% to 2% where there was a joint in the concrete.

7. Physical Characteristics of the Failures

The extent of destruction in the respective failure zones is illustrated in figure 7. It should be mentioned that the end anchorages in Beams U-1 and U-2 had been released before the photograph was taken; thus figure 9 is a better indication of the failure zone in these beams. All failures resulted from crushing of the concrete. However, the failures developed in different manners.

With Beams U-1 and U-2, one of the cracks which had formed under a load point kept increasing in size until it was within two inches of the top of the beam. The crack opened as much as 1/4 of an inch (at the bottom) before the concrete was crushed. In all likelihood the failures were initiated by excessive yielding of the steel (see Plate 57). That is what is commonly called a tension failure with reinforced concrete beams.

With Beams O-1 and O-2, the development of cracks was retarded and the cracks did not progress as high into the beam. Figure 10 shows Beam O-1 while it was carrying 95% of its ultimate load; there are no cracks in the upper half. Just before failure horizontal cracks developed near the midpoint. At failure the concrete above the horizontal cracks burst upwards.

With Beams U-31 and O-31, the failures occurred at the centre joint. Horizontal cracks were observed in the former, see figure 11.

In general, the failures in the more heavily reinforced beams were more destructive and more sudden.

VIII CONCLUSIONS

1. With respect to deflections, the behavior of these beams was, for all practical purposes, elastic at loads up to 70% of the cracking load; there was no marked deviation from the straight line (in the load-deflection curve) with loads up to 90% of the cracking load. After the first cycle of loading, 50% higher residual deflections were observed for beams which had a joint in the concrete at midspan.

2. There is an indication that plane sections rotate about an axis which is initially $\frac{1}{2}$ inch to 1 inch below the centre of gravity axis. The axis of rotation moves upwards as loads are applied.

3. An average value of 0.0039 inches/inch has been obtained for the ultimate compressive strain in the concrete.

4. It has been found that the usual design relationship predicts cracking loads that are 6% to 15% low when the tensile strength of concrete is assumed to be $0.15f_c'$.

5. For concrete beams prestressed with unbonded Lee-McCall tensioning units, the loss in prestress due to creep and shrinkage was found to be of the order of; 7% during the first day, 5% during the first 6 hours.

6. A value of 0.97 has been indicated for the ratio of the moment arm to the effective depth for rectangular beams with a percentage of steel of 0.0073; 0.94 for those with a percentage of steel of 0.012. The values were 1% to 2% lower for beams with a joint in the concrete.

7. The more highly reinforced beams generally gave more destructive failures.

BIBLIOGRAPHY

1. "Prestressed Concrete", Gustave Magnel; Concrete Publications; Limited;
2. "Principles and Practice of Prestressed Concrete", P.W. Abeles; Fredrick Ungar Pub. Co., New York; 1949.
3. "Prestressed Concrete Structures", A.E. Komendant; McGraw-Hill Book Co., Inc., New York; 1952
4. "Prestressed Concrete", Y. Guyon; John Wiley and Sons, inc., New York; 1953.
5. "Proceedings of the First United States Conference on Prestressed Concrete", M.I.T. Publication; 1951.
6. Prestressed Concrete Issue of "Civil Engineering", January 1953, Mag. of A.S.C.E., New York.
7. "A Study of Combined Bending and Axial Load in Reinforced Concrete Members", E. Hognestad; University of Illinois, E.E.S. Bull. 399; 1951.
8. "Modern Developments in Reinforced Concrete", Portland Cement Association, Bulletin 27; 1952.
9. "Stressteel Manual", published by the Stressteel Corp., Wilkes-Barre, Pa.

APPENDIX A

Static Tests Performed on Lee-McCall Bars and Bar-Nut Assemblies

There are presented in this appendix the results of five tensile tests which were performed to determine the stress-strain curve for the $\frac{1}{2}$ " ϕ Macalloy bars that were used in the six beams of the preceeding studies. Two bar-nut assemblies were also tested, and the data from those tests is included.

Two SR-4, Type A-3, Baldwin-Southwark electric gauges, placed on the bar in diametrically opposite locations, were used to measure strains while the load was applied in five kip increments up to the theoretical yield point and in 2 kip increments to approximately 145 k.s.i.. It was possible to follow the strains well up into the plastic region (to 145 k.s.i.) with a Type L Strain Indicator. One specimen was subjected to two loading-unloading cycles as indicated in Plate 59.

The stress-strain curves which were obtained are shown in Plates 58 and 59; the results from all specimens were very consistent with one another. Typical fractures are illustrated in figure 12.

Both bar-nut assemblies fractured in the same region, viz., near the point at which the tapered threads begin. It should be noted that in the case of the nut on the right hand side of figure 12 the relation of the fracture plane to the nut is not as it was when failure occurred.

The efficiencies of the bar-nut assemblies (based on the ultimate strength of the bar in the tensile specimens)

were found to be 93% and 94%. If the nominal bar size of $\frac{1}{2}"\phi$ and the specified minimum ultimate strength of 145 k.s.i. are used as the basis (that is the basis used by the manufacturer), the efficiency of the assemblies computes to 108%. In other words, these two end anchorages satisfied the specifications of their manufacturer.

Some further computations were made to determine the effectiveness of the tapered threads:

observed total load carried by $\frac{1}{2}"\phi$ bar-nut assembly
= 29.5 kips,

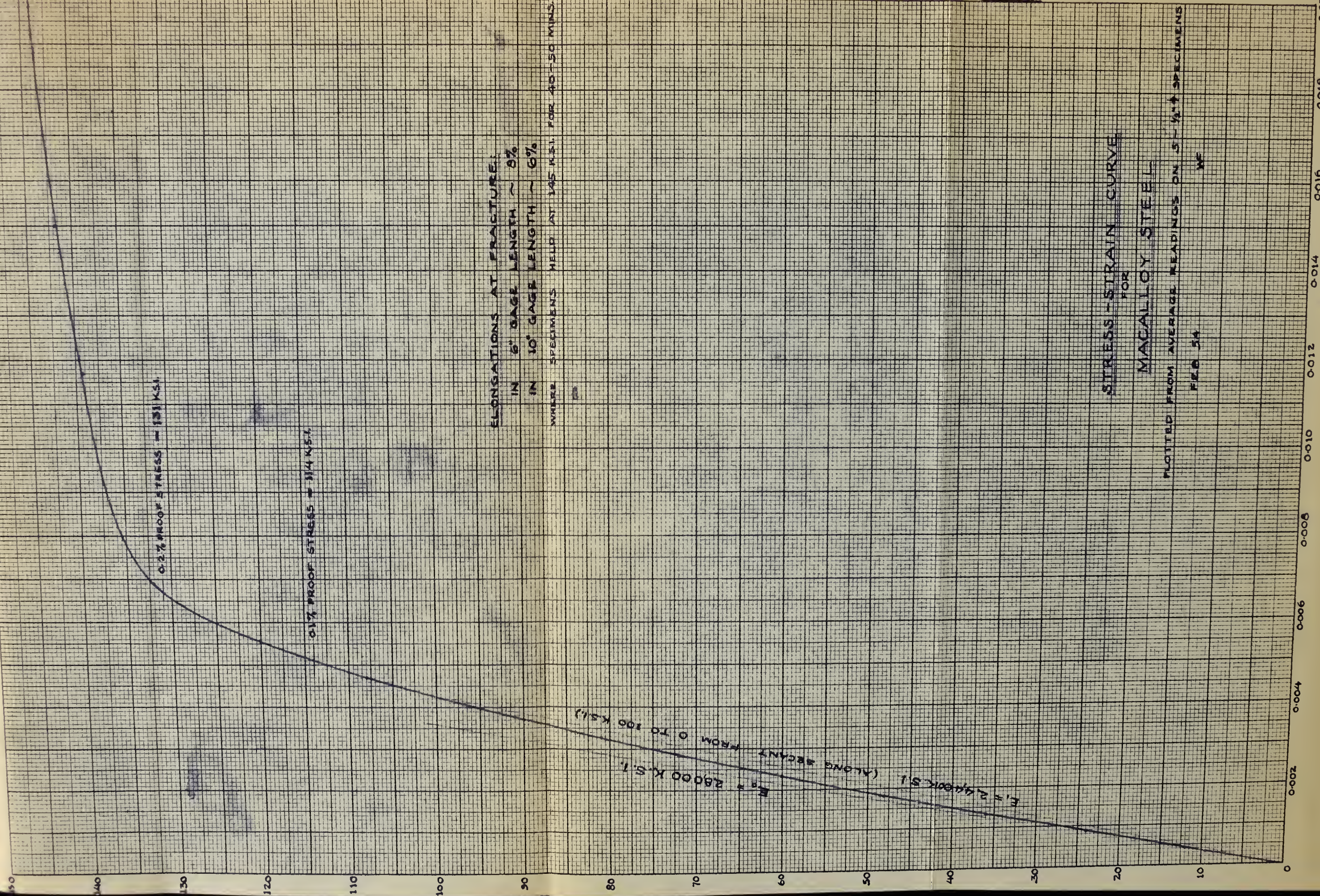
measured root diameter (near failure plane) = 0.435 in.

observed ultimate strength of the steel = 157 k.s.i.
(from tensile tests),

portion of ultimate load carried by the tapered threads
= 29.5 - 23.5 = 6 kips.

Thus the tapered threads carried about 20% of the ultimate load.

ULTIMATE STRENGTH 157.5



ELONGATIONS AT FRACTURE:
IN 6" GAGE LENGTH ~ 8%
IN 10" GAGE LENGTH ~ 6%

WHERE SPECIMENS HELD AT 145 K.S.I. FOR 40-50 MINS.

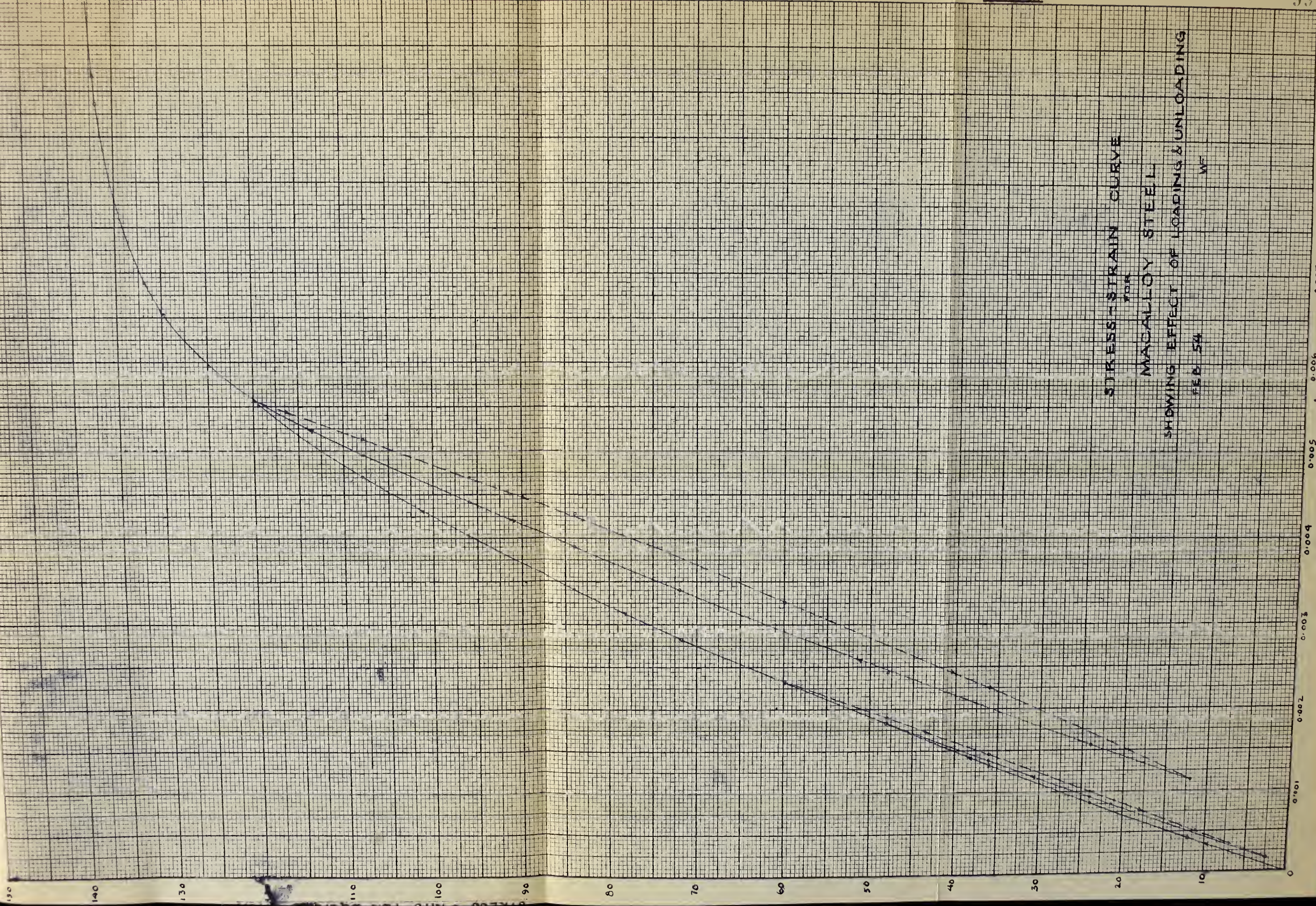
STRESS-STRAIN CURVE
FOR

MACALLOY STEEL

PLOTTED FROM AVERAGE READINGS ON 5-1/2" SPECIMENS

FEB 54

WF



STRESS - STRAIN CURVE

MACALLOY STEEL

SHOWING EFFECT OF LOADING & UNLOADING

FEB 54

WF



Figure 12. Typical fractures in Macalloy Bars.

APPENDIX B

Extensometers

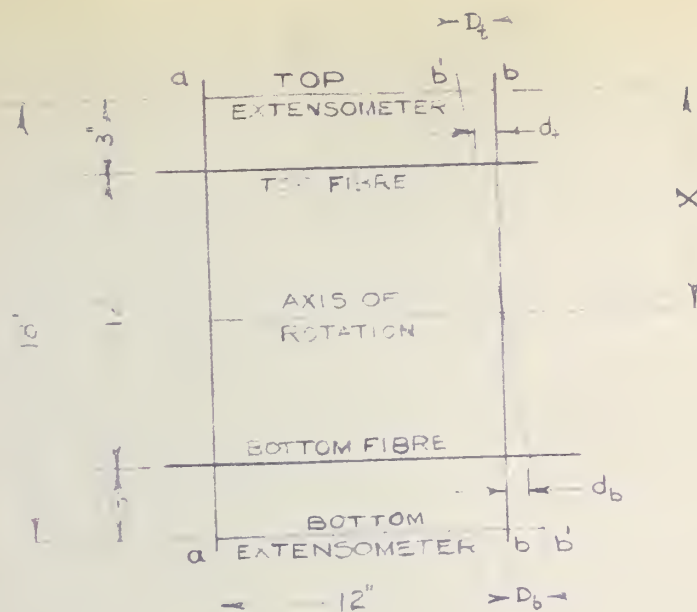
Assuming Bernoulli's Hypothesis that plane sections of a flexural member remain plane, and by measuring the relative rotation of one section with respect to another, then for a given increment of applied moment the following may be determined:

1. the location of the axes of rotation of sections,
2. the resulting strain in the top-most compression fibre.

In the tests reported herein, the angle changes between two sections were measured by observing longitudinal strains in the upper and lower fibers of the beam by means of two extensometers. An extensometer consisted of a jig for supporting an Ames dial (1/1,000th in. per division) that would measure the change in distance between the ends of two pairs of vertical rods which were placed in two separate cross-sections (near the centre of each beam). These rods, 3/8 in. in diameter and 20 ins. long, were placed in the forms a distance of 12 ins. apart, prior to pouring the beams, such that 4 in. of rod protruded above and below the beam. The extensometers were clamped to the rods 3 in. from the top and bottom surfaces of the beams. For a detailed and assembly drawing of the extensometers, see plate 60 of this appendix.

Location of the axis of rotation of sections

In the figure below the sections labeled as "a-a" and "b-b" represent the cross-sections of a test beam which contained the extensometer anchorage rods. Section b'-b'



represents the totated position of section b-b relative to section a-a due to an applied load increment. The length D_t is the shortening of the top extensometer due to the rotation of sections. Both D_t and D_b were measured with Ames dials.

From similar triangles and the dimensions shown in the figure above, the distance (X) of the axis of rotation below the top extensometer is given by:

$$X = \frac{18 D_t}{D_t + D_b} \text{ ins.}$$

Plates 35 to 40 illustrates the position of the axis of rotation for each increment of load - applied to each beam under test.

Strain in the top-most compression fibre

Again, upon consideration of similar triangles in the figure above, the total compressive strain (d_t) in the

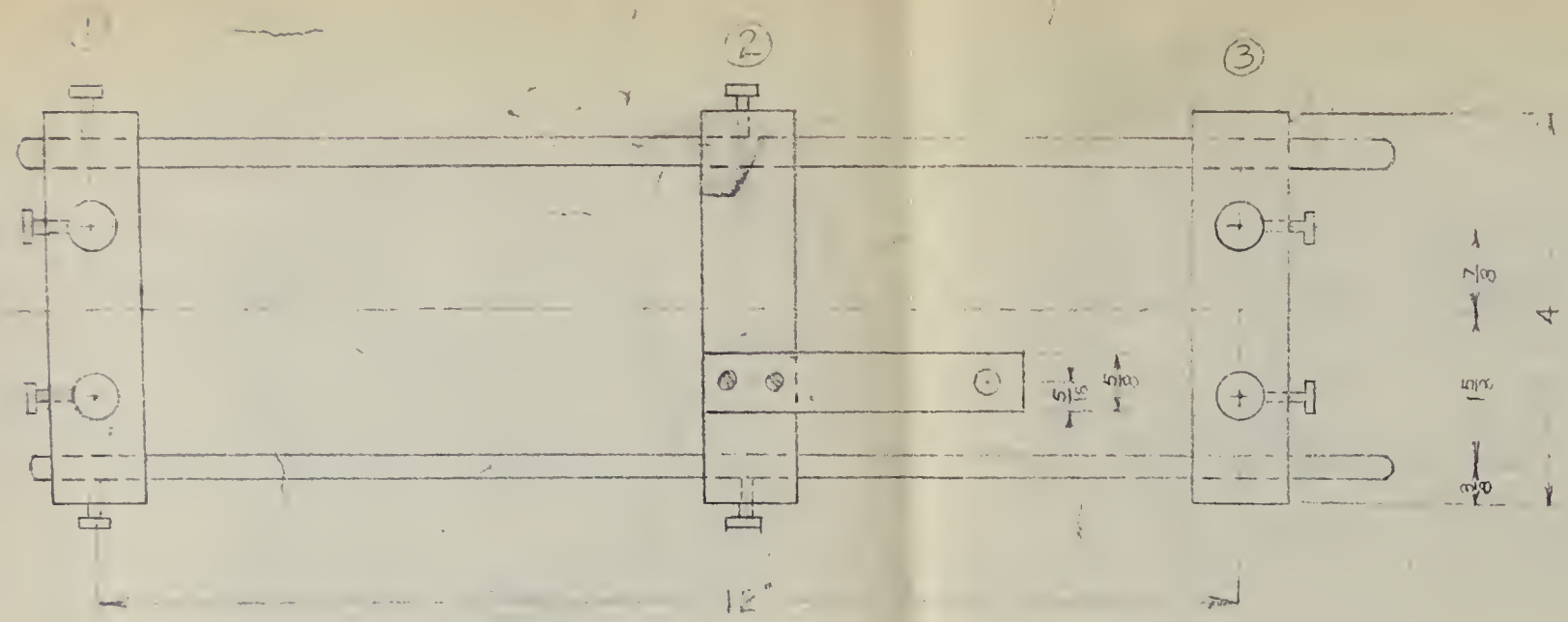
top-most compression fibre of the beam is given by:

$$d_t = \frac{D_t + D_b}{18}(X-3)$$

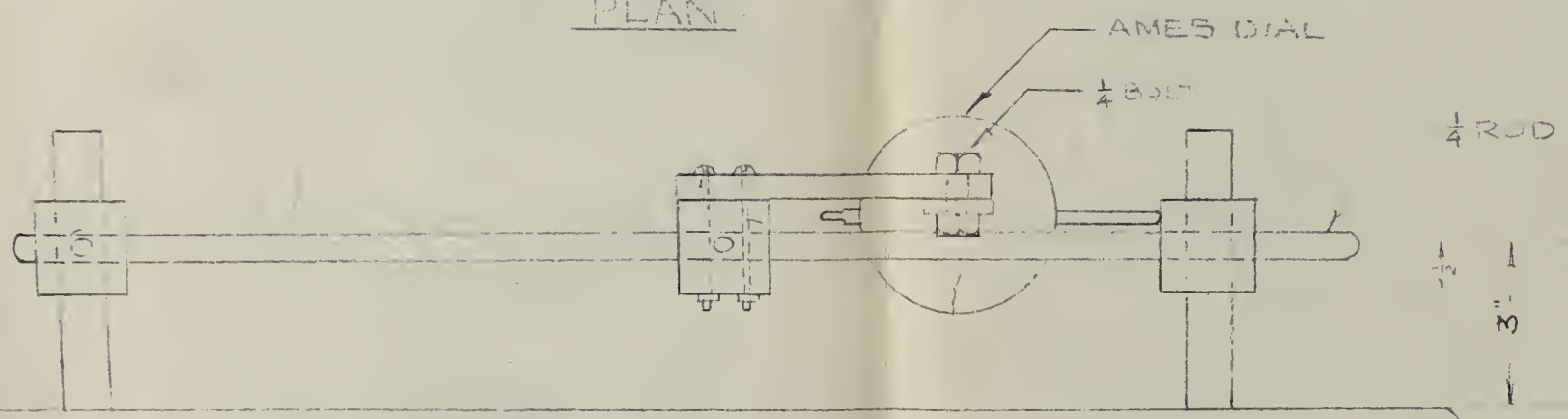
$$= D_t - 1/6 (D_t + D_b) \text{ ins.}$$

Thus, the average unit compressive strain (e_t), as shown in Plates 41 to 46 is given by:

$$e_t = 1/12 (D_t - 1/6(D_t + D_b)) \text{ in./in.}$$



PLAN



12' CONCRETE BEAM

ELEVATION

NOTE

DETAIL OF END COLLAR (3) SAME AS (1) EXCEPT THAT THE END SET SCREWS ARE NOT REQUIRED.

3 - 2 REQ'D.

4 - 1/4" x 1/4" SLIT ROD REQ'D.

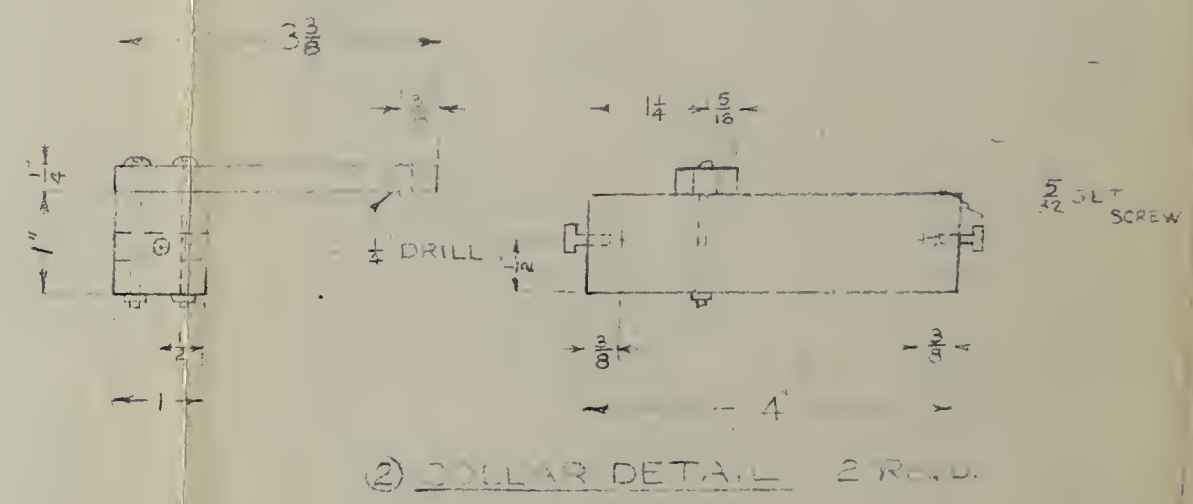
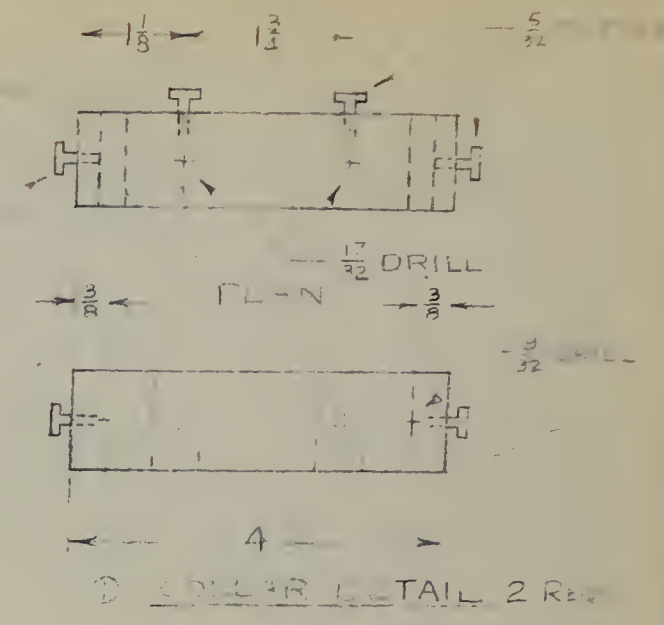
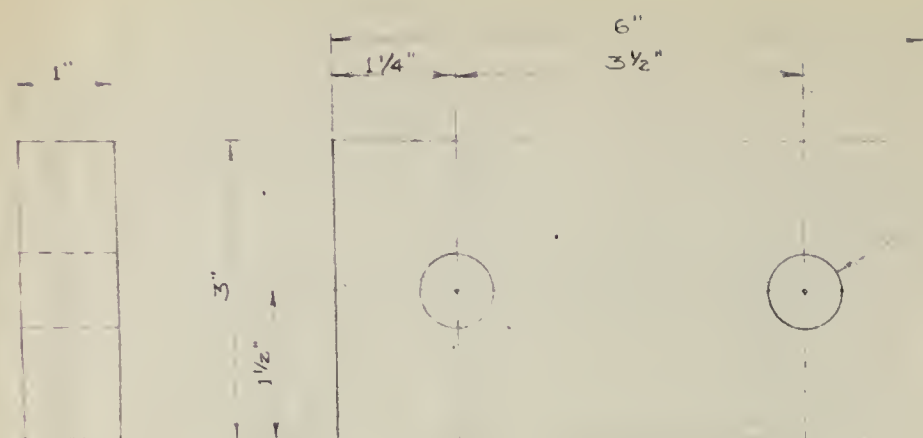


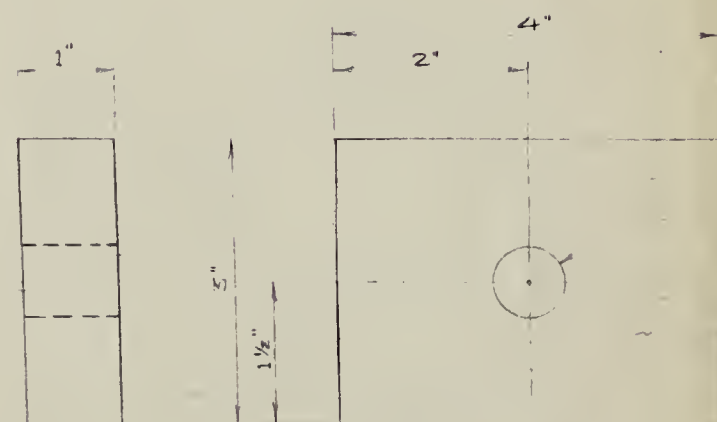
PLATE 60

EXTENSOMETER
ASSEMBLY & DETAILS
PRESTRESS BEAM
INVESTIGATION
UNIVERSITY OF ALBERTA
SCALE - HALF SIZE
DATE - JAN 14/54
T.W.L.



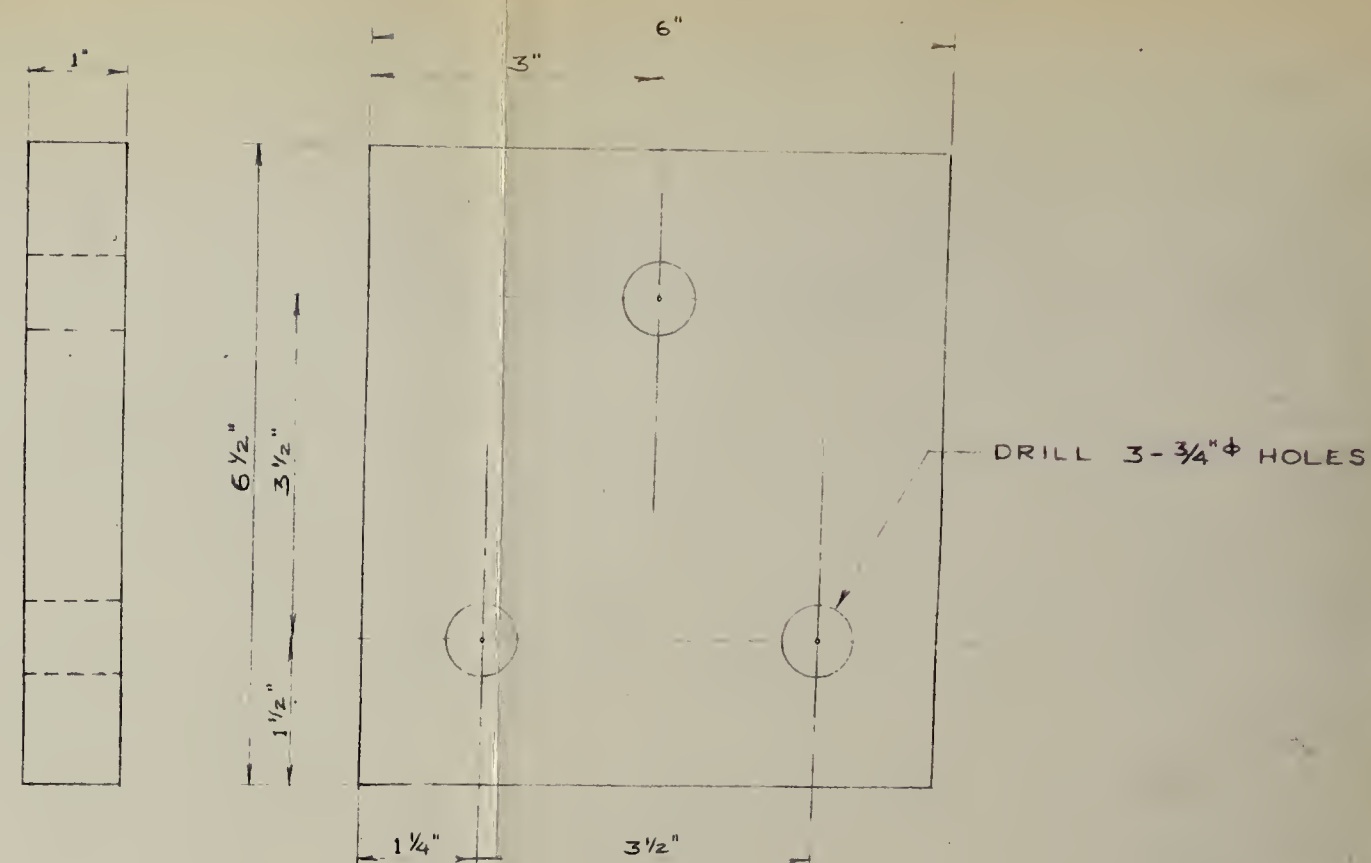
DRILL 2- $\frac{3}{4}$ " ϕ HOLES

ANCHOR PLATE EP1
8 REQ'D.



DRILL 1- $\frac{3}{4}$ " ϕ HOLE

ANCHOR PLATE EP3
2 REQ'D.



ANCHOR PLATE EP2
4 REQ'D.

MATERIAL

STEEL - EQUAL TO ASTM SPEC A7-50T

PLATE 62

END ANCHOR PLATES FOR
PRESTRESSED CONG. BEAMS

DATE JAN 34 TND WF

1/2 SIZE

DWG NO

DWG NO

2x4 PLANKING

3/4" FIR PLYWOOD SHEATHING

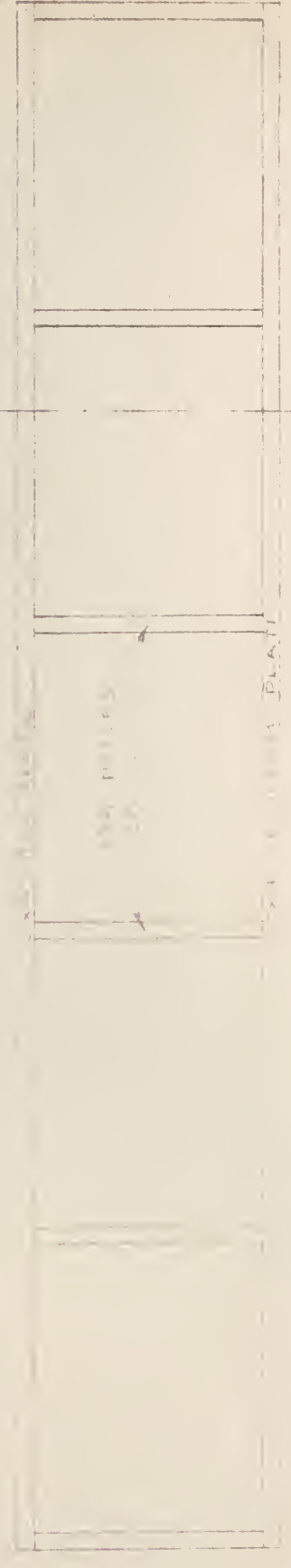
3/8" 1/4"



PLAN

11'-0"

A-A

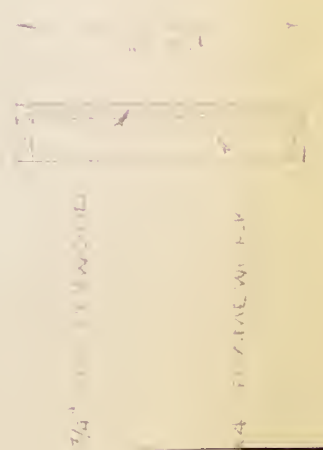


1x4 PLANKS

2x4 PLANK

A-A

1'-0"



3/4" FIR PLYWOOD

2x4 PLANK

BEAM - ONE SIDE OF BEAM FORM

2 SIDES RIGID

1 ALUM. SHEET 24 LIN. FT. 3/4" X 1/2" (WIDE) FIR PLYWOOD
2 PLANKS TO BE AT RIGHT ANGLES TO EACH OTHER
3 PLANKS TO BE FINISHED ONE SIDE (ROUGH FOR TIE-ROPS)

SECTION

